THE ROLE OF NFATC1 IN PROXIMAL TUBULE INJURY AND REPAIR

By

Melissa Marie Langworthy

Dissertation

Submitted to the Faculty of the

Graduate School of Vanderbilt University

in partial fulfillment of the requirements

for the degree of

DOCTOR OF PHILOSOPHY

In

Cell and Developmental Biology

May, 2008

Nashville, Tennessee

Approved:

Professor H. Scott Baldwin

Professor Christopher Wright

Professor Chin Chiang

Professor Mark de Caestecker

Professor Raymond Harris

To my beloved husband, Tom

In loving memory

Timothy Evans

11/09/1976 – 02/23/2008

ACKNOWLEDGEMENTS

"The woman who starts the race is not the same woman who finishes the race. " I saw this quote during a race and believe it accurately describes my life as a graduate student. I entered: excited and naïve, eager to learn, unaware that this process and so many scientists would change my perception of the world outside of the laboratory. I now emerge prepared to apply the knowledge I've gained to future research questions.

I will begin by thanking the Department of Cell and Developmental Biology in the Vanderbilt University School of Medicine for continued support and for fostering an exciting research environment that is both diverse and collaborative.

I would like to thank the Program in Developmental Biology, especially Chris Wright and Kim Kane, for their enthusiasm, support, and commitment to the training of developmental biologists here at Vanderbilt and future scientists in the Nashville schools. The seminars, journal clubs, and retreats sponsored by PDB have significantly enlightened my appreciation for all things that develop.

I would like to thank my mentor, Scott Baldwin, for his patience and continuous support. I am honored that you took me as your first graduate student. Thank you for fostering an environment in which I was able to be an independent and self-sufficient scientist. I would also like to thank the members of the lab, past and present, including, Drew Misfeldt, Kel Vin Woo, Kate Violette, Kathy Boyer, Lorene Batts, Kevin Tompkins, Xianghu Qu, Bin Zhou, Bingruo Wu, Justin Grindley, and Kai Jiao and to the friends of the Baldwin Lab; Lance Prince, Steve Goudy, Ryan Humphreys, Chris Brown, Cyndi Hill and Jaime Hendrix for constant support and more good times than bad.

I thank the members of my committee; Chris Wright, Mark de Caestecker, Chin Chiang, and Ray Harris. I am grateful for your commitment to my education, challenging me with insightful questions, and for rejuvenating my spirits at my annual meetings.

The research presented in this dissertation was performed between 2004 and 2008 and was supported by NIH Pediatric Nephrology Research Center Grant (DK44757) and by the NIH Center for Molecular Toxicology at Vanderbilt (NIH P30 ES000267).

I am grateful to the VMC Flow Cytometry Shared Resource and to Kevin Weller, David Flaherty, and Brittany Matlock for their service. The VMC Flow Cytometry Shared Resource is supported by the Vanderbilt Ingram Cancer Center (P30 CA68485) and the Vanderbilt Digestive Disease Research Center (DK058404).

Mark de Caestecker, thank you for always providing the necessary constructive criticism that pulled my head out of the clouds and put it back on my shoulders, for your critical review of my manuscripts, sponsorship at Renal Week, and for sharing your lab and reagents with me in times of need. And to former members your lab: Scott Boyle and David Frank for your friendship, support, and advice all but too often found at the bottom of a pint glass.

I thank Agnes Fogo for getting me excited about the kidney, Ellen Donnert for teaching me a fraction of what she knows on histology, Gilbert Moeckel for his expertise in pathology and for quantifying the AKI scores, Stephen Dunn at Thomas Jefferson University for performing the HPLC serum creatinine analysis on my samples, and Kim Lim at The University of Michigan for graciously providing the anti-β-Gal antibody.

Thanks to everyone who made the past years less lonely: To Aime Franco for enthusiastically sharing in the love of science and to all the Franco's for being our family

on holidays and all the super bowls, birthday parties, and Sunday dinner's in between. To Drew and Chris for making the lab a fun place to be and for boundless experimental advice. To Kate for keeping me sane and constantly reminding me that I missed my calling to be a paleontologist specializing in the Cretaceous Period. To Kim Roberts for being a loving "mom". To Jen Puster-Rahde for always emailing love and support. To Karen Edelblum for always being there and for reminding me that you love me because I'm just as brutally honest as you are. And the entertainment of WBER… the only station that matters.

To Dad and Denise thank you for your constant love and support and for the occasional, yet lengthy, motivational lectures. They were always appreciated. To Mom, thanks for loving me despite my often-abrasive persona and for always finding a way to make light of stressful situations by reminding me how pretty I am. To my older and wiser sister Jennifer and brother-in-law Brian, for planning and sharing the most important day of your lives with the most important day of Tom and my lives. To my younger and funnier sister Amanda for always making me laugh and look good. To Hal and Nikki Langworthy, you seem to always say the right thing at the right time. Thank you for your love and support.

And to my husband Tom. I love you and cherish you and could not have completed this journey without your infinite love and support and willingness to listen. Thank you for keeping me up-to-date on pop-culture and for re-teaching me geographical locations and historic events that I should have learned in school. You take me the way I am, and I am forever grateful.

TABLE OF CONTENTS

LIST OF FIGURES

LIST OF TABLES

LIST OF ABREVIATIONS

AdSC	Adipocyte derived stromal cell
AKI	Acute kidney injury
APC	Allophycocyanin
APEMP	Adult parietal epithelial multipotent progenitors
AQ	Aquaporin
BMC	Bone marrow cell
BMP	Bone morphogenic protein
BMSC	Bone marrow stromal cell
BrdU	Bromodeoxyuridine
BUN	Blood urea nitrogen
C	Carboxyl
CAA	Chloroacetaldehyde
CABIN	Calcineurin-binding protein 1
caNFATc1	Constitutively active NFATc1
CDK4	Cyclin dependent kinase 4
CK1	Casein kinase 1
CRAC	Calcium-release activated calcium channels
CsA	Cyclosporine A
DSCR	Down's syndrome critical region
E_	Embryonic day
EMT	Epithelial to mesenchymal transition
EnMT	Endothelial to mesenchymal transition
ES	Embryonic stem (cell)
FACS	Fluorescence activated cell sorting
FISH	Fluorescent in situ hybridization
GFP	Green fluorescent protein
GSK3β	Glycogen-synthase kinase 3β
$HgCl_2$	Mercuric Chloride
HMG	High-mobility group
hRPTEC	Human renal proximal tubule epithelial cells
HSC	Hematopoietic stem cell
IC	Inner cortex
IL-2	Interleukin-2
$InsP_3$	Inositol-1,4,5-trisphosphate
iPSC	Induced pluripotent stem cells
I/R	Ischemia/reperfusion
KHS	Krebs-Henseleit saline
KHS+	KHS with 1.5% FBS
KIM-1	Kidney injury molecule 1
KSP	Kidney specific protein
LTL	Lotus tetragonolobus lectin
MCIP	Modulatory calcineurin-interacting protein

MET	Mesenchymal to epithelial transition
mpkCCD	Murine collecting duct principal cells
MRPC	Multipotent renal progenitor cells
N	Amino
ND	Not determined
NF-κβ	Nuclear factor-κβ
NFAT	Nuclear Factor of Activated T-Cells
NLS	Nuclear localization sequence
NHR	NFAT homology region
OC	Outer cortex
OREBP	Osmotic response enhancer-binding protein
PCNA	Proliferating cell nuclear antigen
PI	Propidium iodide
PTC	Proximal tubule epithelial cells
PTPC	Proximal tubule progenitor cells
REC	Renal epithelial cells
RHR	REL homology region
SCID	Severe combined immunodeficiency
SEM	Standard error of measurement
Sglt2	Sodium glucose cotransporter member 2
SP	Side population
SP#	Serine-proline (2 and 3)
SPXX	Serine-proline-X-X
SRR	Serine-rich region
T	Brachyury
TA	Transiently amplifying
TAD	N-terminal transactivation domain
TNF	Tumor necrosis factor
TonEBP	Tonicity element binding protein
TUNEL	Terminal dUTP nick-end labeling
vWF	von Willebrand factor
WT	Wild Type
X	Amino acid
YFP	Yellow fluorescent protein

CHAPTER I

INTRODUCTION

Overview

Recovery from acute kidney injury (AKI) caused by a nephrotoxic insult requires renal tubule cell regeneration. The AKI can be induced by a toxic insult to the nephron following acute or chronic exposure to an environmental and/or occupational toxin, by ischemia/reperfusion (IR) injury typically induced by transient hemodynamic shock, or from treatment with chemotherapeutic and/or immunosuppressive drugs. The mechanism of repair from AKI is not clear.

The NFAT proteins are dynamic regulators of transcriptional activity and were first identified in T cells where their activation is a critical component in the initiation of an immune response. Cyclosporine A (CsA), an immunosuppressive drug inhibits the phosphatase activity of calcineurin thus preventing the dephosphorylation of NFATc1 proteins necessary for the transcriptional activity of NFAT proteins. A clinical side effect of CsA is nephrotoxicity having both acute and chronic effects on renal structure and function. However, a mechanism has not been identified for the nephrotoxicity of CsA.

Extensive work has been performed to characterize NFAT expression and signaling in T-cells, the cardiovascular system, and numerous other tissues where roles for NFAT proteins have been described in controlling the cell cycle and activating transcriptional targets. In contrast, very little is known about the expression of NFAT proteins in renal tissues. Our laboratory made the novel observation that a member of the

nuclear factor of activated T cells (NFAT) family of transcription factors, NFATc1, is expressed in a subset of proximal tubule epithelial cells (PTC) following AKI. In addition, using a transgenic reporter mouse utilizing NFATc1 regulatory elements, expression was observed in the cortical region of the adult kidney. Our lab has previously described an important role for NFATc1 plays in maintaining the endocardial phenotype. Therefore, we hypothesize that NFATc1 might play a role in maintaining the epithelial phenotype of proximal tubule epithelial cells (PTCs).

The primary focus of my research has been to determine the function of NFATc1 in PTCs in a mouse model of AKI in both normal tissue and during AKI. In Chapter I, I will discuss 1) the proposed models for tubular epithelial repair, 2) the regulation of NFAT transcription and function in the kidney, and 3) AKI and the nephrotoxicity of CsA and mercuric chloride ($HgCl_2$). The first experiment that I performed in the kidney was to induce AKI with a single dose of $HgCl_2$ in WT and in *Nfatc1*$^{+/-}$ mice over a brief time course. This experiment was the basis for the work described in Chapter II of this dissertation where I demonstrate that the *Nfatc1*$^{+/-}$ mice have sustained AKI, reduced expression of NFATc1, and increased proximal tubule apoptosis compared to WT mice. To further attenuate NFATc1 expression, Cyclosporine A was administered to mice and resulted in increased serum creatinine concentration, increased apoptosis, and reduced proximal tubule cell proliferation following $HgCl_2$ injury as described in Chapter III. Chapters IV focus on the use of a novel NFATc1 transgenic lines to demonstrate accentuated NFATc1 expression in a subpopulation of proximal tubule cells following $HgCl_2$ injury and Chapter V on the isolation and characterization of this unique subpopulation of proximal tubule progenitor cells (PTPCs). Further lineage analysis

documented that the NFATc1 labeled PTPCs are resistant to apoptosis and subsequently proliferate to repair the damaged proximal tubule segment and thus represent a progenitor population. In Chapter VI, I will conclude with a discussion of the significance of a self-renewing resident PTC progenitor population and suggest future experiments to further characterize the role for NFATc1 in proximal tubule regeneration.

Kidney structure

An adult human kidney is comprised of greater than one million individually functioning units called nephrons [Fig. 1.1. (McKinley and O'Loughlin, 2006)]. Each nephron contains a glomerulus and a segmented renal tube. The glomerulus purifies and filters the blood and is composed of Bowman's space, capillaries, glomerular basement membrane, podocytes, and mesangial cells. The glomerular capillaries are composed of a network of fenestrated endothelial cells that create pores for plasma filtration. Mesangial cells have a phagocytic function and are located within the extracellular matrix between capillaries. The glomerular basement membrane maintains the structure of the glomerulus by fusing the basal lamina of the capillary endothelial cells with podocytes. Podocytes have interdigitating processes that cover the external side of the glomerular basement membrane and control the filtration of proteins from the capillary lumen into Bowman's space, the portion of the glomerulus connected to the lumen of the renal tubule.

The glomerulus begins the formation of urine by filtrating plasma into Bowman's space through the glomerular capillary wall into the adjacent processes that are separated by slit pores within the slit diaphragm. The filtration barrier established by the slit diaphragm allows water and small plasma solutes to pass through the filtration barrier

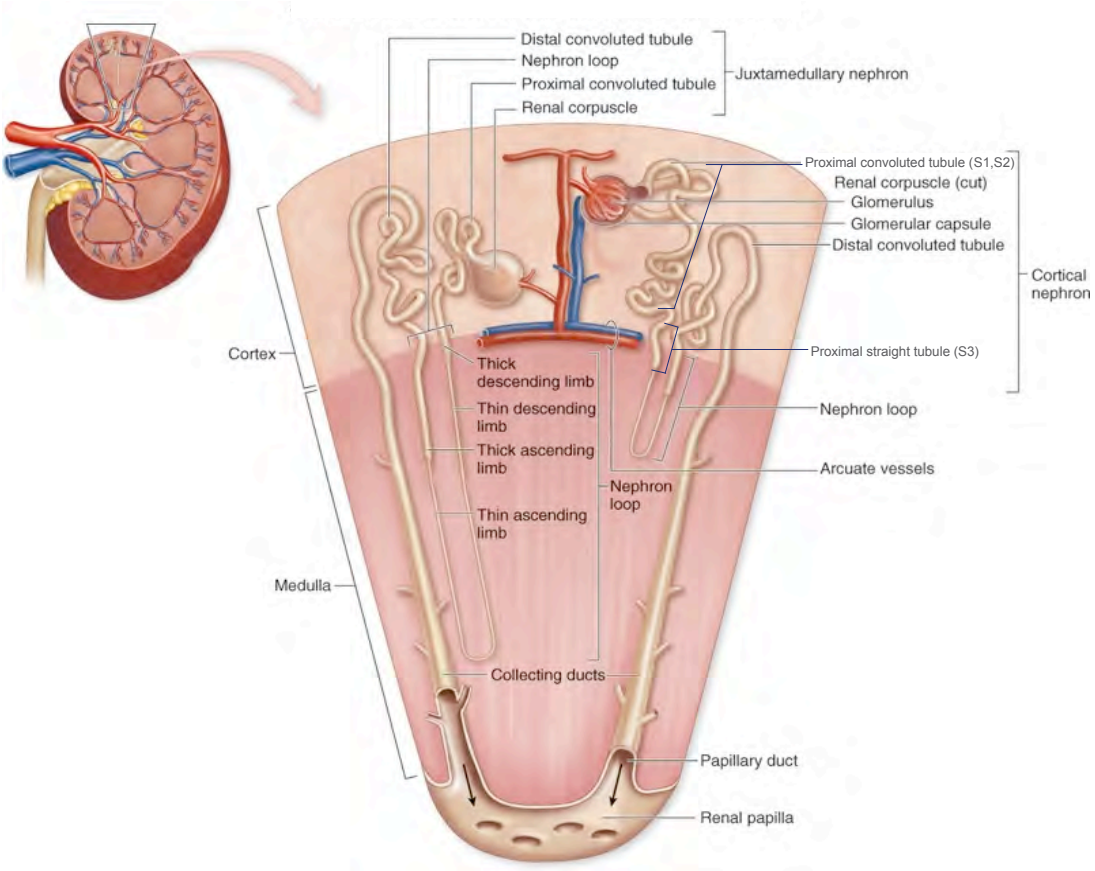

Figure 1.1. ***Nephron structure.*** Figure adapted from McKinley and O'Loughlin's Human Anatomy (2006).

easily and restricts large proteins from being excreted into the urine through the renal tubule.

The renal tubule absorbs nutrients and water, concentrating the toxins. The renal tubule connects the Bowman's capsule to the ureter and is made up of the proximal tubule, loop of Henle, and the distal tubule. The proximal convoluted tubule (S1, S2) is comprised of cuboidal epithelial cells with round nuclei and a luminal brush border composed of microvilli. The proximal tubule is located within the kidney cortex and actively reabsorbs water, NaCl, glucose, amino acids, and vitamins. Continuing from the proximal convoluted tubule is the proximal straight tubule (S3). The proximal tubule is followed by the loop of Henle that is composed of the thick descending limb, thin descending limb, thin ascending limb, and thick ascending limb. The thick and thin segments are comprised of cuboidal and squamous epithelium, respectively and functions to further concentrate the urine by removing water and NaCl. The distal convoluted tubule is lined with cuboidal cells that have distinct lateral borders and lack a brush border. The distal tubule reabsorbs sodium and empties into the collecting ducts found in the medulla that further reabsorbs water and excretes urine into the ureter.

Acute Kidney Injury

Acute kidney injury (AKI, also called acute renal failure, acute tubular necrosis, and acute renal injury) is an important clinical problem resulting from insults that cause functional and structural changes in the kidney. The insult leading to AKI can be induced by a toxic insult to the nephron following acute or chronic exposure to an environmental and/or occupational toxin, treatment with chemotherapeutic and/or immunosuppressive

drugs, or by ischemia/reperfusion (IR) injury typically induced by transient hemodynamic shock (Basile, 2007). AKI is characterized by apoptosis of cells in the straight portion of the proximal tubular and thick ascending limb of the loop of Henle and is associated with changes in the serum chemistry and urine with increased concentrations of serum creatinine, blood urea nitrogen (BUN), and increased expression of kidney injury molecule 1 (KIM1) in tubule epithelial cells. If the injury stimulus is removed or inhibited the injury phase is followed by partial or complete regeneration of injured tubules.

Models of AKI

To identify mechanisms of renal injury, AKI is modeled in rodents by administration of renal toxins or surgical manipulations that mimic clinical nephrotoxic ischemia. Cisplatin, a chemotherapy drug used to treat pediatric and adult patients, induces renal injury of tubular cells marked by apoptosis and necrosis. A single injection of Adriamycin causes acute glomerular injury and loss of podocytes as well as tubular cell injury and progressive renal failure. A number of heavy metals of unknown biological function (cadmium, chromium, mercury, lead, uranium) excessive concentration of metals with known biological function (cobalt, copper, iron, zinc) and those used in chemotherapeutic drugs (platinum, vanadium) are accumulated in the proximal tubule and cause AKI (Sabolic, 2006). Ischemia/reperfusion is a surgical model of AKI performed by applying a temporary clamp on the renal pedicle, blocking the flow of blood for a short period of time under anesthesia followed by the release of the clamp. The AKI of ischemia/reperfusion injury is marked by vasoconstriction, hypoxic injury to

the microvascular endothelial cells and tubular epithelial cells, and leukocyte-mediated cytotoxicity. The cellular injury from ischemia/reperfusion injury is accompanied by depletion of ATP and an increase in intracellular Ca^{2+} and mimics the ischemia/reperfusion injury that occurs during kidney transplantation. During the process of renal transplantation, there is a period of anoxia during cold preservation followed by a period of reperfusion after implantation resulting in significant injury to the transplanted organ (Foley and Chari, 2007).

The body of literature published documenting causes of, treatments for, and prevention of AKI is extensive. Therefore, I will focus the presentation on two forms of nephrotoxicity that are relative to this dissertation: nephrotoxicity induced by exposure to inorganic mercury (presented below) and nephrotoxicity associated with the immunosuppressive drug CsA (presented in the following section).

Mercury nephrotoxicity

All forms of mercury, elemental and organic and inorganic conjugates, are toxic with inorganic mercury being more acutely nephrotoxic. Organic forms of mercury, including methylmercuric chloride and dimethylmercury, are less nephrotoxic and require multiple exposures to large doses in order to cause renal injury (Zalups, 2000). Inorganic mercury conjugates are more toxic and a single dose of mercuric chloride ($HgCl_2$) causes AKI in mice and rats causing a marked injury in the PTCs preferentially in the S2 and S3 segments (Hultman and Enestrom, 1986).

Cellular uptake of mercury

Mercury is transported into PTCs by interacting with thiol-containing compounds transported into the cell. There are two mechanisms involved in the uptake of mercury by PTCs: luminal membrane transport and basolateral membrane transport. At the luminal membrane, γ-glutamyltransferase and cysteinylglycinase import mercury conjugates of glutathione and cysteine, in particular dicysteinylmercury into the cell. At the basolateral membrane, the dicarboxylate and organic anion transport systems import mercury conjugates of cysteine, glutathione, homocysteine, and N-acetylcysteine into the cell. Mercury conjugated molecules interfere with subsequent metabolism causing changes in heme metabolism, lipid peroxidation, mitochondrial dysfunction, and oxidative stress. Renal tubular injury was increased in animals when they were administered a mercuric conjugate of cysteine (Zalups and Barfuss, 1996). Transportation, accumulation, and excretion of mercury containing molecules appears to be a mechanism exclusive to the proximal tubule as other segments of the nephron have not been shown to have a similar mechanisms (Zalups, 2000).

Indices of injury

Depending on the form and dose of mercury administered, cellular injury and cell death can be detected along the length of the proximal tubule segment and cortex from beneath the outer capsule to the junction with the outer medulla (Zalups, 2000). During the early stages of mercury toxicity, proximal tubule cells undergo a number of structural changes including the shortening and lose brush border microvilli, detachment of cells from the basement membrane, blebbing, vesiculation of cytoplasm, derangement of the

cytoskeleton, cellular swelling, lysosomal swelling, and mitochondrial injury including vacuolation and fragmentation [Rev. in (Sabolic, 2006)]. Injury can be observed after 1 hour, particularly after exposure to a high dose, and the peak in injury occurs at 24 hours and lasts roughly 3 days. Following injury, the proximal tubule is regenerated and function is restored within 2 weeks. Death from exposure to a high dose of inorganic mercury is due to AKI as well as cardiovascular collapse, shock, and severe gastrointestinal damage and bleeding.

The cellular response to injury from exposure to $HgCl_2$ injury results in necrosis or apoptosis. Apoptosis resulting from AKI occurs from both the intrinsic mitochondrial pathway and from the extrinsic death-receptor pathway (Foley and Chari, 2007). Following cellular uptake (as described above), the cell is exposed to oxidative stress measured by the increased production of free radicals and the accumulation of reactive oxygen species, leading to the accumulation of intracellular cytoplasmic Ca^{2+}. Synergistic action of reactive oxygen species and Ca^{2+}cause mitochondrial damage and loss of mitochondrial function and in turn activates the cleavage of procaspases into active caspases. If the mitochondria are able to maintain the production of ATP as injury persists, the cell proceeds to undergo apoptosis. If production of ATP is inactivated and/or ATP stores are depleted, the cell undergoes cellular death by necrosis. Cells in the proximal tubule segment that do not undergo cell death launch a number of effects that favor cell survival including the activation of antiapoptotic proteins and induction of a number of protective proteins that decrease the injury caused by the oxidative stress and free radicals. [Rev. in (Sabolic, 2006)].

Strain sensitivity

The nephrotoxicity of inorganic mercury varies between different inbred strains of mice. Mice on the C57BL/6 background are less sensitive to inorganic mercury exposure than mice on the 129/Sv, C3H/He, B6C3Fi, and Balb/c backgrounds. Mice on the C57BL/6 background are able to tolerate exposure to higher doses of $HgCl_2$ without elevating serum creatinine and/or BUN concentrations and C57BL/6 mice excreted greater amounts of mercury in urine compared to other backgrounds (Satoh et al., 1997; Tanaka-Kagawa et al., 1998; Yasutake and Hirayama, 1986).

Questions about mercury nephrotoxicity

There are a number of questions about mercury toxicity that are not addressed in the literature. How is the remaining toxicity handled by nephrons with denuded proximal tubule segments and an overall reduction of functioning nephrons? How do damaged nephrons regenerate PTCs? Are there resident cells, either proximal tubule or of another cell type that replace them via proliferation and/or dedifferentiation or a circulating cell of hematopoietic origin that repairs the nephron? The following section will cover the proposed role of circulating and resident stem cell populations in repairing the damaged kidney.

Mechanisms of proximal tubule epithelial repair

Stem cells verses progenitor cells

Following AKI, it is necessary for the proximal tubule segment to repair itself in order to restore renal function and avoid complete renal failure. The cell population responsible for repair has been proposed to be either a stem cell or a progenitor cell. Stem cells are pluripotent, self-renewing, slow cycling, undifferentiated and reside in a stem cell niche – a microenvironment that directly promotes the maintenance of the stem cell population. The stem cell niche may be a great distance from the tissue in which they are active, as in bone marrow derived stem cells or the niche may be in close contact to the tissue and cell types in which they sustain and repopulate, such as stem cells located in hair follicles and intestinal crypts. In contrast, progenitor cells are differentiated, amplify transiently to undergo self-renewal, and cycling is dependent on the rate of proliferation necessary to either maintain or replenish the population [Rev. in (Morrison and Spradling, 2008)].

There are three proposed mechanism for how proximal tubule repair occurs (Fig. 1.2). One model suggests that bone marrow stem cells (BMC) circulating within the blood are able to incorporate and dedifferentiate into PTCs. A second model suggests that adjacent less injured mesenchymal cells in the interstitium undergo the process of mesenchymal to epithelial transition (MET) in order to repair the proximal tubule. A third mechanism suggests that it is the proximal tubules themselves that proliferate to repair and restore renal function. I will discuss the literature supporting each of these proposed models.

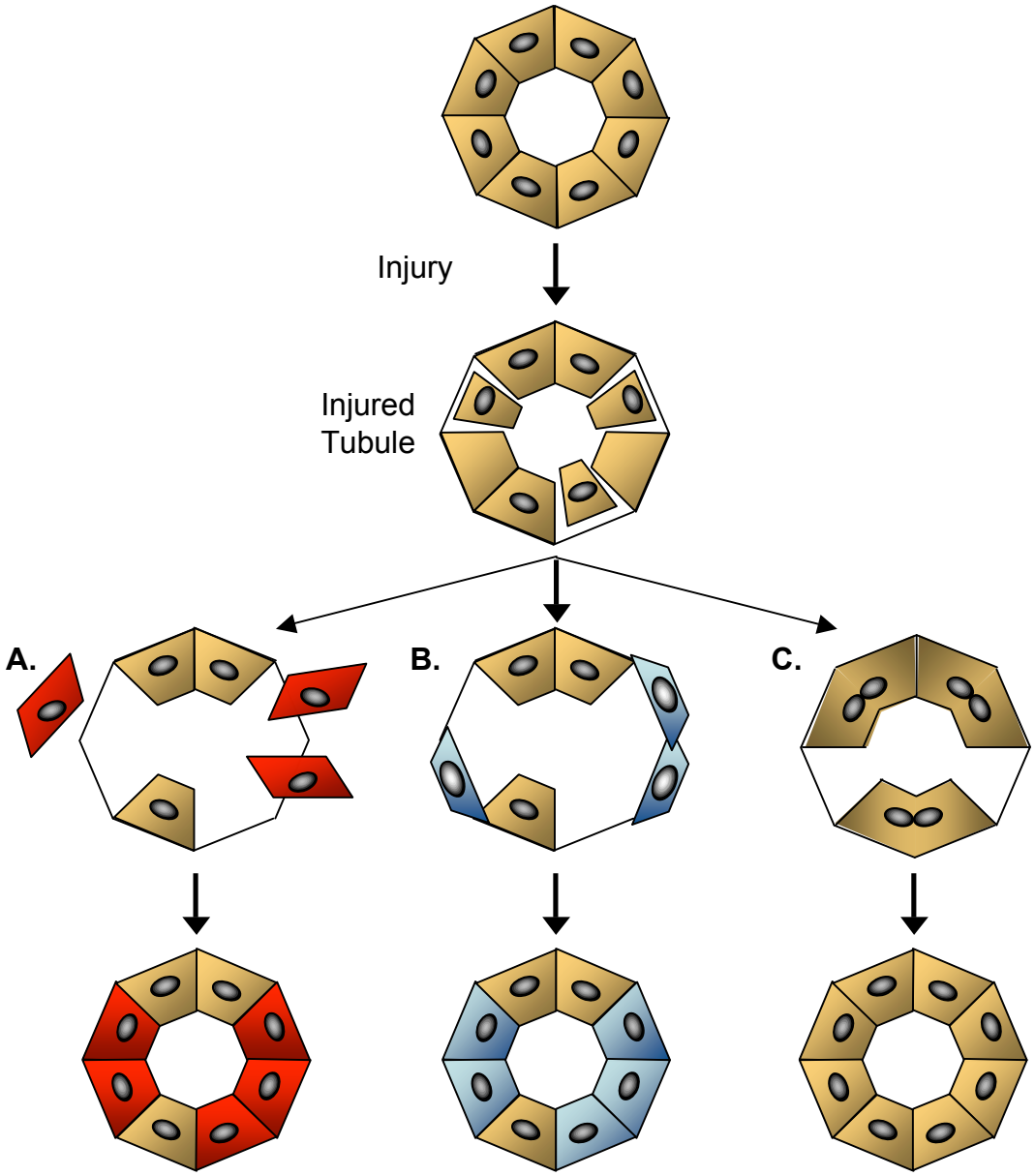

Figure 1.2. ***The origin of tubule epithelial progenitors.*** Following AKI, the proximal tubule segment regenerates to restore renal function and prevent renal failure. There are three proposed mechanisms for repair. **A.** One model suggests that BMCs circulating within the blood dedifferentiate and incorporate into the proximal tubule. **B.** A second model suggests that adjacent interstitial cells undergo the process of mesenchymal to epithelial transition (MET) in order to repair the proximal tubule. **C.** Finally, regeneration may occur via proliferation of intrinsic self-renewing proximal tubule progenitor cells.

Circulating progenitor cells

BMCs specifically hematopoietic stem cells (HSC) have been shown to be able to differentiate into numerous nonhematopoietic cell types. BMCs have been shown to localize to the kidney following a renal injury and have been identified as podocytes, endothelial, interstitial, mesangial, and tubular epithelial cells. Three mechanisms are proposed to describe the differentiation and incorporation of bone marrow derived stem cells into the host kidney. One, a subset of the BMC are pluripotent and able to differentiate into any cell type by responding to environmental signals. Two, BMC fuse with injured cells, providing undamaged cytoplasmic components, and form either synkaryons (one nucleus in a common cytoplasm) or heterokaryons (two nuclei in a common cytoplasm). And in a third proposed mechanism, cells do not undergo a proliferative process but instead transdifferentiate by epigenetic reprogramming into the new cell type, however, little evidence has been shown to support this important possibility. The therapeutic potential repairing renal damage via BMC transplantation BMC has been studied by injecting crude male BMC suspensions into female immunocompromised mice or rats.

Fusion of BMC with ES cells *in vitro* occurs at a ratio of 1 to 10^6 BMC. *In vivo*, fusion has been shown to occur in a number of tissues, including the chronically injured kidney, in which the proximal tubule was shown to be repopulated by fusion of donor BMC with host proximal tubules (Held et al., 2006). Fusion events can be demonstrated by fluorescent *in situ* hybridization (FISH) to identify the presence of the Y chromosome of the donor male in female recipient. If male donor BMC are injected into an immunocompromised female host, a fusion event between the male BMC and an existing

renal cell would result in a change in the karyotype of the nuclei containing 2X1Y or 3X1Y.

Lin and colleagues used a sophisticated genetic approach and injected male BMC of *R26R-EYFP* genetic background (Srinivas et al., 2001) into immunocompromised female hosts with a Ksp-Cre background. Ksp-Cre is a transgenic line that expresses Cre using regulatory elements for the kidney specific protein (ksp) cadherin and is expressed in tubular epithelial cells as well in other epithelial cells in the developing urinary/genital system (Shao et al., 2002). This genetic approach allows for fusion events to be identified in tubules cells not only by FISH but also by the identification of cells that express yellow fluorescent protein (YFP). The injected BMCs express YFP due to a floxed stop codon that prohibits reporter expression and in the presence of Cre, the stop codon is removed and YFP expressed. Using this technique, FISH was used to identify BMC that incorporated into collecting ducts, distal tubules, proximal tubules, and thick ascending limbs of female recipients following I/R injury. They identified that 1.8% of the tubular epithelial cells were bone-marrow-derived 4 weeks after injury. Extensive quantification revealed that 0.93% and 0.34% of these BMC underwent fusion and were identified to have karyotypes that were 3X1Y and 2X1Y, respectively. Immunolabeling with an anti-YFP antibody showed that YFP was expressed in renal tubules, however the authors did not quantify the frequency of YFP expressing fused cells (Li et al., 2007a). Fusion events resulting in YFP expression in non-tubular cell types could not be detected due to limited expression of Ksp to renal tubules. While these experiments are novel and show evidence that a small number of tubular epithelial cells are repaired by fusion with BMC following

I/R injury, they would have been more informative in defining of the potential of fusion of BMC if the host expressed a ubiquitous Cre and if the YFP was observed real time.

Duffield and colleagues used three models of transplantation to create chimeras. Female mice were lethally irradiated and bone marrow was replaced with bone marrow from male mice, or bone marrow that would constitutively express GFP or constitutively express β-Gal. Six weeks after bone marrow replacement, mice underwent unilateral I/R injury. They identified an increase in BMC in the interstitium but not in tubular epithelia of the I/R injured kidney. BMC-derived cells were not observed in the contralateral uninjured kidney. BMC that appeared to be tubular epithelia were shown by deconvolution microscopy to be interstitial cells. Duffield and Bonventre explain that previous researchers did not use such sensitive microscopy and BMC-derived tubular epithelia described previously were misidentified (Duffield and Bonventre, 2005).

Bi *et al*. cultured bone marrow stromal cell (BMSC) and adipocyte derived stromal cells (AdSC) and injected them into mice following cisplatin induced AKI. BMSC and AdSC did not incorporate into regenerating renal tissue but did show that treatment with these cells reduced renal injury as measured by BUN concentrations. They suggested that the increased renal function was accredited to cytokines secreted by BMSC and AdSC that inhibit cisplatin-induced apoptosis and could be used clinically to increase renal function but not permanently repair the kidney (Bi et al., 2007). Thus the work by Duffield and colleagues and by Bi and colleagues suggests a limited direct therapeutic potential of BMC by their incorporation into or fusion with renal tubule segment of the nephron but rather suggests the major benefit was from paracrine signaling events.

Adjacent less injured cells

The mammalian kidney forms through the process of mesenchymal to epithelial transition (MET). The definitive mammalian kidney arises at day 35-37 of human gestation (embryonic day 10.5-11 in mouse) when a population of cells at the caudal end of the Wolffian duct known as the ureteric bud grows out into the surrounding metanephric mesenchyme. Reciprocal signaling events between the ureteric bud and metanephric mesenchyme allow the ureteric bud to branch and the metanephric mesenchyme to condense. Condensed metanephric mesenchyme at the tips of the ureteric branches undergo MET to form the proximal and distal tubules of the nephron and epithelial component of the developing glomerulus. Migrating endothelial cells form the remainder of the glomerulus and the ureteric branch develops into the collecting duct. Development of the kidney is unique in that mobile and unorganized mesenchymal cells receive signals to form organized polarized epithelia with distinct adhesion properties to undergo MET (Vainio and Lin, 2002). The second proposed mechanism for tubule repair is based on a recapitulation of normal renal developmental processes marked by dedifferentiation and migration of adjacent uninjured or less injured cells into damaged epithelial tubules by MET. Because transgenic markers have not been identified, this hypothesis is tested using a common experimental design: sorted or cultured cell populations are labeled with a tracer molecule, such as a fluorescent protein, and reintroduced into the kidney via engraftment under the renal capsule or injection into the blood stream.

Little and colleagues studied side population (SP) cells in the adult kidney and their ability to integrate into regenerating tissue. SP cells are proposed to be a resident

progenitor population of cells and were identified by retaining low levels of Hoechst fluorescent dyes because their membrane transport pumps can efflux the dye rapidly out of the cell. FACS analysis showed that SP cells account for 0.14% of the adult kidney and are further characterized to be CD45-, CD34-, c-kit-, Sca1+, CD24+ and CD31+. This expression pattern distinguishes SP cells from bone marrow SP cells, which are CD45+, CD34+, c-kit+, Sca1+, CD24+ and CD31+. AKI was modeled by a single injection of Adriamycin, which causes acute glomerular injury and loss of podocytes as well as tubular cell injury and progressive renal failure. After injecting Adriamycin into the tail vein to induce AKI, isolated adult kidney SP were injected both directly under the kidney capsule and into the circulatory system via the renal vein. SP cells incorporated into proximal tubule, distal tubule, collecting duct, glomerulus, and interstitium but not into endothelial cells of the blood vessel. The authors used microarrays to identify a set of additional markers that were upregulated in SP of adult and embryonic kidney samples compared to adult kidney. *In situ* hybridization was used to confirm expression of those markers and identify a cell population that expressed these cells. Most of the identified markers were expressed in proximal tubules and interstitial cells with the exception of CD24 that was not expressed in proximal tubules (Challen et al., 2006). The SP cells show potential to be a stem cell population because they were able to incorporate into multiple cell types thus demonstrating multipotency, however the endogenous location of these cells is unclear due to the inability to identify a specific population that expressed the predicted markers. Yet it is unclear whether incorporation of the injected SP was due to cells that were circulating in the blood or due to injection under the renal capsule. The

identification of the cells in the interstitium suggests that a role for regeneration via an adjacent cell population.

Al-Awqati and colleagues propose the renal papilla as the niche for adult renal stem cells and following AKI these cells migrate and repair damaged tubules. They pulsed 3-day-old neonatal rats with the thymidine analog bromodeoxyuridine (BrdU) for 3.5 days and examined retention of the label after 2 months. The mitotic interval for cells during early *ex utero* development was 3 days and thus all cells would label with BrdU during the pulse. During the 2 month chase, cells that were rapidly dividing would reduce the individual cell chromatin labeling with BrdU to levels that would not be able to be detected and cells retaining the label were slow-cycling stem cells are called "label-retaining cells". They found that the renal papilla contained an abundant population of cells that retained a strong BrdU signal. However, these cells disappeared from the papilla following I/R injury despite the finding that the papilla did not undergo apoptosis after injury. These cells were not incorporated into the recovering renal tissues and the authors proposed that these cells migrated into the damaged regions of the nephron and underwent multiple rounds of proliferation, thus reducing the level of BrdU to a level that cannot be detected (Oliver et al., 2004). Thus the proposed mechanism for tubule repair is through the uninjured niche of papilla stem cells. However, the authors did not document evidence of a genetic marker that would allow lineage tracing or evidence showing observations of migration of these cells Furthermore, due to the high osmotic stress that renal papillary cells are exposed to, the label retention of BrdU may result in artifact labeling (Burg, 2002).

Goligosky and colleagues further studied the papilla stem cells using Nestin-GFP (green fluorescent protein) transgenic mice created by Mignone *et al*. (Mignone et al., 2004) as a genetic marker. Nestin has been proposed to be a stem cell marker expressed by intraepithelial stem cells, mesonephric mesenchyme, and endothelial cells and in the adult kidney. In adult mice, Nestin-GFP was identified in the papilla as well as in the medulla, podocytes of the glomerulus, and in the parietal epithelial cells that line the Bowman's capsule. They performed I/R and analyzed changes in Nestin-GFP expression. Nestin-GFP expression was enhanced in the glomerulus and peritubular capillaries, although the number of cells expressing GFP after I/R injury did not change. They observed the migration of GFP cells *ex vivo* and concluded that GFP cells in the papilla migrated toward the cortex. However, they did not observe expression of Nestin-GFP in proximal or distal tubules (Patschan et al., 2007). This study shows that Nestin expression is increased in endothelial-like cells following renal injury. The transgenic Nestin-GFP reporter is dependent on nestin regulation and it is proposed that as labeled cells begin to differentiate into epithelial like cells, they lose expression of nestin and therefore GFP expression. Lineage tracing performed with a nestin-Cre and the *R26R-EYFP* reporter would address this lingering question.

Multipotent renal progenitor cells (MRPC) were isolated from adult rat kidneys that were digested with collagenase (Gupta et al., 2006). MRPC were grown on fibronectin-coated plates for 4 to 6 weeks until spindle-shaped cells were formed and then plated at a single cell density to form individual colonies. Undifferentiated MRPC expressed CD90, CD44, vimentin, and Oct4 but did not express SSEA-1, CD-11b, CD45, CD133, CD106, MHC class I and II, CD31, CD56, and Cytokeratin. Undifferentiated

MRPC could be differentiated and induced to express endothelial, epithelial, hepatocyte, and neural markers. Undifferentiated MRPC were used in two *in vivo* models: injection under the renal capsule and injection following I/R injury. When injected under the renal capsule, MRPC formed cyst-like structures and tubular-like structures that no longer expressed Oct-4, a pluripotent stem cell marker, suggesting that these cells were differentiated. Rats were subjected to 30 minutes of ischemia followed by injection of MRPC into the abdominal aorta. MRPC were found in renal tubules at a frequency of 5-10% and lodged in the glomeruli, an adverse effect that the authors attributed to the administration of the exogenous cells not observed in sham treated animals. However, the injected MRPC did not increase renal function over saline injected or sham operated rats. The authors conclude that MRPC are renal stem cells that can differentiate into renal tubules following injury despite the fact that they could not histologically mark endogenous MRPC in the rat (Gupta et al., 2006).

Romagnani and colleagues identified adult parietal epithelial multipotent progenitors (APEMP) located in Bowman's capsule expressing stem cell markers CD24 and CD133. They isolated these cells and injected them into adult severe combined immunodeficiency (SCID) mice with glycerol-rhabdomyolysis induced AKI and found that APEMP incorporated into proximal and distal tubules and increased renal function as seen by decreased BUN levels compared to SCID mice without injection of APEMP cells (Sagrinati et al., 2006). This suggests evidence for an adjacent less injured cell population, although genetic markers have not been identified to label APEMP *in vivo* to question whether or not they can migrate and differentiate into proximal and distal tubules.

Romagnani and colleagues identified a population of human renal multipotent progenitor cells isolated from human embryonic kidneys (aborted fetuses) identified by markers for CD24 and CD133 (CD24+CD133+ REC, renal epithelial cells). *In vitro*, CD24+CD133+ REC were able to differentiate into adipogenic, endothelial, osteogenic, stromal, and epithelial cell types. When subcutaneously injected into SCID mice, CD24+CD133+ REC spontaneously formed vessel like structures that express the endothelial marker von Willebrand factor (vWF). The role of CD24+CD133+ REC in recovery from glycerol-rhabdomyolysis induced AKI was studied by injecting cells into the tail vein of SCID mice at the peak of renal injury. CD24+CD133+ REC incorporated into various renal cell types including, proximal tubule, distal tubule, collecting duct, and endothelial cells. Injection of these cells showed protection against renal injury, as BUN levels were decreased in mice treated with REC at the peak of injury and BUN levels were further reduced with administration of REC and glycerol concurrently (Lazzeri et al., 2007). This study suggests that CD24+CD133+ REC further differentiated in the *in vivo* host setting and migrated into injured tubule segments and support a mechanism that adjacent less injured non-tubular epithelial cell populations repair injured tubules.

Self-renewal of PTCs

The final mechanism for proximal tubule repair is through proliferation of proximal tubule cells that survive the AKI. This model is the most difficult to prove because either a subset of regulatory markers specifically expressed by the proximal tubule progenitor cells and/or genetic markers are needed to show proliferation within the proximal tubule progenitor cell population.

Evidence of tubular progenitor cells was examined in rats by investigating the cell cycle rate. Continuous BrdU labeling for 7 days showed strong nuclear labeling particularly in the S3 segment of proximal tubule cells. The labeling period was extended to 14 days rationalizing that the cell cycle time in various epithelia is 1-3 days and rapidly cycling transiently amplifying (TA) cells should have all gone through the cell cycle during the labeling period and thus should all be BrdU positive. In order to identify slow-cycling cells, they performed immunohistochemistry with the Ki-67 marker to identify Ki-67+BrdU- cells. They expected all proliferating cells to pass though the S-phase during the 14-day long BrdU labeling period and incorporate BrdU. If further labeling with the marker Ki-67 occurred, this would identify a cell that is Ki-67+ BrdU–, and that cell would be a slow cycling cell. They did identify Ki-67+BrdU- slow-cycling cells in the proximal tubule and these cells expressed proximal tubule markers suggesting that they were fully differentiated. The authors conclude that the proximal tubule is regenerated via division of differentiated slow-cycling cells and rapidly proliferating cells (Vogetseder et al., 2007). However, the authors did not question which of these populations of proximal tubules, slow-cycling or rapid-cycling cells, was responsible for regeneration following an injury stimulus.

A hypothesis has been proposed that the self-renewing proximal tubule progenitor cells are differentiated epithelia that can express embryonic stem (ES) cell markers. Testing this hypothesis, Vigneau *et al*. differentiated ES cells into embroid bodies *in vitro*. The cells were *LacZ/T/GFP+* where LacZ was targeted into the ubiquitously expressed *ROSA26* locus (*R26R*) and GFP was cloned into one allele of the mesodermal marker brachyury (T) locus. Thus, all cells will express β-Gal but only cells adopting a

mesodermal fate will express GFP. The *LacZ/T/GFP+* cells were injected into developing newborn mouse kidneys and the *LacZ/T/GFP+* cells integrated into proximal tubules with normal morphology and polarization. Mice that had received these ES derived cells did not form teratomas as adults, a concern when working with ES cells. These cells were further purified as renal proximal tubular progenitor cells and are proposed to be a major step towards clinical regenerative therapies (Vigneau et al., 2007). However, the therapeutic potential of these cells has ethical limitations because they are derived from ES cells Furthermore, based on the experiments performed, observations are limited to pediatric therapy as the authors did not perform experiments injecting these cells into adult mice with/without renal injury or identify brachyury expressing adult proximal tubules.

Lessons from renal stem cells and progenitor cells

The work described in the preceding sections support multiple mechanisms for tubular repair: via differentiation of circulating bone marrow derived stem cells, proliferation and trans-differentiation of adjacent less injured non-epithelial cells, and intrinsic self-renewal progenitor proximal tubule cells. However the significance of each of these mechanisms is hindered by the lack of a genetic and/or transgenic model systems and proper lineage tracing paradigms to document the circulation, migration, and/or proliferation of the stem/progenitor cell population. These studies suggest further investigations of renal progenitor populations require development of genetic/transgenic model systems that would 1) label the progenitor cell population prior to and throughout the period of regeneration, 2) apply a permanent genetic mark by a reporter on the

stem/progenitor cell thus providing lineage tracing, and 3) be independent of cell phenotype thus not limiting expression to a specific cell fate allowing for observation of trans-differentiation. The studies presented in this dissertation will directly address some of these concerns.

The NFAT family of transcription factors

Nuclear factor of activated T cells (NFAT) are named for the T cells in which they were initially identified. The NFAT family of transcription factors contains five proteins that were initially thought to be specific regulators of cytokine gene activation in the immune system because they bound the interleukin-2 (IL-2) promoter in activated T-cells (Crabtree, 1999; Crabtree and Olson, 2002; Hogan et al., 2003; Rao et al., 1997). Alternatively spliced forms have been identified for NFATc1, NFATc2 and NFATc4 and these splicing events allow for variation at the amino (N) and carboxyl (C) termini with the core region being conserved (Fig. 1.3a). All members of the NFAT family contain the NFAT homology region (NHR) and a highly conserved DNA binding domain, the REL homology region (RHR), which is the unifying characteristic of NFAT proteins establishing DNA binding specificity (Fig. 1.3b). The NHR is relatively conserved amongst family members and contains the transactivation domain, several serine residues that are phosphorylated in resting cells, and docking sites for calcineurin and the NFAT kinases, casein kinase 1 (CK1) and glycogen-synthase kinase 3 (GSK3β). The RHR links NFAT proteins to the REL-family of transcription factors also named the nuclear factor-κβ (NF-κβ) family of transcription factors.

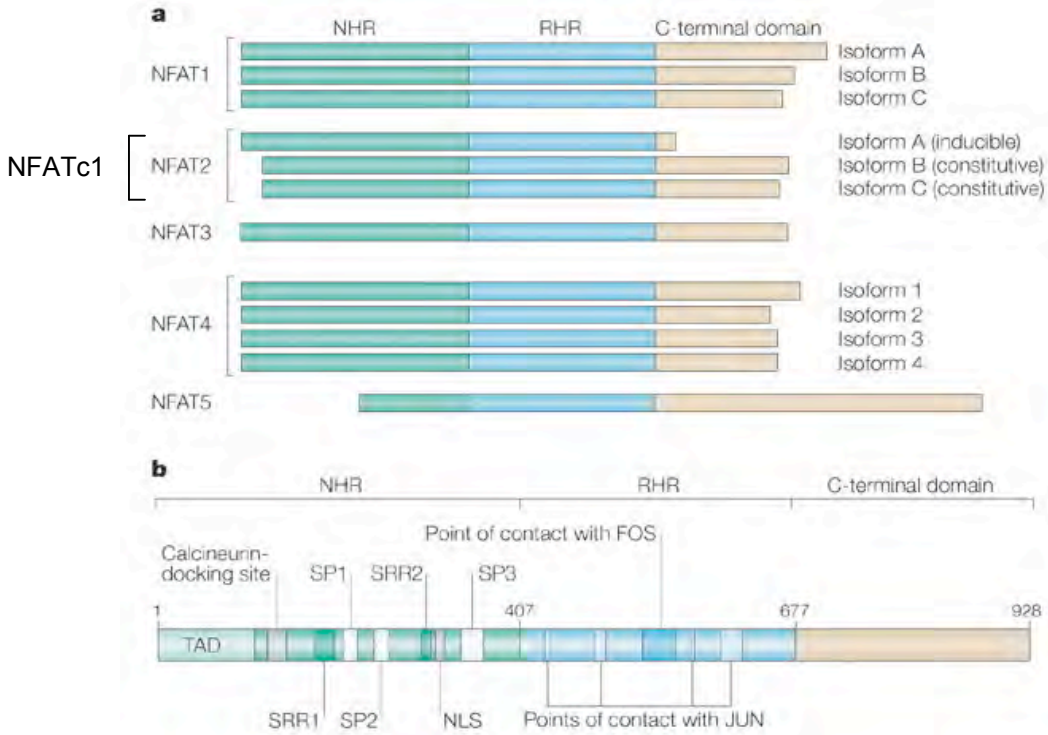

Motif	Amino-acid sequence	Maintenance kinase	Export kinase
SRR1	SPASSGSSASFISD	CK1	CK1
SP2	SPRTSPIMSPRT	ND	GSK3
SP3	SPQRSRSPSPQPSP	ND	ND (GSK3 for NFAT2)

Figure 1.3. ***The NFAT family of transcription factors*****. A.** Isoforms of the NFAT family of transcription factors. **B.** A schematic representation of the transactivation, regulatory, DNA-binding and C-terminal domains of NFATc proteins. This figure from Macian *et al*. (2005) is reprinted with permission from the Nature Publishing Group, license number 1865010844872.

NFAT signaling

The NFATc proteins, NFATc1, NFATc2, NFATc3 and NFATc4, are regulated by calcium signaling (Fig. 1.4) (reviewed in (Crabtree and Olson, 2002; Macian, 2005). Phosphorylated NFATc proteins are localized in the cytoplasm and are transcriptionally inactive. Activation of NFATc proteins requires an influx of intracellular calcium. Receptor signaling, such as the activation of T cell receptor in T cells, activates phospholipase C-γ, which hydrolyzes phosphatidylinositol-4-5-bisphosphate to make inositol-1,4,5-trisphosphate ($InsP_3$). $InsP_3$ triggers the release of calcium from intracellular stores. This intracellular increase in calcium also triggers calcium-release activated calcium channels (CRAC) at the plasma membrane to open thus sustaining the increased intracellular calcium levels.

Calmodulin binds calcium, in turn activating the calmodulin dependent phosphatase calcineurin forming an active phosphatase complex that dephosphorylates NFAT, exposes the nuclear localization sequence, and shuttles NFAT to the nucleus where it binds DNA targets at specific recognition sites. Calcineurin has two functional units; A contains the phosphatase domain and mediates interaction with phosphorylated substrates, and B binds calcium and calmodulin and, when bound to A, causes a conformational change that exposes the phosphatase domain of the A subunit. There are 3 isoforms of calcineurin A, α, β, and γ and 2 isoforms of calcineurin B, 1 and 2. Calcineurin-Aα and -Aβ and calcineurin-B1 are ubiquitous. Calcineurin Aγ and calcineurin-B2 are found primarily in the testes with little expression in the brain (Rev. in (Gooch, 2006; Macian, 2005).

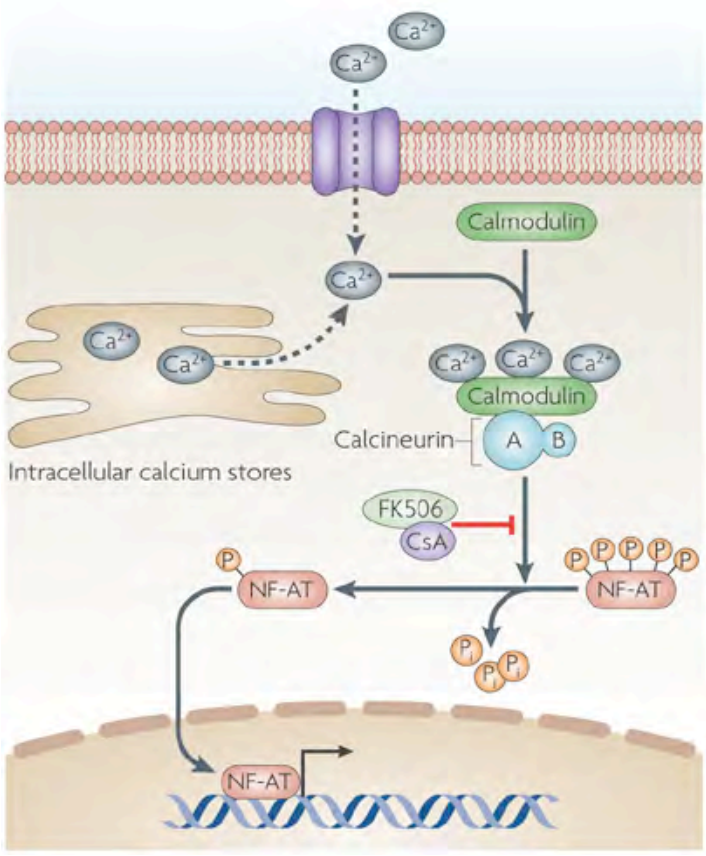

Figure 1.4. ***Regulation of NFAT activation.*** Following an increase in intracellular calcium, the active calcium-calmodulin-calcineurin complex dephosphorylates NFAT allowing nuclear localization and subsequent transcriptional activity. Calcineurin phosphatase activity is inhibited by pharmacologic drugs, Cyclosporine A (CsA) and FK506 (tarcolimus). This figure from Steinbach *et al*. (2007) is reprinted with permission from the Nature Publishing Group, license number 1873810550481.

Nuclear export of NFATc, and thus transcriptional deactivation, is regulated by GSK3β and CK1. These kinases phosphorylate NFATc masking the nuclear localization sequence and facilitating nuclear export (Beals et al., 1997). Thus, transcriptional activity of NFAT is dependent on the phosphorylation state and a balance between nuclear import and export. Phosphorylation sites are found in serine-rich motifs: serine-rich region 1 (SRR1) motif, serine-proline-X-X (SPXX) repeat motif (where X is any amino acid), and serine-proline 2 (SP2) and SP3. Calcineurin dephosphorylates 13 of the 14 conserved phosphorylation sites in NFATc proteins and dephosphorylation exposes the nuclear localization signal allowing nuclear transport of the NFATc proteins and may also control RHR DNA binding affinity.

NFAT5, the tonicity element binding protein (TonEBP), does not contain these binding domains and is regulated by hypertonic/osmotic stresses (Huang and Rubin, 2000; Lopez-Rodriguez et al., 2001; Lopez-Rodriguez et al., 1999; Miyakawa et al., 1999). NFAT5 is expressed by almost every cell as it responds to changes in osmotic stress (Lopez-Rodriguez et al., 2001; Miyakawa et al., 1999). NFAT5 controls the osmotic stress-induced expression of several cytokines, including tumor necrosis factor (TNF) and lymphotoxinβ and NFAT5 null mice have impaired T-cell function under hyperosmotic stress conditions (Go et al., 2004; Lopez-Rodriguez et al., 2001). NFAT5 is the primordial member of the NFAT family and expression of this protein emerged as early as *Drosophila* by evolution from the REL-family of transcription factors and the NFATc proteins are thought to have evolved as mammals evolved and adopted the calcineurin regulatory domains (Stroud et al., 2002).

NFATc1

Three isoforms have been identified for NFATc1 (Fig. 1.5). NFATc1/A is expressed using the P1 promoter and the polyadenylation site pA1. NFATc1/B and NFATc1/C are expressed using either the P1 or P2 promoter, have a truncated N-terminal with transcription starting with exon 2, a long C-terminal, and use the polyadenylation site pA2 (Chuvpilo et al., 1999).

As described above, NFATc is regulated by calcium and calcineurin. However, NFATc1, more specifically the NFATc1α isoform, an N-terminal splice variant of NFATc1, is unique as transcriptional regulation also occurs via an autoregulatory loop requiring an NFAT-dependent inducible promoter. In T cells, when sufficient levels of constitutively expressed NFATc1 are attained, NFATc2 acts with NFATc1 to turn on expression of the inducible isoform of NFATc1 leading to persistent NFATc1 transcriptional activation (Chuvpilo et al., 2002b; Zhou et al., 2002).

Two research groups concurrently but independently created single-exon deletions of NFATc1 with the intentions of studying NFATc1 null T cells. The *Nfatc1*$^{-/-}$ allele created by Ranger *et al.* mutated the RHR and de la Pompa *et al.* mutated the NHR (de la Pompa et al., 1998; Ranger et al., 1998a). In both cases, Nfatc1$^{-/-}$ embryos died in *utero* of cardiac valve and septal defects. These studies identified NFATc1 as the only NFAT member expressed in endocardial cells during valve development. The role of NFATc1 was further delineated in valve formation via endothelial to mesenchymal transition (EnMT). In the endothelial cells, NFATc1 expression was dephosphorylated and nuclear localized suggesting constitutive transcriptional activity. NFATc1 expression was not detected in the mesenchymal cells that fill the cushions of valves of the

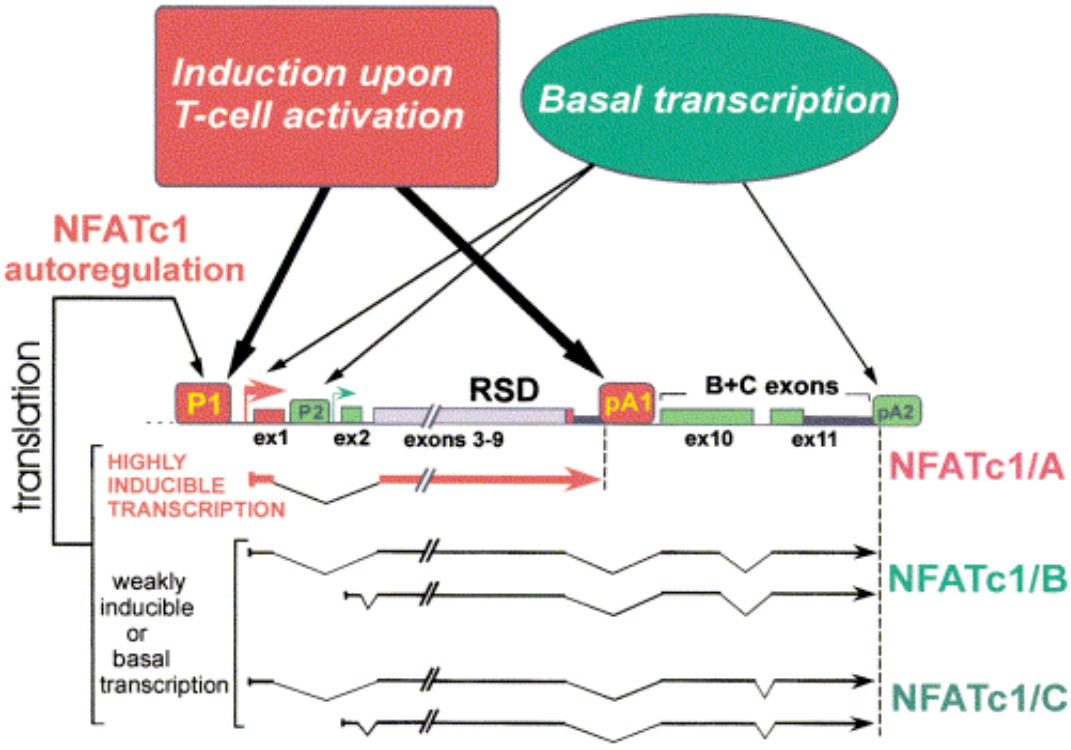

Figure 1.5. ***Model of transcription of NFATc1.*** Nfatc1 transcription is controlled by two promoters, P1 and P2, and two poly A sites, pA1 and pA2. The strong promoter P1 and the weak polyadenylation site pA1 control the highly inducible transcription and autoregulation of the short isoform NFATc1/A. The synthesis of the longer isoforms NFATc1/B and NFATc1/C is controlled by either P1 or P2 and by the strong polyadenylation site pA2. The autoregulation of P1 promoter by NFATc1 or NFATc2 results in an increase of NFATc1/A but not NFATc1/B and/or NFATc1/C synthesis. Adapted from Chuvpilo *et al.* (1999).

developing out-flow track and atrial-ventricular canal (Ranger et al., 1998a). These findings suggested that NFATc1 signaling maintained the specificity of the endocardial cells.

Unpublished work performed within the Baldwin laboratory has investigated the role of NFATc1 during cardiac EnMT, a necessary process for valve formation. *Nfatc1*$^{-/-}$ stem cells (Ranger et al., 1998b) were injected into WT blastocysts creating chimeric embryos. Quantification of the identity of cells within cardiac valves showed that chimeric valves had a decreased number of *Nfatc1*$^{-/-}$ endocardial cells and an increased number of *Nfatc1*$^{-/-}$ mesenchymal cells suggesting that *Nfatc1*$^{-/-}$ cells progressed to EnMT more frequently than WT cells. Therefore it was hypothesized that NFATc1 is at least partially responsible for maintaining the endocardial pro-valvular phenotype during development of the heart and may be responsible for establishing and maintaining the phenotype of other cell populations.

NFATc1 expression in stem cells

While preparing this dissertation, a role for NFATc1 was described in hair follicle stem cells. A microarray screen was performed to identify genes that are differentially expressed in the niche of stem cells of a hair follicle, the bulge, compared to the epidermis (Horsley et al., 2008). NFATc1 expression was identified in the quiescent bulge cells in the hair follicle. NFATc1 was shown to be involved in a mechanism to control stem cell cycling. NFATc1 expression is activated by bone morphogenic protein (BMP) signaling and represses cyclin dependent kinase 4 (CDK4) signaling in order to maintain stem cell quiescence and when the stem cells are activated to grow a hair,

NFATc1 is downregulated, removing the repression of CDK4 and allowing proliferation. Inhibition of calcineurin phosphatase activity using CsA (described below) increased hair growth, a phenotype that was also observed in calcineurin B1 null mice (Mammucari et al., 2005). When Horsley *et al*. inhibited NFATc1/calcineurin signaling by deleting a conditional allele of NFATc1 or treated mice with CsA, the quiescent phase of the stem cell was removed resulting in rapid hair growth (Horsley et al., 2008). This was the first report for NFATc1 in a stem cell population, and shows that NFATc1 plays a functional role in maintaining the rate of proliferation in stem cells.

Inhibition of NFATc signaling

NFATc proteins have an important role in an immune response. Therefore, it is not surprising that inhibition of this family of proteins would have significant clinical implications in the treatment of patients with autoimmune diseases and improving the survival of grafted tissues. Identifying calcineurin inhibitors has been a major focus as a way of preventing NFAT activation. Synthesis of molecules that interfere with the interaction of NFAT and calcineurin has been possible due to structural analysis of this interaction. In the NHR, a conserved sequence PXIXIT (where X is any amino acid) has been identified as the calcineurin binding sequence. A similar peptide, VIVIT (MAGPHPVIVITGPHEE full length sequence), has a high affinity to this sequence and has been used to block NFAT dephosphorylation *in vitro* (Aramburu et al., 1999). In rats, VIVIT has been shown to be a potential therapeutic agent in treating several cardiovascular disorders including angiogenesis, atherosclerosis, cardiac hypertrophy,

and restenosis. Clinical trials with VIVIT are in preclinical stages and no patient data is currently available (Yu et al., 2007a).

CsA and Tacrolimus (FK506) are pharmaceutical drugs that block phosphatase activity of calcineurin (Ho et al., 1996) thereby blocking nuclear translocation and function of all NFATc proteins. However, these drugs have unintended neurotoxic and nephrotoxic side effects (discussed below). The mechanistic cause for these side effects is thought to occur through the inhibition of unintended targets because they block calcineurin activity and not NFAT activity directly (reviewed in (Bechstein, 2000; Olyaei et al., 2001). A number of endogenous calcineurin inhibitors have been identified in recent years. These include the A-kinase anchor protein (AKAP), calcineurin-binding protein 1 (CABIN), and members of the Down's syndrome critical region (DSCR)/modulatory calcineurin-interacting protein (MCIP) family of calcineurin inhibitors, known as calcipressins (Coghlan et al., 1995; Rothermel et al., 2000; Sun et al., 1998).

Acute and chronic CsA nephrotoxicity

CsA has been shown to have dramatically different cell specific effects on endothelial, epithelial, and fibroblast cells (Esposito et al., 2000b), thus the toxic effects of CsA are likely multifactorial. Adverse renal complications have been associated with CsA including nephrotoxicity, interstitial fibrosis, and decreased glomerular filtration rate. CsA has both acute and chronic effects on renal function.

Acute CsA nephrotoxicity causes injury in PTCs characterized by disrupted brush border and disrupted cytoplasm (Esposito et al., 2000b). CsA has an antiproliferative

response in endothelial and epithelial cells and is associated with initiation of apoptosis (Esposito et al., 2000a). Acute effects of CsA can also include glomeruloarteriolar constriction with a hemodynamically mediated decrease in the glomerular filtration rate directly related to endothelial injury (Gauthier and Helderman, 2000; Kahan, 1989). Vacuolization, degeneration and apoptosis of arteriolar smooth muscle cells are also part of the injury spectrum (Blair et al., 1982; Mihatsch et al., 1988).

Chronic CsA nephrotoxicity is characterized by progressive renal dysfunction, concentric arteriolar hyalinization, inflammatory cell influx, glomerular scaring, increased intrarenal immunogenicity, and striped tubular interstitial fibrosis (Burdmann et al., 1994; Li et al., 2004; Myers et al., 1988; Young et al., 1995a; Young et al., 1995b), which has been shown to be initiated by epithelial to mesenchymal transformation (EMT) of the PTCs (Iwano and Neilson, 2004; Iwano et al., 2002). Chronic effects of CsA have been shown to inhibit the renin-angiotensin-aldosterone pathway, activate profibrotic genes, and maintain intrarenal ischemia causing cycles of injury and repair eventually culminating in kidney dysfunction seen in organ transplant recipients (Rezzani, 2004). Although several molecules have been identified that play a role in this disease process, the mechanism by which CsA causes acute and chronic nephrotoxicity is still poorly understood. Alternative immunosuppressive drugs have been identified and clinically tested but are not as effective as CsA. Thus, in the face of the nephrotoxic side effects of CsA, it is a necessary therapeutic drug.

NFAT and calcineurin expression in renal tissue

NFATc proteins have been shown to regulate the development and function of a variety of cells and tissues including, components of the cardiovascular, immune, nervous, skeletal and vascular systems. However, information on the expression and function of NFAT proteins in renal cells received little attention in the literature prior to my dissertation research. I will focus now on publications prior to and during my thesis research documenting expression and function of NFAT and calcineurin in renal tissues.

NFATc1 has been identified in glomerular mesangial cells, *in vitro*, where it regulates COX2 expression following increase in endothelin-1 (Sugimoto et al., 2001) and COX2 expression is suppressed following CsA treatment (Hocherl et al., 2002). However, expression of NFATc1 has not been observed in mesangial cells, *in vivo*, but has been shown to be predominantly expressed in cortical tubules using and anti-NFATc antibody (Gooch et al., 2003; Puri et al., 2004). However, the antibody used to document NFATc expression recognizes all NFATc proteins and does not distinctively label NFATc1.

Li *et al*. analyzed the relationship between the calcium-dependent calcineurin-NFATc pathway and NFAT5 *in vitro* in immortalized murine collecting duct principal cells (mpkCCD). They showed that NFAT5 and NFATc1 bound to NFAT binding sequences on the promoter of aquaporin-2 (AQ-2), a water channel protein specifically expressed in the distal tubule and collecting duct. Expression of AQ-2 increased in response to hypertonicity and increased intracellular calcium concentrations. The increased in AQ-2 is important in maintaining the transfer of water from the apical membrane of the collecting duct epithelial cells to the medullary interstitium when

interstitial osmolality increases. This allows collecting duct epithelial cells to respond to local changes in osmotic stress independent of the normal function of these cells to remove water and electrolytes when concentrating urine (Li et al., 2007b). In addition, rats treated daily with CsA had decreased expression of AQ-1 (a proximal tubule specific aquaporin), decreased expression of hypertonicity protective genes, and increased renal tubular apoptosis (Lim et al., 2004). These findings suggest that the chronic nephrotoxicity of calcineurin inhibitors in renal tubules may result from a defect in calcineurin-mediated regulatory mechanisms.

NFAT5 is the only NFAT null allele documented to have a renal phenotype. NFAT5 knock out mice (*Nfat5*$^{-/-}$) die in the late embryonic or perinatal period, though the etiology of death has not been delineated. Some *Nfat5*$^{-/-}$ mice survive into early adulthood and have disrupted kidney morphology resulting from increased hypertonic stress including irregularly shaped tubules and epithelial cells, incomplete papilla formation, enlarged renal pelvis, and progressive atrophy of the medulla (Lopez-Rodriguez et al., 2004). Cells within the medulla compensate for increasing extracellular hypertonic stress by increasing membrane transporters and enzymes that increase intracellular osmolites including aldose reductase, Na^+/Cl^- coupled betaine/γ-aminobutyric acid transporter, and Na^+ dependent myoinositol transporter, which were down-regulated in the kidneys of *Nfat5*$^{-/-}$ mice. NFAT5 was previously shown to maintain transcription of these enzymes and transporters in order to protect cells from hypertonicity. The severe renal abnormalities observed in *Nfat5*$^{-/-}$ mice that survived into adulthood show demonstrated reduced capacity of the epithelium to endure high osmotic

stress. However, NFAT5 activation, unlike NFATc proteins, is not dependent on calcineurin phosphatase activity, as described above.

A floxed allele of calcineurin-B was deleted using a Pax3-Cre transgene. The Pax3-Cre transgenic mice have strong Cre expression in neural crest cells and is strongly expressed in the metanephric mesenchyme (Li et al., 2000). Calcineurin-B null mice had progressive renal obstruction that lead to renal failure and death (Chang et al., 2004a). Specific knockouts of calcineurin-Aα and calcineurin-Aβ had similar renal developmental defects. However, further inhibition of each knockout by treatment with CsA showed that CsA inhibition was specific to the Calcineurin-Aα isoform and reproduced features of CsA nephrotoxicity *in vivo* and *in vitro*. [Rev. in (Gooch, 2006)] Calcineurin-Aα has been shown to be the main isoform expressed in the proximal tubule (Tumlin et al., 1995). This localization correlates with some of the indices of the nephrotoxic injury and interstitial fibrosis associated with CsA and may indicate disruption of NFATc function in the PTCs.

Proposing a link for CsA, NFATc1 and nephrotoxicity

In lymphocytes, CsA inhibits calcineurin preventing the dephosphorylation and transcriptional activation of NFATc proteins. The benefits of CsA are equally meet by side effects such as nephrotoxicity, thus decreasing the therapeutic potential of CsA. One of the renal cell populations damaged by CsA-associated nephrotoxicity is the proximal tubule, in which expression of calcineurin-Aα, the isoform of calcineurin specifically targeted by CsA has been documented as well as expression of NFATc proteins (Gooch, 2006; Puri et al., 2004). Therefore, one important questions remains: Is this mechanism

of disrupted calcineurin/NFATc signaling and transcriptional inactivation responsible for the immunosuppressive activity of CsA specific to lymphocytes *or* is disrupted calcineurin/NFATc signaling replicated in other cell types causing the observed nephrotoxicity? Identification of the expression and function NFATc proteins in the proximal tubule will be important for understanding the mechanism of CsA as inhibition of calcineurin/NFATc signaling may disrupt transcriptional targets of NFATc proteins and may be partially responsible for the nephrotoxicity.

Aims of dissertation

The main objective of my thesis research was to study the role of NFATc1 in PTCs following an AKI in mice. When I proposed this thesis project, evidence that NFATc1 could play a role in maintaining the epithelial phenotype was based on unpublished experiments performed in the lab using chimeras and observations of NFATc1 expression in the proximal tubule. Chimeric embryos, created by injecting *Nfatc1*$^{-/-}$ cells into WT blastocysts, showed that *Nfatc1*$^{-/-}$ cells were found at a lower frequency in endocardial cells and at a greater frequency in the mesenchyme derived cushion suggesting that NFATc1 played a role in maintaining the endothelial phenotype. We propose that NFATc1 may have a similar mechanism of maintaining the epithelial phenotype of PTCs during the process of kidney injury and repair. We proposed to test this hypothesis in the kidney focusing on PTCs because of the observed NFATc1 expression in the proximal tubule and because CsA has nephrotoxic effects specifically affecting the proximal tubule.

CHAPTER II

NFATC1$^{+/-}$ MICE HAVE DELAYED RECOVERY FROM AKI

Introduction

AKI is an important clinical problem resulting from insults that causes functional and structural change in the kidney. The insult leading to AKI can be induced by a toxic insult to the nephron following acute or chronic exposure to an environmental and/or occupational toxin, from treatment with chemotherapeutic and/or immunosuppressive drugs or from an ischemic injury (Basile, 2007). The AKI is marked by changes in the serum chemistry and urine with increased concentrations of serum creatinine, BUN, and kidney injury molecule 1. Recovery from AKI caused by a nephrotoxic insult requires renal tubule cell regeneration. However, the source of the regenerative cells remains undefined, as described in Chapter I.

Taking into account the nephrotoxicity of calcineurin inhibitors and having documented expression of NFATc1 in the kidney, we hypothesize that NFATc1 plays a role in modifying epithelial regeneration following renal injury. A single dose of $HgCl_2$ was used to induce AKI in the PTCs of WT mice and mice heterozygous for a null mutation in NFATc1 (*Nfatc1*$^{+/-}$). Following $HgCl_2$ injury, the *Nfatc1*$^{+/-}$ mice demonstrated increased apoptosis, sustained injury, and delayed regeneration, compared to the WT mice. In addition, the *Nfatc1*$^{+/-}$ mice have decreased expression of NFATc1 mRNA and protein throughout the time course compared to WT mice. These data suggest a critical role for NFATc1 in regeneration of injured proximal tubule cells. To our knowledge, this

is the first example of a phenotype identified in the *Nfatc1*$^{+/-}$ mouse and suggests a role for NFATc1 in the regeneration of injured PTCs.

Methods

Mice

NFATc1 knock out mice created by excising the Rel DNA binding domain were maintained as a heterozygous colony on a pure Balb/c background and genotyped as previously described (Ranger et al., 1998a). Primer sequences used to genotype mice are listed in Table 2.1. The Institutional Animal Care and Use Committee of Vanderbilt University approved all animal studies.

Experimental Protocol

All experiments were performed on 6-8 week old female littermates. A single subcutaneous dose of 8.14 mg/kg $HgCl_2$ (Fisher Scientific) in normal saline causes significant AKI in mice on the Balb/c background (Miyaji et al., 2002). Wild type and *Nfatc1*$^{+/-}$ mice were administered $HgCl_2$ and sacrificed 24 hours (1 day), 72 hours (3 days), 5 days or 10 days later and compared to mice not administered $HgCl_2$, 0 day. WT mice analyzed at 0, 1, 3, 5, and 10 days n = 8, 8, 10, 8, and 5, respectively. *Nfatc1*$^{+/-}$ mice analyzed at 0, 1, 3, 5, and 10 days n = 8, 7, 8, 11, and 5, respectively. See Figure 2.1 for schematic diagramming the experimental time course and periods of injury and repair.

Table 2.1 Oligonucleotide sequences of primers used to genotype transgenic mice.

Marker gene	Primer sequence	Annealing Temperature (C°)	Cycles	Fragment length (bp)
NFATc1	AGCGTTGGCTACCCGTGATATTGCTGAAGA GTTCCAGGTGACCCAGAAATCAAGGGTCAG CTTCCCTGATGTGTGTTGTGGCAGACAAGAT	68	35	270 WT 350 KO
NFATc1-P2-Cre	CCTGGAAAATGCTTCTGTCCG CAGGGTGTTATAAGCAATCCC	54	81	105
NFATc1-P2-LacZ	GCAGCAGGCAGGGTCACAGAGA ACCCCAGGCTGCAAGGAGGATT	58	80	176
R26R	AAAGTCGCTCTGAGTTGTTAT GCGAAGAGTTTGTCCTCAACC GGAGCGGGAGAAATGGATATG	58	40	500 WT 250 KO
R26R-EYFP	AAAGTCGCTCTGAGTTGTTAT GCGAAGAGTTTGTCCTCAACC GGAGCGGGAGAAATGGATATG	58	40	500 WT 250 KO
Z/EG	CGGCGGCGGTCACGAACTC TTCAAGGACGACGGCAACTACAAGA	62	30	385

Primer sequences for NFATc1 (Ranger et al, 2000), NFATc1-P2-LacZ (Zhou et al., 2005), sglt2-Cre used to genotype NFATc1-P2-Cre (Rubera et al., 2004), and R26R, R26R-YFP (Soriano et al., 1999) have been previously published.

Histology

Dissected kidneys were bisected and fixed in PBS containing 4% paraformaldehyde overnight at 4˚, dehydrated in an ethanol gradient and xylene and embedded in paraffin. 5 μm sections were cut on a microtome. The AKI score for tubular injury was assessed in hematoxylin and eosin stained sections using a semiquantitative scale in which ten high power fields (200X) were blinded and scored by Dr. Gilbert Moeckel for the percentage of tubules with AKI and assigned a score: 0 = normal; 1 = <10%; 2 = 10–25%; 3 = 26–75%; 4 = >75% as previously described (Ramesh and Reeves, 2002). Weigert's Iron Hematoxylin Solution (Sigma) and the Accustain Trichrome Stain (Sigma) were used to stain and score interstitial collagen deposits.

Blood serum creatinine concentration

Blood samples drawn from the orbital vein at each end point were analyzed to determine the serum creatinine concentration as previously described (Dunn et al., 2004).

RNA extraction

A fragment of the outer cortex was snap-frozen and stored at –80˚C. RNA was isolated from 40mg of tissue using the Versagene™ Total RNA Purification Kit and DNA contamination was removed using the Versagene ™DNase Treatment Kit. RNA quality and concentration was determined using capillary electrophoresis (RNA 6000 Nano LabChip Kit and Bioanalyzer, Agilent). Samples within each experimental group were pooled and single-stranded cDNA was prepared from 10 ug of total RNA using oligo dT_{16} primer and a standard protocol (Transcriptor Reverse Transcriptase, Roche).

Quantitative Real-Time PCR (qRT-PCR)

qRT-PCR was performed in a Light Cycler (Roche). All experiments were done using the Light Cycler DNA Master SYBR Green I Kit, 0.5 μM of each primer, 3-5 mM $MgCl_2$, and 200 ng cDNA. DNA primer sets (Table 2.2) were designed using different exons, when possible, to ensure that the product was from mRNA and not genomic DNA. The specificity of the amplified product was evaluated using the melting curve analysis and a no template control reaction included in each run. The housekeeping gene, GAPDH, was used to normalize the data. The relative change in gene expression was determined using the critical threshold (C_t) and the equation Fold Induction = $2^{-\Delta\Delta Ct}$ using the wild type 0 Day sample as the calibrator sample and a two-fold increase or decrease in expression was considered significant (Livak and Schmittgen, 2001).

Isolation of proximal tubules

PTCs were isolated using modification of the methods of Vinay *et al.* (Vinay et al., 1981) and as modified in Xu *et al.* (Xu et al., 2007). Briefly, cortices from $HgCl_2$ treated WT or *Nfatc1*$^{+/-}$ mice were collected and minced in Krebs-Hensleit saline (KHS) buffer containing 115 mM NaCl, 24 mM $NaHCO_3$, 10 mM HEPES, 5 mM glucose, 5 mM KCl, 2 mM NaH_2PO_4, 1.5 mM $MgSO_4$, 1 mM alanine. The KHS was then enriched with 0.15% (wt/vol) collagenase type I, 0.5% (wt/vol) bovine serum albumin, and 0.01% soybean trypsin inhibitor and incubated at 37˚C for 1 hour to digest the cortices. The suspension was strained through a 100-μm sieve, washed and centrifuged at 600 rpm 3 times. The pellets were combined with 47% Percoll (Amersham) solution mixed with 2X

Table 2.2 Oligonucleotides for qRT-PCR analysis of NFATc expression.

Marker gene	Primer sequence	Annealing Temperature (C°)	Product Temperature (C°)	Fragment length(bp)
GAPDH	CACTGGCATGGCCTTCCGTG AGGAAATGAGCTTGACAAAG	55	80	253
Nfatc1	GGTGGCCTCGAACCCTATC TCAGTCTTTGCTTCCATCTCCC	55	86	204
Nfatc2	CATCCGCGTGCCCGTGAAAGTC CTGCCCCTGCCCCTGAGAACCA	64	86	430
Nfatc3	GAGCCCATTATGAAACTGAAGGTA AAGTTAGCTGGCTGGAGATAGAGG	56	83	419
Nfatc4	CTTTGGCCCTGACGTGGACTTCTC TAGCCTGGCCCCACCTCATTGTAG	62	86	413

Sequences are listed in the order antisense, sense-primer.

KHS and centrifuged at 16,300 rpm for 30 minutes at 4˚C. The lowest band enriched with proximal tubule segments was washed with KHS buffer 3 times and utilized for protein isolation.

Protein isolation and Western blotting

Proximal tubule segments were pelleted and lysed in 25 mM HEPES pH 7.4, 150 mM NaCl, 5 mM EDTA, 1% Triton X-100, 10% Glycerol, 50 mM NaF (tyrosine phosphatase inhibitor), 2 mM NaVO4 (phosphatase inhibitor) and 1% protease cocktail inhibitor (Sigma). Concentration was determined by Bradford assay, and 50μg of protein was analyzed per lane. NFATc1 was detected by Western blot analysis (mouse monoclonal, 7A6, BD Pharmingen). Protein loading was confirmed by Western blot analysis for β-actin (mouse monoclonal, Sigma-Aldrich). To quantify the concentration of active NFATc1 protein, the dephosphorylated protein band was quantified by densitometry (EpiChem; UVP Bioimaging System) and the results were normalized as a ratio of NFATc1 to β-actin for each preparation as compared to WT samples at Day 0.

Antibody staining

PCNA and TUNEL staining were performed on paraffin sections using the PCNA Staining Kit (Zymed) and ApopTag ® Apoptosis Detection Kit (Serologicals), respectively. 10 high power fields from each mouse were scored blindly for the number of PTCs that were TUNEL or PCNA positive.

Statistics

All data are presented as mean ± SEM. All scoring was performed blinded. Two-way ANOVA was used to assess the relationship between genotype, and acute kidney score, serum creatinine, apoptosis, proliferation, collagen, or NFATc1 mRNA level at each time point. Differences between groups were assessed with two-way ANOVA and posttest using Bonferroni correction to compare Day 1, 3, 5, and 10 to Day 0 for each genotype and to reduce Type I error. A result was considered significant when $P<0.05$.

Results

$Nfatc1^{+/-}$ mice have sustained AKI

AKI can be induced by the administration of a single dose of $HgCl_2$ (8.14mg/kg) causing a marked injury in the S2 and S3 segments of the proximal tubule in Balb/C mice (Hultman and Enestrom, 1986). While *$Nfatc1^{-/-}$* null mice die *in utero* at E13.5 due to cardiovascular defects (de la Pompa et al., 1998; Ranger et al., 1998a) and thus unavailable for postnatal studies, we induced AKI in WT (Balb/C) (Myers et al.) and heterozygous null *$Nfatc1^{+/-}$* mice (Ranger et al., 1998a) to determine if genetic attenuation of NFATc1 effected the severity of renal injury or the rate of PTC repair. We administered $HgCl_2$ to mice and analyzed indices of AKI 1, 3, 5, and 10 days after injury compared to day 0 mice that were not treated with $HgCl_2$ (Fig. 2.1 Schematic).

Compared to the WT mice (Fig. 2.1A), we did not observe any morphological or histological differences in the *$Nfatc1^{+/-}$* mice before $HgCl_2$ administration (Fig. 2.1F). One day after $HgCl_2$ injury, AKI marked by tubular dilation, cellular necrosis, nuclear dropout

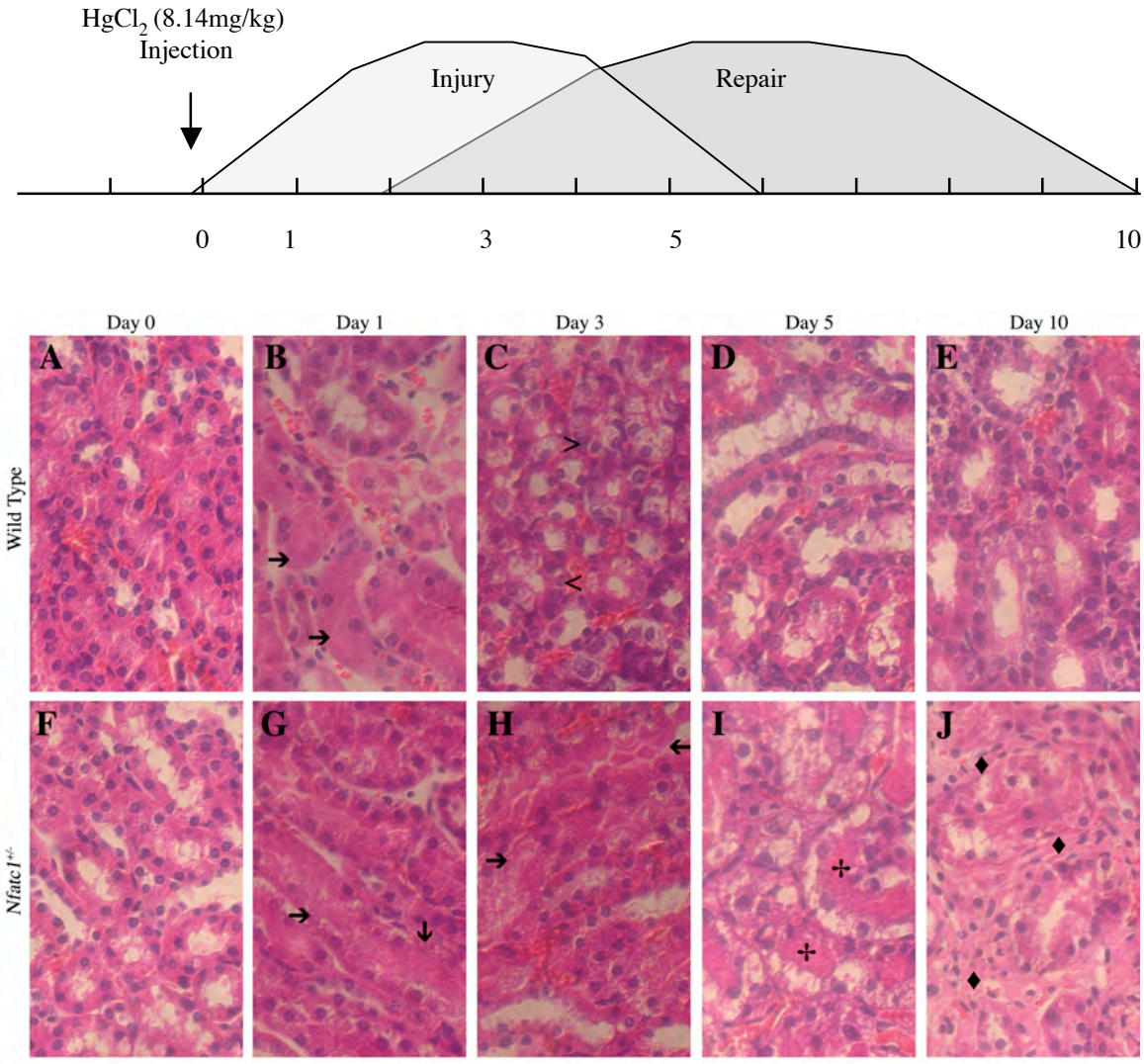

Figure 2.1. ***Genetic attenuation of NFATc1 causes sustained $HgCl_2$ induced AKI.*** Schematic diagramming experimental time course. There was no detectable difference between WT (**A**.) and *Nfatc1*$^{+/-}$ (**F**.) mice before administration of $HgCl_2$. 1 day after a single injection of $HgCl_2$ (3mM), AKI, marked by tubular dilatation, nuclear dropout, and loss of brush borders was observed in both WT (**B**.) and *Nfatc1*$^{+/-}$ mice (**G**.). 3 days after $HgCl_2$ injury, PTCs in WT mice (**C**.) contained large basophilic nuclei in the regenerating proximal tubule segment of the nephron. *Nfatc1*$^{+/-}$ mice (**H.**) showed fewer basophilic nuclei suggesting that the PTC remained in an injured state. 5 days after injury, the WT (**D**.) mice have basophilic nuclei and fewer injured tubules. *Nfatc1*$^{+/-}$ (**I**.) PTCs have basophilic nuclei 5 days after $HgCl_2$ injury. 10 days after injury, the injured PTCs of WT (**E**.) mice have regenerated and have recovered from the injury as indicated by defined cellular membranes and brush borders. *Nfatc1*$^{+/-}$ (**J**.) mice have disorganized PTC nephron segment. A-J Hematoxylin and eosin stained sections. Arrow, nuclear dropout; >, proliferating nuclei; +, tubular dilatation; diamond, disorganization of the PTC nephron segment. 400X Magnification.

and the loss of defined brush border membranes in PTCs was observed in both WT and *Nfatc1*$^{+/-}$ mice (Fig. 2.1B, G). Three days after $HgCl_2$ injury, PTCs in WT mice (Fig. 2.1C) contained large basophilic nuclei characteristic of proliferation. Damaged PTCs of *Nfatc1*$^{+/-}$ mice showed fewer basophilic nuclei, suggesting that the proximal tubules remained in an injured state (Fig. 2.1H). Five days after injury, PTCs of WT mice (Fig. 2.1D) show reorganization of the epithelial tubules while the PTCs of *Nfatc1*$^{+/-}$ mice were disorganized or dilated (Fig. 2.1I). Ten days after injury, the injured PTCs of WT mice regenerated and recovered from the injury as indicated by defined cellular membranes and brush borders (Fig. 2.1E). However, the injury from $HgCl_2$ was sustained at 10 days in the *Nfatc1*$^{+/-}$ as the PTCs nephron segment was not remodeled into a proper tubule and was fibrotic (Fig. 2.1J).

To assess the severity of renal injury, we employed a quantitative evaluation of PTC injury defined by the severity of tubular dilation, cellular necrosis, nuclear dropout and the loss of defined brush border membranes in PTCs (Fig. 2.2) (Ramesh and Reeves, 2002). As indicated by the histology in Figure 1, *Nfatc1*$^{+/-}$ mice had a significant increase in AKI throughout the $HgCl_2$ time course compared to WT mice ($p<0.0001$, Two-way ANOVA). Significant AKI was measured in both WT and *Nfatc1*$^{+/-}$ mice at 1, 3, and 5 days indicating that the initial response to injury was similar in each group ($p<0.001$, Bonferroni posttest). However, the injury from $HgCl_2$ was sustained in *Nfatc1*$^{+/-}$ mice and significantly higher after 10 days in the *Nfatc1*$^{+/-}$ mice ($p<0.001$, Bonferroni posttest) while recovery to pre-injury levels occurred in the WT mice by day 10.

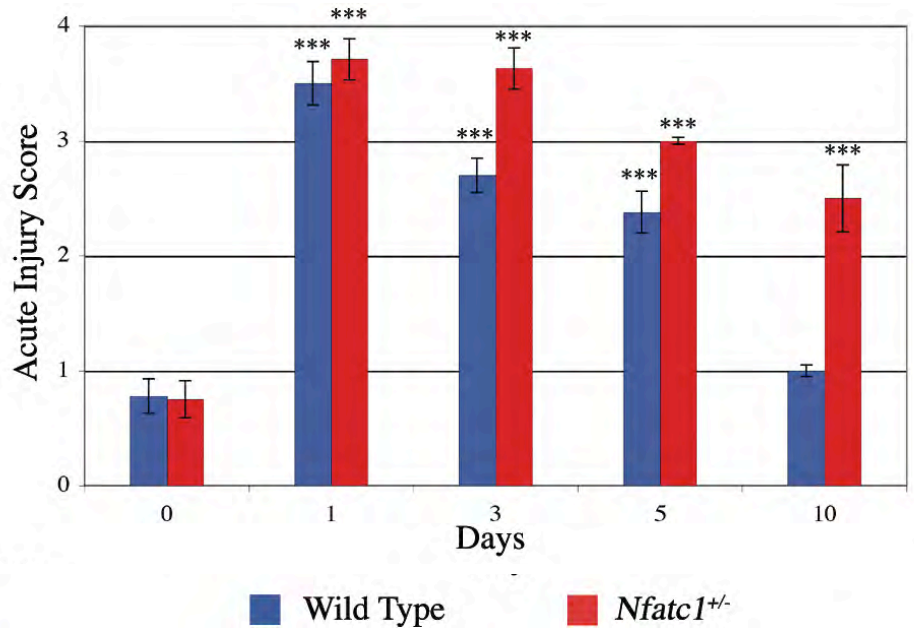

Figure 2.2. ***Nfatc1$^{+/-}$ mice have significant AKI compared to WT.*** Acute injury scores to quantify $HgCl_2$ induced injury. Acute injury scores were significantly higher in the WT and *Nfatc1*$^{+/-}$ mice after $HgCl_2$ ($p<0.0001$ WT vs. *Nfatc1*$^{+/-}$ mice, two-way ANOVA, ***$p<0.001$ Bonferroni post test verses day 0). AKI scoring, 0 = normal; 1 = <10%; 2 = 10–25%; 3 = 26–75%; 4 = >75% PTC injury.

Nfatc1 transcription is decreased in Nfatc1$^{+/-}$ mice

Expression of NFATc1 is strongly induced through autoregulation of the endogenous promoter by transcription factors NFATc1 and NFATc2 (Chuvpilo et al., 2002a; Zhou et al., 2002). We used quantitative qRT-PCR to measure alterations in NFATc1 expression, which was significantly increased in the WT mice throughout the time course ($p<0.0001$, WT vs. *Nfatc1*$^{+/-}$, two-way ANOVA) (Fig. 2.3). Before $HgCl_2$ injury, *Nfatc1*$^{+/-}$ mice and had a 20% reduction in NFATc1 expression compared to WT mice. After $HgCl_2$ injury, Nfatc1 expression was immediately upregulated in the WT mice during the initial phase of the injury, Day1. Nfatc1 expression was significantly increased in WT mice 3 days after $HgCl_2$ injury correlating with the period of regeneration of the PTCs ($p<0.001$, Bonferroni posttest). However, in *Nfatc1*$^{+/-}$ mice, Nfatc1 expression was attenuated and did not significantly increase throughout the time course. Expression of other NFATc transcription factors (Nfatc2, Nfatc3, and Nfatc4) were not significantly altered throughout the $HgCl_2$ time course in WT and *Nfatc1*$^{+/-}$ mice (Fig. 2.4) suggesting that other NFATc transcription factors do not compensate for the decreased Nfatc1 expression in *Nfatc1*$^{+/-}$ mice. This is consistent with previous data showing that when the expression of a single NFATc family member is decreased, other NFATc proteins are unable to compensate (Wilkins et al., 2002).

NFATc1 protein is upregulated in proximal tubules following $HgCl_2$ injury

We were interested in addressing if the amount of NFATc1 protein was specifically decreased in the proximal tubule segment of *Nfatc1*$^{+/-}$ mice compared to WT

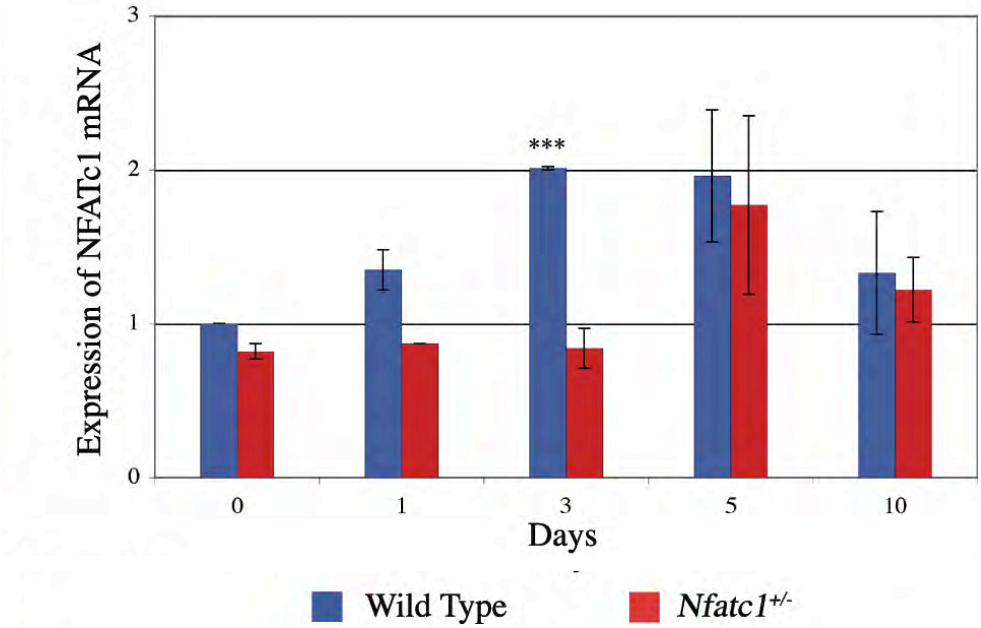

Figure 2.3. ***Nfatc1 expression in the renal cortex is blunted in Nfatc1$^{+/-}$ mice compared to WT mice following $HgCl_2$ injury.*** Following treatment with $HgCl_2$, the WT mice have a significant increase in NFATc1 expression at day 3. ($p<0.0001$ WT vs. *Nfatc1*$^{+/-}$ mice, two-way ANOVA, ***$p<0.001$ Bonferroni post test verses day 0).

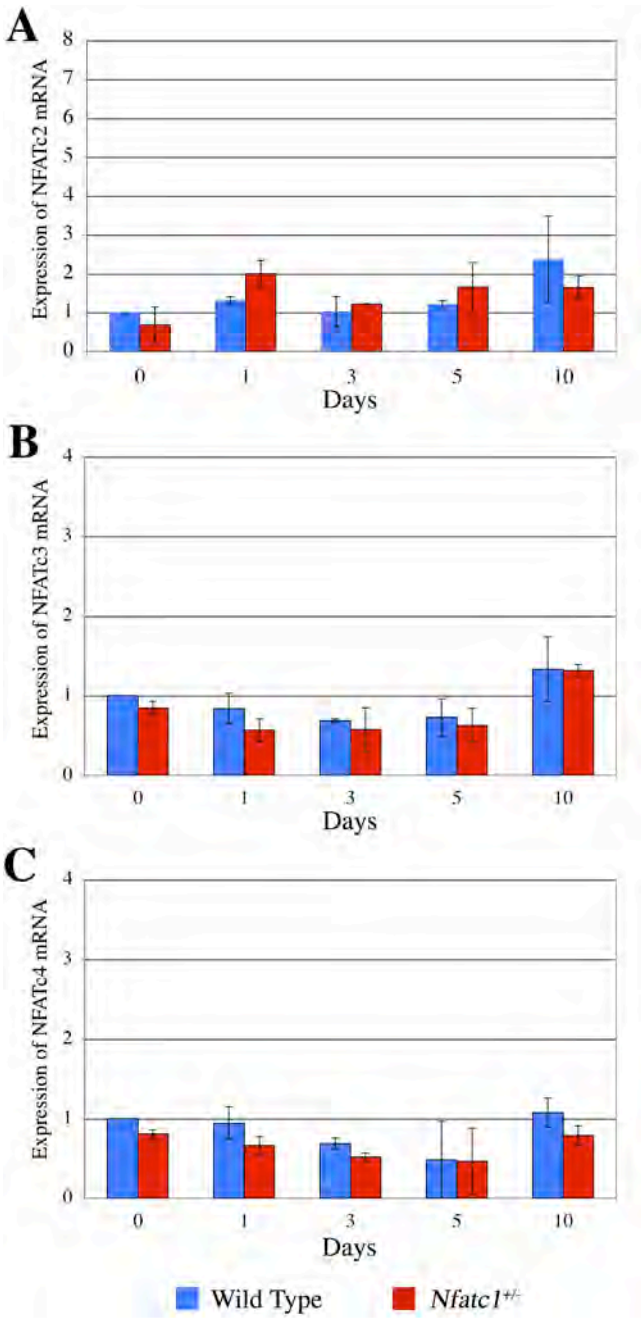

Figure 2.4. ***Transcription of other NFATc family members was not altered following $HgCl_2$ induced AKI.*** The relative expression of **A.** Nfatc2, **B.** Nfatc3, and **C.** Nfatc4, in mRNA samples isolated from whole kidney cortex of adult mice.

mice. Therefore, we repeated the $HgCl_2$ time course in WT and *Nfatc1*$^{+/-}$ mice and isolated proximal tubule fractions from 3 individual mice at each time point. The purity of the isolated proximal tubule fractions was greater than 95%. Protein extracted from the proximal tubule fractions were analyzed by western blot (Fig. 2.5A). We observed both phosphorylated and dephosphorylated NFATc1 as the antibody used recognizes NFATc1 regardless of phosphorylation status as previously published (Hesser et al., 2004; Pan et al., 2007). We quantified the amount of dephosphorylated NFATc1 protein and normalized the expression to the amount of β-actin detected. Throughout the $HgCl_2$ time course, the expression of NFATc1 was significantly increased in the WT mice compared to the *Nfatc1*$^{+/-}$ mice ($p = 0.0014$, two-way ANOVA, Fig. 2.5B). Before $HgCl_2$ injury, *Nfatc1*$^{+/-}$ mice had a 10% reduction in NFATc1 expression compared to WT mice. The dephosphorylated NFATc1 was significantly increased 3.5-fold in the proximal tubules of WT mice 3 days after treatment with $HgCl_2$ ($p<0.001$, Bonferroni posttest) compared to only a 2-fold increase in *Nfatc1*$^{+/-}$ mice 3 days after treatment ($p<0.05$, Bonferroni posttest vs. Day 0).

NFATc1 attenuation results in increased interstitial collagen following AKI.

While interstitial fibrosis is not a characteristic of $HgCl_2$ induced AKI, it is one of the hallmarks of CsA induced nephrotoxicity (Burdmann et al., 1994). Therefore, we questioned whether, genetic attenuation of NFATc1 might produce a fibrotic response in the setting of AKI. After $HgCl_2$ treatment, we observed severe cortical interstitial changes and observed more extensive collagen deposition in the kidneys of *Nfatc1*$^{+/-}$ mice compared to WT mice (Fig. 2.6A-B). We quantified interstitial collagen in the cortex

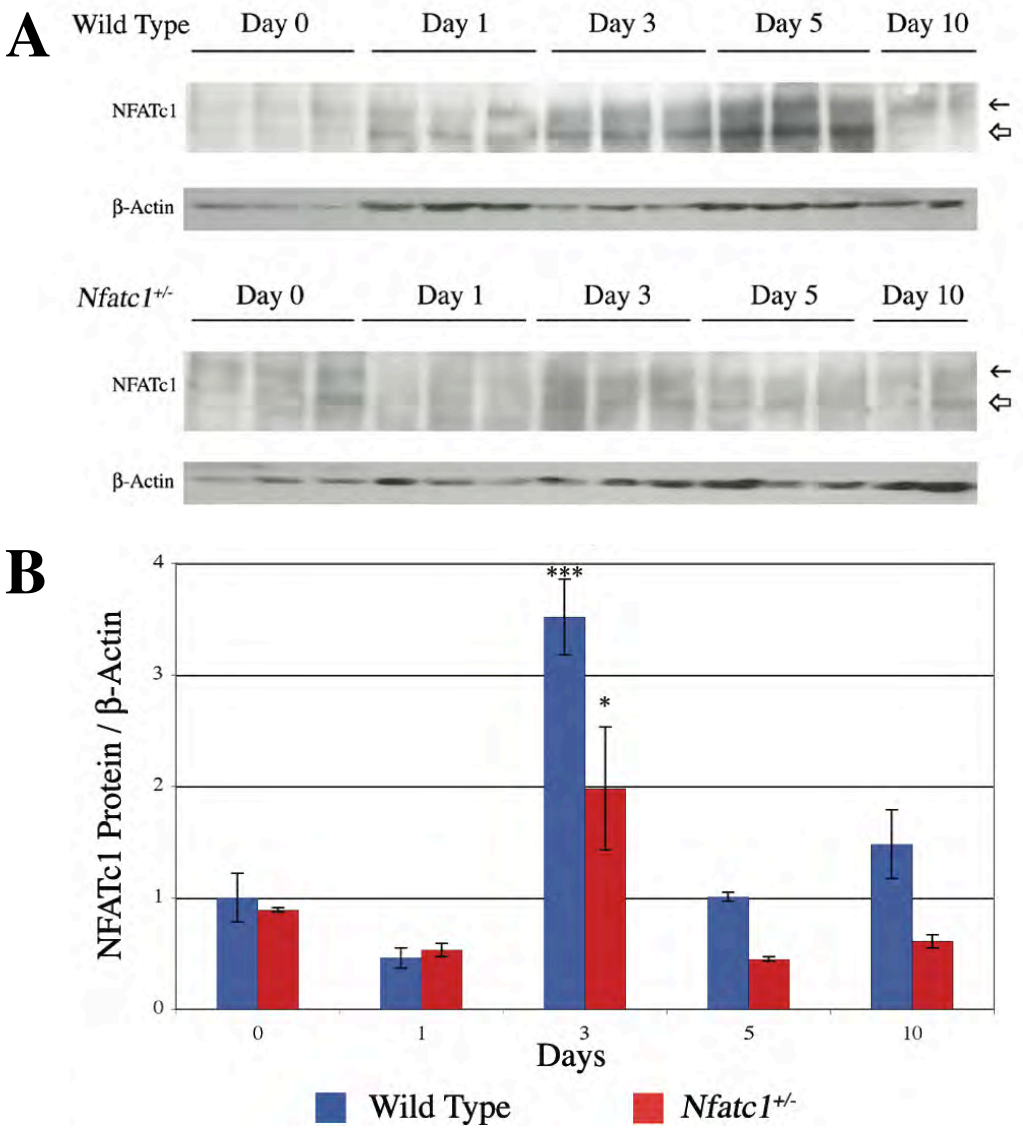

Figure 2.5. ***Dephosphorylated NFATc1 protein is upregulated in proximal tubules following $HgCl_2$ injury.*** **A.** Western blot for NFATc1 and β-actin protein from isolated proximal tubules. Each lane represents proximal tubule cell lysate from different mice. Open and closed arrows indicate the dephosphorylated activated and phosphorylated cytosolic forms of NFATc1, respectively. **B.** Comparison of dephosphorylated NFATc1 expression levels normalized to β-Actin in WT and *Nfatc1*$^{+/-}$ mice. (p=0.0014 WT vs *Nfatc1*$^{+/-}$ mice, two-way ANOVA, ***p<0.001 and * p<0.05 Bonferroni posttest verses day 0).

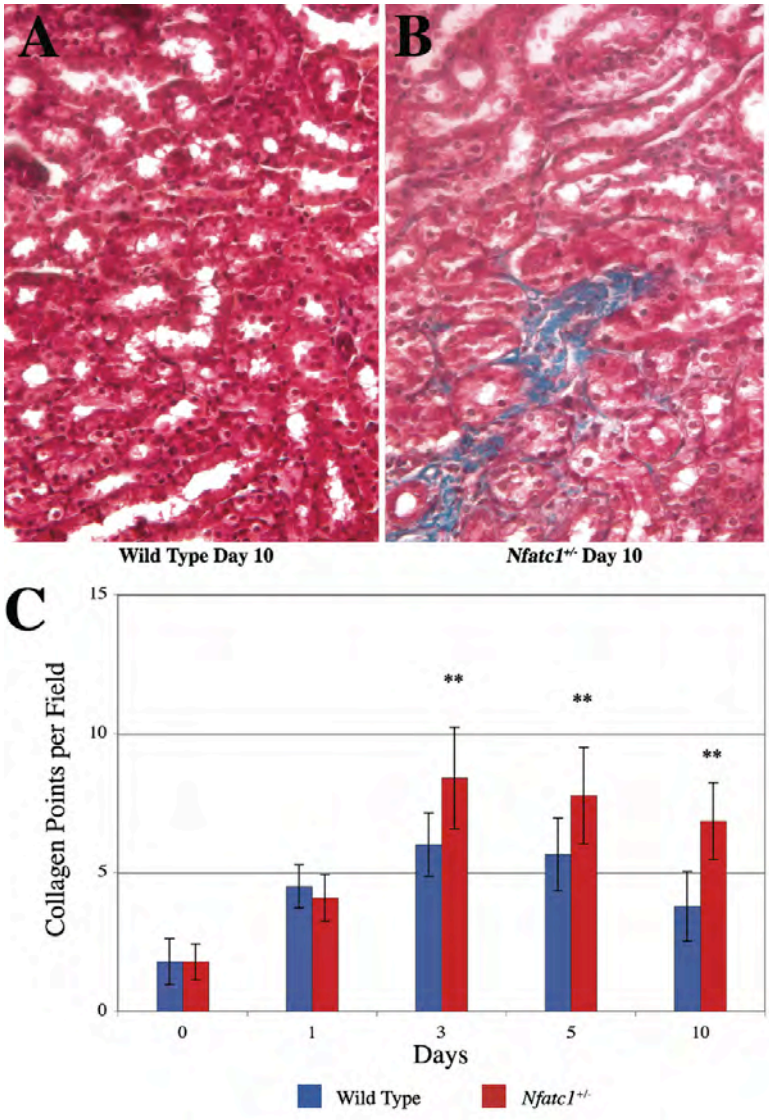

Figure 2.6. ***Following treatment with $HgCl_2$, Nfatc1+/- mice have increased interstitial collagen deposits and disrupted proximal tubule segments.*** Trichrome staining 10 days after $HgCl_2$ injury in WT (**A.**), *Nfatc1*$^{+/-}$ (**B.**). **C.** Quantitative point counting of interstitial collagen deposits. *Nfatc1*$^{+/-}$ mice had significantly higher interstitial collagen 3, 5, and 10 days after $HgCl_2$ injury compared to that seen at Day 0. (**p<0.01 by two-way ANOVA with Bonferroni post test verses day 0)

using a point counting assay (Fig. 2.6C) (Ma et al., 1998). The interstitial collagen of *Nfatc1*$^{+/-}$ mice was not different compared to WT mice before $HgCl_2$ injury. The interstitial collagen in WT mice did not change significantly throughout the time course. However, *Nfatc1*$^{+/-}$ mice had enhanced interstitial collagen deposition 3, 5, and 10 days after injury that was not detected before injury ($p<0.01$, two-way ANOVA, Bonferroni posttest).

Treatment with $HgCl_2$ increased serum creatinine

The nephrotoxicity of $HgCl_2$ was assessed by measuring serum creatinine levels in blood samples collected before treatment with $HgCl_2$ (Day 0), and at each end point 1, 3, 5, and 10 days as described above (Fig. 2.7A). As anticipated, the rise in serum creatinine peaked at day 3 following $HgCl_2$ administration consistent with the onset of maximal renal damage. There was no difference in serum creatinine concentrations of *Nfatc1*$^{+/-}$ mice compared to WT mice before treatment with $HgCl_2$ suggesting that there was no intrinsic renal pathology in the *Nfatc1*$^{+/-}$ mice prior to $HgCl_2$ administration. Similarly, there was no difference in serum creatinine concentrations following $HgCl_2$ documenting equivalent amounts of injury in both groups.

NFATc1 attenuation results in increased PTC apoptosis

CsA nephrotoxicity triggers the apoptotic pathway in mitochondria resulting in CsA-induced tubular cell toxicity, *in vivo* and *in vitro* (Justo et al., 2003). NFATc1 is upregulated in activated T cells and can attenuate CsA induced apoptosis in several cell types (Chuvpilo et al., 2002b; Eckstein et al., 2005; Roy et al., 2006). We hypothesized

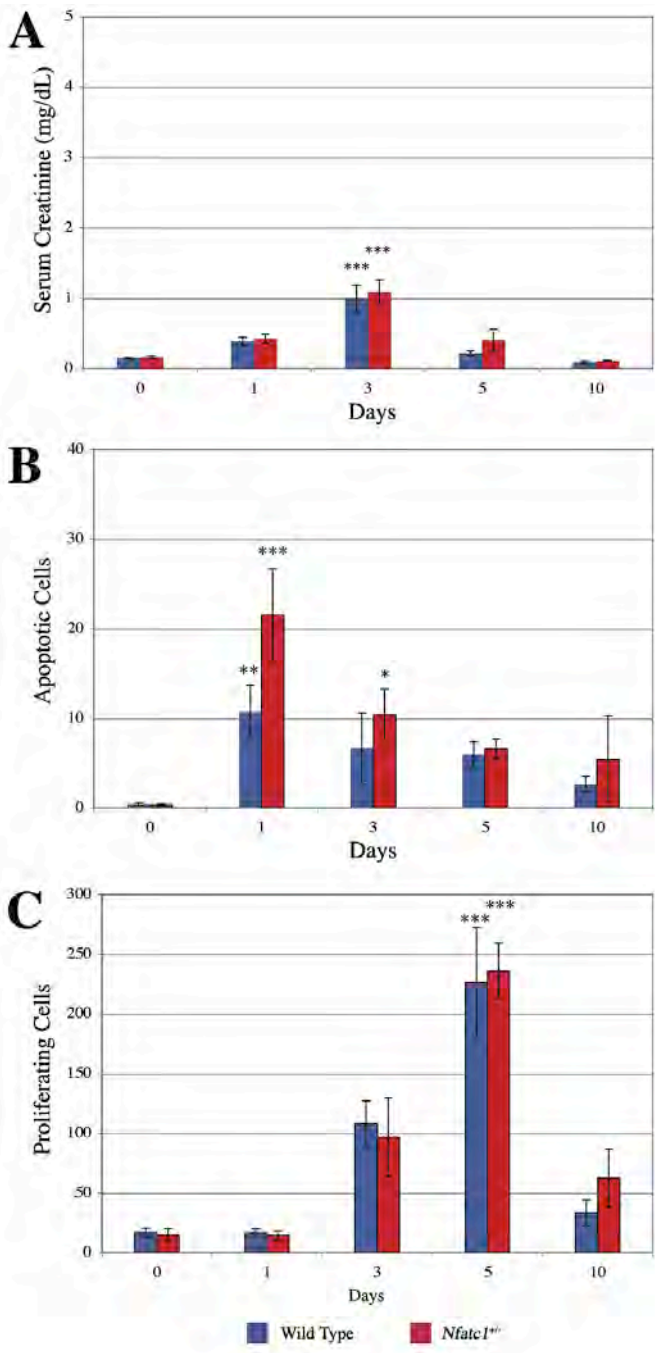

Figure 2.7. ***Attenuation of NFATc1 causes increased serum creatinine concentrations, increased apoptosis and decreased PTC proliferation following $HgCl_2$ injury.*** **A.** Serum creatinine concentrations were elevated in WT and *Nfatc1*$^{+/-}$ mice following $HgCl_2$ induced AKI. (***p<0.001 Bonferroni post test verses day 0) **B.** Apoptosis following $HgCl_2$ induced AKI. 1 and 3 days after $HgCl_2$ injury, there was a significant increase in the number of apoptotic PTCs in *Nfatc1*$^{+/-}$ mice. (p=0.043 WT vs *Nfatc1*$^{+/-}$ mice, two-way ANOVA, ***p<0.001, **p<0.01 and * p<0.05 Bonferroni post test verses day 0) **C.** Proliferation following $HgCl_2$ induced AKI. (***p<0.001 Bonferroni posttest verses day 0)

that NFATc1 protected PTCs from apoptosis associated with AKI. We quantified TUNEL stained PTCs in the cortex (Fig. 2.7B). The number of apoptotic PTCs in *Nfatc1*$^{+/-}$ mice was significantly increased throughout the time course compared to WT mice ($p = 0.043$, two-way ANOVA, Fig. 2.7B). One day after $HgCl_2$ injury, there was a significant increase in the number of apoptotic PTCs in WT and *Nfatc1*$^{+/-}$ mice ($p<0.1$ and $p<0.001$, respectively, Bonferroni posttest). Three days after $HgCl_2$ treatment, the number of apoptotic cells remained significantly increased compared to Day 0 in the *Nfatc1*$^{+/-}$ mice ($p<0.05$, Bonferroni posttest) while the number of apoptotic cells had decreased to pretreatment levels by day 3 in Wt mice. These observations were consistent with our previous observation of increased injury in *Nfatc1*$^{+/-}$ mice and suggest that even a moderate attenuation of NFATc1 results in increased susceptibility to apoptosis in PTCs.

Proliferation is not altered in Nfatc1$^{+/-}$ *mice*

Immunohistochemistry was performed with the proliferation marker proliferating cell nuclear antigen (PCNA) and the PCNA+ PTCs were quantified (Fig. 2.7C). Although the number of surviving PTCs was decreased in the *Nfatc1*$^{+/-}$ mice due to apoptosis, proliferation was not altered in the *Nfatc1*$^{+/-}$ mice compared to WT. Thus, while tubular regeneration was delayed, the PTC population that escapes apoptosis and survives the AKI was able to regenerate the damaged kidney.

Discussion

NFATc1 was upregulated during the period of regeneration following $HgCl_2$ induced AKI and modest attenuation of NFATc1 expression through genetic deletion of one allele, results in increased apoptosis in PTCs, delayed regeneration, and increased fibrosis in response to PTC injury. This is the first direct evidence that NFATc1 has a role in maintaining the proximal tubule segment following AKI and to our knowledge, is the first example to our knowledge of a phenotype identified in the *Nfatc1*$^{+/-}$ mice.

Before $HgCl_2$ administration, we did not observe any morphological or histological differences in the *Nfatc1*$^{+/-}$ mice compared to WT mice. After $HgCl_2$ injury, AKI marked by tubular dilation, cellular necrosis, nuclear dropout and the loss of defined brush border membranes in PTCs was observed in both WT and *Nfatc1*$^{+/-}$ mice. Throughout the time course of injury, the *Nfatc1*$^{+/-}$ mice had sustained AKI as seen by fewer basophilic nuclei characteristic of proliferation suggesting that the proximal tubules remained in an injured state, tubules were disorganized or dilated, and the proximal tubule segment was not remodeled into a proper tubule and was fibrotic. Quantification of the AKI revealed that the *Nfatc1*$^{+/-}$ mice had a significant increase in AKI throughout the time course.

The injury induced by NFATc1 attenuation phenocopies the nephrotoxic injury previously associated with CsA. The toxicity and interstitial fibrosis associated with CsA is dose independent and it is tempting to speculate that these “side effects” are secondary to inhibition of normal NFATc1 activity in the tubule epithelial cells, though this has not been proven. We would speculate that it is critical for the proximal tubule cells to regenerate rapidly as delayed regeneration in *Nfatc1*$^{+/-}$ mice was accompanied by

increased interstitial collagen deposition and fibrosis, although interstitial collagen deposition was not significantly altered compared to WT.

NFATc1 mRNA and protein were significantly decreased in the *Nfatc1*$^{+/-}$ mice during the period of regeneration following $HgCl_2$ mediated AKI. The Real-time PCR analysis of renal cortex mRNA shows that NFATc1 was upregulated in WT mice at Days 3 and 5, during the period of regeneration following $HgCl_2$ induced AKI. Likewise, protein isolated from the proximal tubule segment shows that NFATc1 protein expression was increased in the proximal tubule at Day 3, during the period of regeneration. The decrease in NFATc1 transcription and protein content in the proximal tubule segment of *Nfatc1*$^{+/-}$ mice is due to the genetic deletion of one allele of NFATc1. Decreased NFATc1 expression from allelic deletion of one allele also was likely to be compounded by an attenuation in the autoamplification of NFATc1 from the NFAT dependent inducible promoter, a mechanism of transcriptional regulation that is unique to NFATc1, as described in Chapter I. These data suggest that a modest attenuation of NFATc1 through genetic deletion hinders the course of regeneration.

However, while we observed histochemical evidence of progressed AKI in *Nfatc1*$^{+/-}$ mice, we did not observe a significant decrease in the serum creatinine and proliferation rates in *Nfatc1*$^{+/-}$ mice compared to WT. We would question whether further attenuation of NFATc1 results in a more severe renal injury marked by increased serum creatinine concentrations, sustained AKI, and decreased regeneration of the proximal tubule segment. The *Nfatc1*$^{-/-}$ genotype is lethal and embryos die in utero of cardiovascular phenotypes and are thus unavailable for adult studies. Therefore, we would propose to use CsA to attenuate all NFATc proteins, as described in Chapter III.

CHAPTER III

PHARMACOLOGIC ATTENUATION OF NFATC PROTEINS WITH CSA

Introduction

Nephrotoxicity is the main adverse effect resulting from the therapeutic use of the immunosuppressive drug, CsA. CsA inhibits the phosphatase calcineurin, and prevents the dephosphorylation and transcriptional activation of NFATc proteins. The nephrotoxicity of CsA is pleiotropic affecting endothelial, epithelial, immune, and fibroblast cells (Esposito et al., 2000b). CsA has been shown to be associated with the initiation of apoptosis in endothelial and epithelial cells. Acute CsA nephrotoxicity causes injury in PTCs characterized by disrupted brush borders, mitochondrial injury, vacuolization, and disrupted cytoplasm (Esposito et al., 2000b). Chronic CsA nephrotoxicity has been shown to cause PTCs to undergo EMT causing tubular interstitial fibrosis *in vivo* (Iwano and Neilson, 2004; Iwano et al., 2002). *In vitro* CsA induces PTCs to form mesenchymal cells accompanied by increased TGF-β1 and connective tissue growth factor proteins (McMorrow et al., 2005). Arteriolar smooth muscle cells are also part of the injury spectrum with histology showing apoptosis, or degeneration and vacuolization (Blair et al., 1982; Mihatsch et al., 1988). Although several molecules have been identified that play a role in this disease process, the mechanism by which CsA causes nephrotoxicity is still poorly understood.

Heterozygous Nfatc1 mice demonstrate only a moderate reduction in NFATc1 mRNA and protein as discussed in Chapter II, and homozygous null mice die *in utero*

and are unavailable for post-natal studies. Therefore, we sought to further reduce the amount of NFATc1 in the proximal tubules. WT mice were treated daily with 5mgCsA/kg or10mgCsA/kg prior to and following $HgCl_2$ induced AKI to inhibit calcineurin and, therefore, dephosphorylation and activation of all NFATc proteins. Serum creatinine concentrations were significantly increased in mice treated with 10mgCsA/kg following $HgCl_2$ induced AKI and the severity of injury in 10mgCsA/kg treated mice was associated with high mortality, as no mice survived longer than 5 days after $HgCl_2$ treatment. This work provides additional insights into potential mechanisms of CsA induced nephrotoxicity suggesting that NFATc1 is involved in mediating regeneration of proximal tubules.

Methods

All experiments were performed on inbred 6-8 week old female Balb/c mice. CsA was administered daily until each end point. CsA prepared in polyoxyethylated castor oil and absolute alcohol (Bedford Labs) was diluted in normal saline and administered in the peritoneal cavity at a daily dose of either 5 mg CsA/kg or 10 mg CsA/kg bodyweight. On day 8, animals were treated with a single dose of $HgCl_2$ and compared to animals that did not receive $HgCl_2$ (n=5 mice/group/time point). A vehicle group was treated with polyoxyethylated castor oil and absolute alcohol daily prepared in normal saline (n=3/group/time point).

For all other experimental methods see Chapter II.

Results

Pharmacologic attenuation of all NFATc proteins with CsA results in severe $HgCl_2$ induced AKI

Nfatc1$^{-/-}$ null mice die *in utero* at E13.5 due to cardiovascular defects (de la Pompa et al., 1998; Ranger et al., 1998a) and are thus unavailable for postnatal studies. The *Nfatc1*$^{+/-}$ mice demonstrate only a moderate reduction in NFATc1 mRNA and protein as described in Chapter II. We sought to further reduce the amount of NFATc1 in the proximal tubule. Therefore, we used a pharmacologic approach to attenuate all NFATc proteins by treating WT mice daily with CsA. Mice were treated with vehicle or CsA daily and we administered $HgCl_2$ to mice after one week of CsA conditioning and analyzed indices of AKI 1, 3, 5, and 10 days after injury compared to Day 0 mice that were not treated with $HgCl_2$ (Fig. 3.1A). Our initial analysis used a dose of 10 mg CsA/kg. The severity of the injury from the combined treatment of 10 mg CsA/kg and $HgCl_2$ was evident, as mice did not survive longer than 5 days after $HgCl_2$ injury (Fig. 3.1B). We repeated the experiments with a reduced dose of 5 mg CsA/kg.

CsA was administered daily prior to treatment with $HgCl_2$ in order to precondition the mice. After 7 days of preconditioning, both 5mgCsA/kg (Fig. 3.2A) and 10mgCsA/kg (Fig. 3.2F) treatment groups showed significant vacuolization of the proximal tubule compared to controls confirming toxicity of CsA in both treatment groups. One day after $HgCl_2$ injury, the histology for WT mice treated with low or high dose of CsA was not significantly different. These findings indicate that the initial response to injury was similar in each group (Fig. 3.2B,G,K). Three days after injury, the histology of damaged PTCs in the 5mgCsA group and 10mgCsA group showed fewer regenerating basophilic

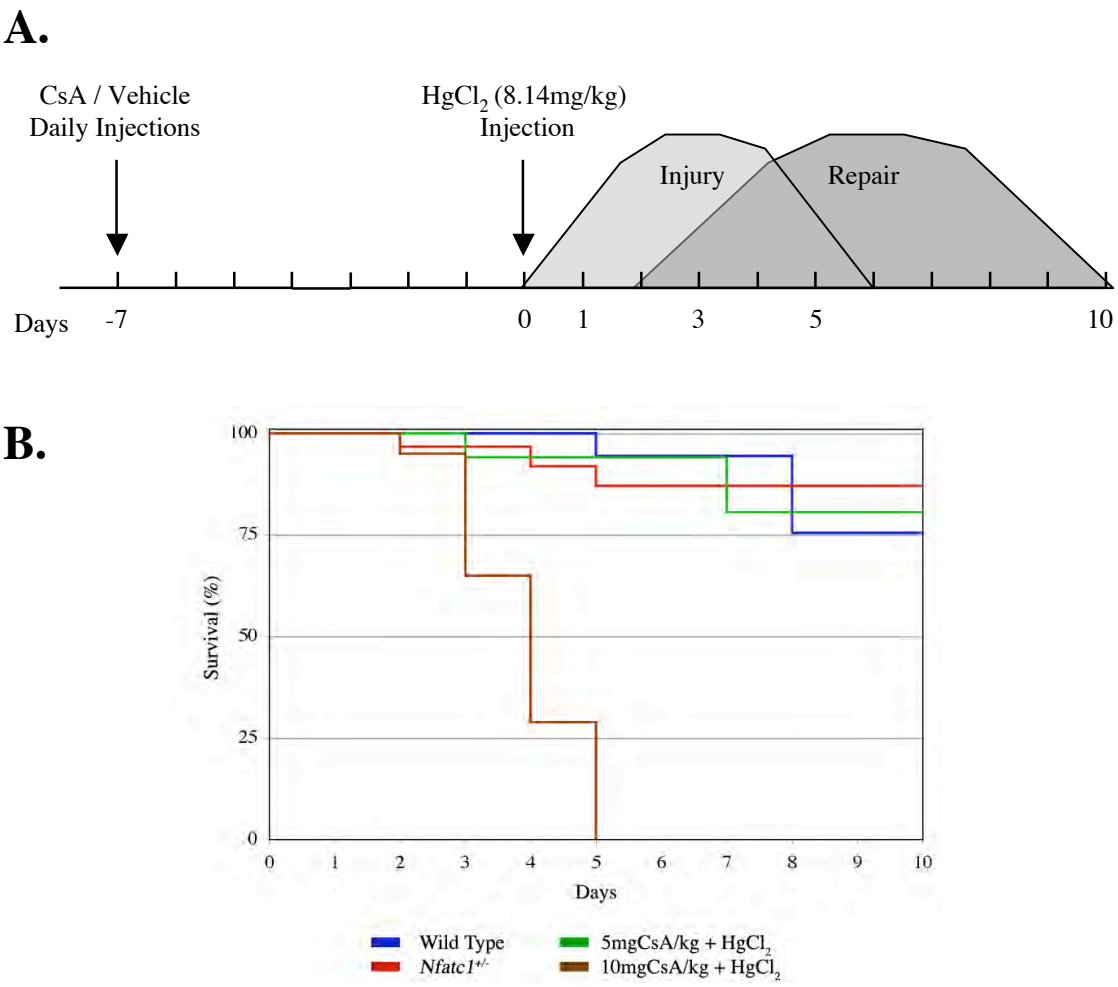

Figure 3.1. ***Experimental design and survival of mice treated with CsA and $HgCl_2$.*** **A.** Schematic diagramming experimental time course. **B.** Kaplan-Meier survival curve of WT (n = 40), NFATc1$^{+/-}$ (n = 42), 5mgCsA/kg treated mice (n = 27), and 10mgCsA treated mice (n = 30) following treatment with $HgCl_2$. No deaths occurred in mice treated with daily with vehicle, 5mgCsA/kg and 10mgCsA/kg without $HgCl_2$ during the time course (data not shown).

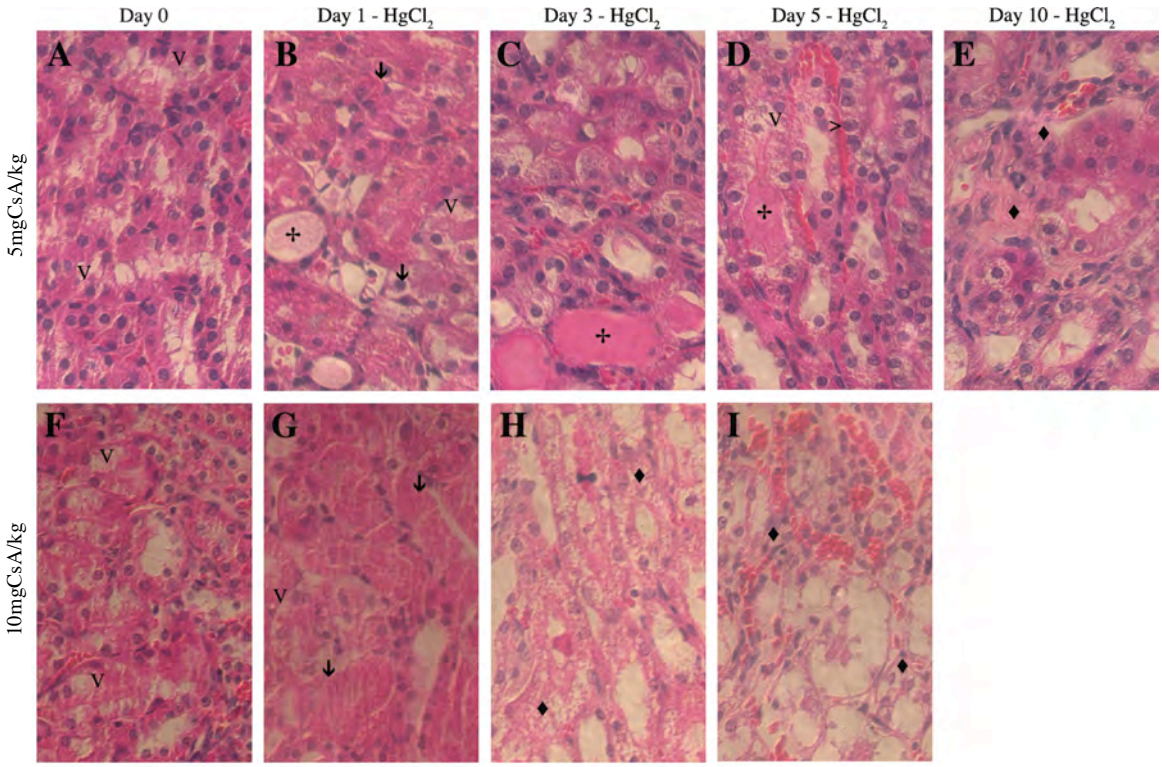

Figure 3.2. ***Pharmacologic attenuation of NFATc1 with either low or high doses of CsA (5mgCsA/kg and 10mgCsA/kg, respectively) causes sustained AKI in mice following treatment with $HgCl_2$.*** After daily conditioning with CsA, mice treated with 5mgCsA/kg (**A**.) and 10mgCsA/kg (**F**.) showed vacuolization of the PTCs not observed in the vehicle treated control (data not shown). 1 day after $HgCl_2$ injury, acute kidney injury is observed in 5mgCsA (**B**.) and 10mgCsA (**G**.) treated mice. 3 days after $HgCl_2$ injury, the histology of damaged PTCs of 5mgCsA (**C**.) and 10mgCsA (**H**.) treated mice showed no basophilic nuclei suggesting that the proximal tubules remained in an injured state. 5 days after injury, the PTCs of 5mgCsA (**D**.) treated mice have basophilic nuclei, a sign of proliferation. **I.** 5 days after injury, kidneys of the 10mgCsA treated mice show tubule casts and severe nephrotoxicity. 10 days after injury, the PTCs of the 5mgCsA (**E**.) treated mice are severely disorganized. A-I; Hematoxylin and eosin stained sections. (V, vacuolization; arrow, nuclear dropout and loss of brush borders; >, proliferating nuclei; +, tubular dilatation; diamond, disorganization of the PTC nephron segment.) 400X Magnification.

nuclei than WT and vehicle treated controls suggesting persistent injury in the proximal tubules (Fig. 3.2C, H). Five days following $HgCl_2$ administration, PTCs in the 5mgCsA group showed evidence of regeneration (Fig. 3.2D). However, 5 days after injury, all PTCs of 10mgCsA mice are injured, without evidence of regeneration (Fig. 3.2I). In the 5mgCsA Group, the injury from $HgCl_2$ was sustained at 10 days compared to WT mice and was accompanied by disorganization of the PTCs nephron segment (Fig. 3.2E).

As indicated by the histology in Figure 3.2, 5mgCsA/kg and 10mgCsA/kg treated mice had a pronounced AKI throughout the $HgCl_2$ time course compared to WT mice ($p=0.0063$ WT vs. 5mgCsA/kg and $p<0.0001$ WT vs. 10mgCsA/kg compared by two-way ANOVA, Fig. 3.3). After $HgCl_2$ injury, significant AKI was measured in both 5mgCsA/kg and 10mgCsA/kg treated mice indicating that the initial response to injury was similar in each group at days 1, 3, and 5 ($p<0.001$, Bonferroni posttest). The 5mgCsA/kg treated mice had sustained AKI at day 10 similar to the *Nfatc1*$^{+/-}$ mice ($p<0.001$, Bonferroni posttest).

Nfatc1 transcription is repressed in CsA treated mice

Because NFATc1 expression can be modulated via an autoregulation at the transcriptional level, we used qRT-PCR to measure the expression of Nfatc1 in the kidney following daily treatments with CsA. Compared to WT mice, the expression of Nfatc1 was significantly reduced in mice treated with 5mgCsA/kg and 10mgCsA/kg ($p=0.0045$ WT vs. 5mgCsA/kg and $p<0.0001$ WT vs. 10mgCsA/kg compared by two-way ANOVA). The 5mgCsA group had a 20% reduction in Nfatc1 expression, similar to *Nfatc1*$^{+/-}$ mice and the 10mgCsA group had a 40% reduction in Nfatc1 expression before

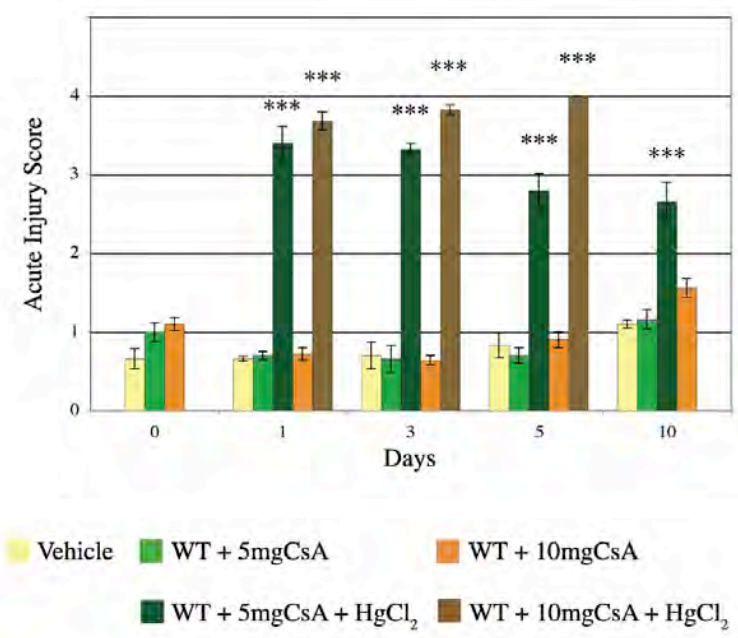

Figure 3.3. ***Quantification of $HgCl_2$ induced acute kidney injury.*** Acute kidney injury scores are significantly increased in mice treated with CsA following $HgCl_2$ induced injury ($p=0.0063$ WT vs. 5mgCsA/kg treated mice and $p<0.0001$ WT vs 10mgCsA/kg treated mice, two-way ANOVA; ***$p<0.001$ Bonferroni posttest compared to Day 0). Acute kidney injury score 0 = normal; 1 = <10%; 2 = 10–25%; 3 = 26–75%; 4 = >75% of PTC are injured showing loss of brush borders, dilated tubules, or nuclear dropout.

$HgCl_2$ injury compared to WT mice (Fig. 3.4). Nfatc1 expression remained suppressed and did not significantly increase in 5mgCsA/kg treated mice until 5 days after $HgCl_2$ injury, similar to the *Nfatc1*$^{+/-}$ mice ($p<0.001$, Bonferroni posttest vs. day 0).

Treatment with the high dose of CsA showed that Nfatc1 expression remained significantly reduced after $HgCl_2$ injury in 10mgCsA group. Nfatc1 expression was not significantly altered in groups of mice treated with vehicle, 5mgCsA/kg or 10mgCsA/kg without $HgCl_2$ throughout the duration of the time course. The transcription of other NFATc proteins Nfatc2, Nfatc3, and Nfatc4, was analyzed by qRT-PCR (Fig. 3.5A-C). The expression of Nfatc3 and Nfatc4 were decreased in response to CsA treatment and there was not a significant change in their expression throughout the $HgCl_2$ time course. However, the expression Nfatc2 was significantly increased at day 5 in 5mgCsA/kg treated compared to expression at day 0 ($p<0.001$, Bonferroni posttest compared to 5mgCsA/kg at day 0) and the transcription of Nfatc2 in 5mgCsA/kg treated mice was significantly increased compared to WT ($p=0.0117$, WT vs. 5mgCsA/kg compared by two-way ANOVA).

Combined treatment with $HgCl_2$ and CsA causes severe mitochondrial injury

CsA has been shown to cause tubular cell apoptosis resulting from mitochondrial injury and treatment with $HgCl_2$ has been shown to form giant mitochondria or mitochondria with flocculent matrix deposits within tubular epithelia (Justo et al., 2003; McDowell et al., 1976). We therefore performed ultrastructure analysis on mice treated with both 5mgCsA and $HgCl_2$ and examined the mitochondria of tubular epithelial cells (Fig. 3.6). One day after treatment with $HgCl_2$, the mitochondria appeared normal and do

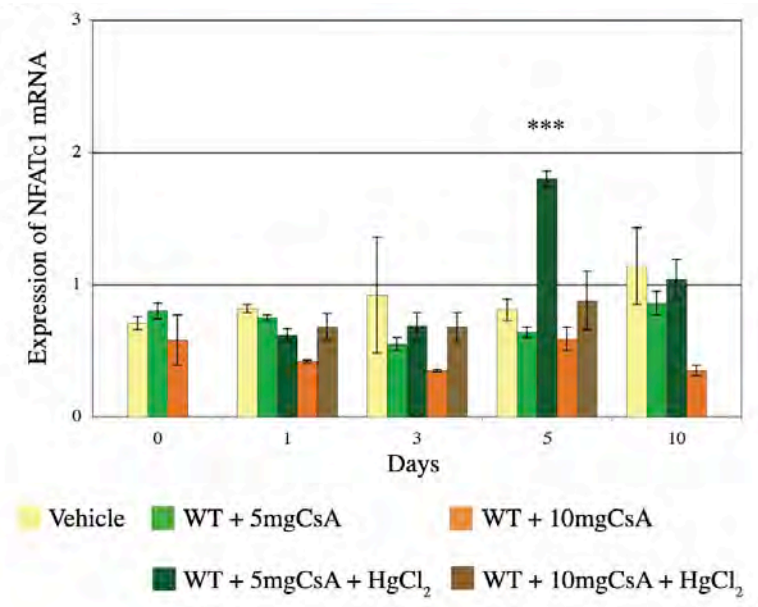

Figure 3.4. ***Nfatc1 transcription is decreased in the cortex following $HgCl_2$ injury.*** The relative expression of Nfatc1 in RNA isolated from the cortex shows blunted NFATc1 expression in CsA treated mice ($p=0.0045$ WT vs. 5mgCsA/kg treated mice and $p<0.0001$ WT vs. 10mgCsA/kg treated mice, two-way ANOVA; *** $p<0.001$ Bonferroni posttest compared to Day 0)

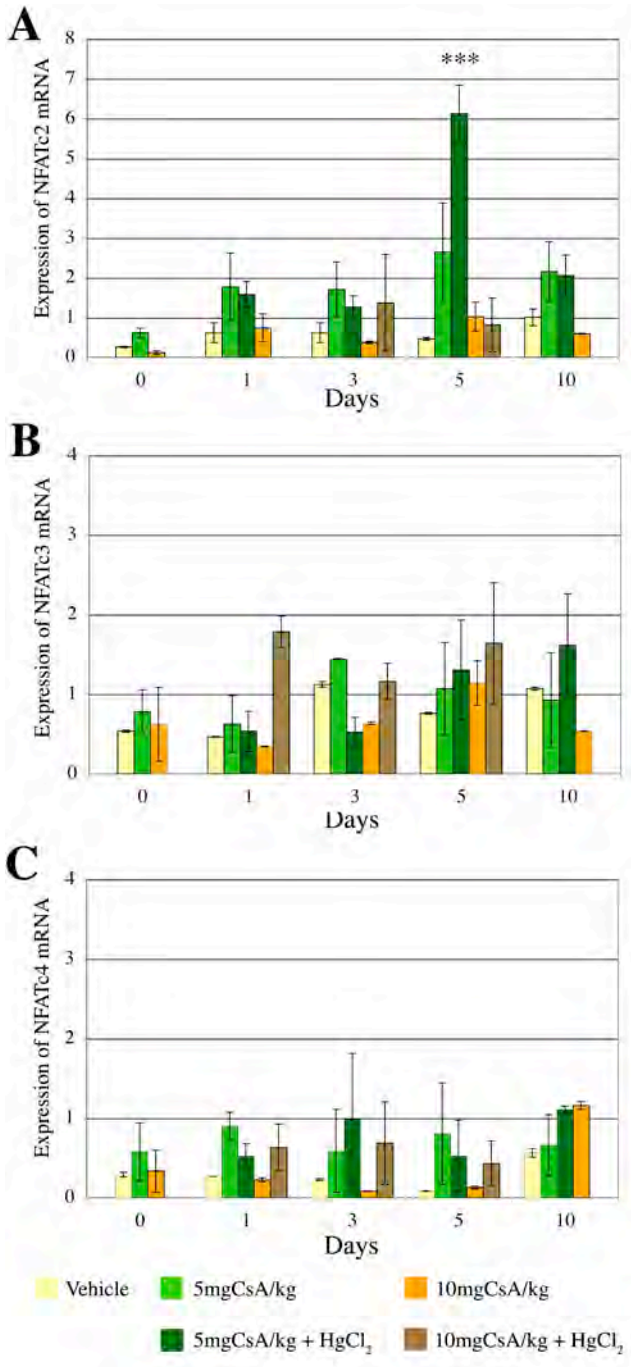

Figure 3.5. ***Transcription of other NFATc family members was not altered following $HgCl_2$ induced acute kidney injury.*** The relative expression of **A.** Nfatc2, **B.** Nfatc3, and **C.** Nfatc4, in mRNA samples isolated from whole kidney cortex of adult mice.

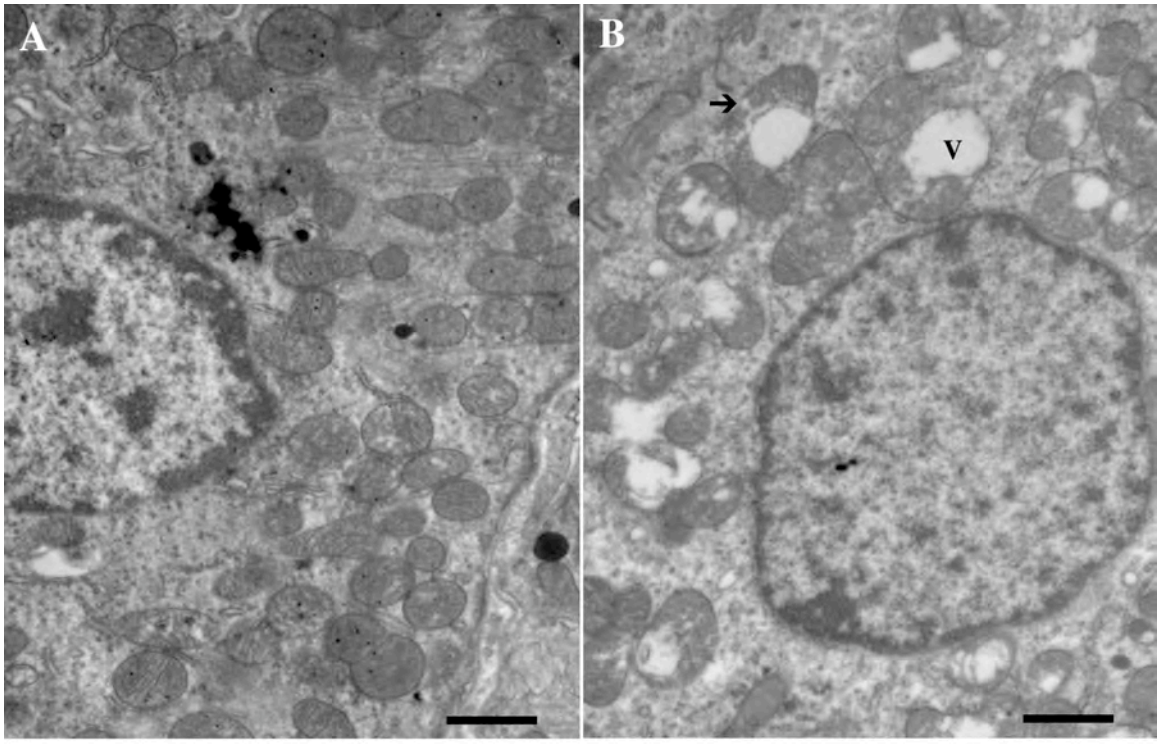

Figure 3.6. ***Prolonged exposure to 5mgCsA/kg after $HgCl_2$ induced AKI causes severe mitochondrial injury characterized by vacuolization and disrupted cristae.*** **A**. 1 after $HgCl_2$ injury. **B**. 10 days after $HgCl_2$ injury. Bar represents 1μm. (V, vacuole; arrow, disrupted cristae)

not have the flocculent matrix deposits as previously reported in rats 24 hours after $HgCl_2$ injury (McDowell et al., 1976). However, 10 days after treatment with $HgCl_2$, the mitochondria contained large vacuoles and showed disorganized cristae. The combined treatment of CsA and exposure to $HgCl_2$ causes a severe injury that is greater than exposure to CsA or $HgCl_2$ alone.

NFATc1 attenuation results in increased interstitial collagen following AKI.

Interstitial fibrosis is one of the hallmarks of CsA induced nephrotoxicity. After $HgCl_2$ treatment, we observed severe cortical interstitial changes and observed more extensive collagen deposition in the kidneys of mice treated with low and high doses of CsA compared to WT mice (Fig. 3.7A,B), as described in Chapter II. We quantified interstitial collagen in the cortex using a point counting assay (Fig. 3.7C) (Ma et al., 1998). There was no significant difference in interstitial collagen between the groups of mice treated with vehicle, 5mgCsA/kg, or 10mgCsA/kg before treatment with $HgCl_2$. Following $HgCl_2$ injury, mice treated with 10mgCsA/kg had significantly higher interstitial collagen compared to WT mice ($p=0.0013$ WT vs. 10mgCsA/kg compared by two-way ANOVA). Mice treated with vehicle, 5mgCsA/kg, or 10mgCsA/kg without $HgCl_2$ did not have a significant change in interstitial collagen deposits throughout the time course.

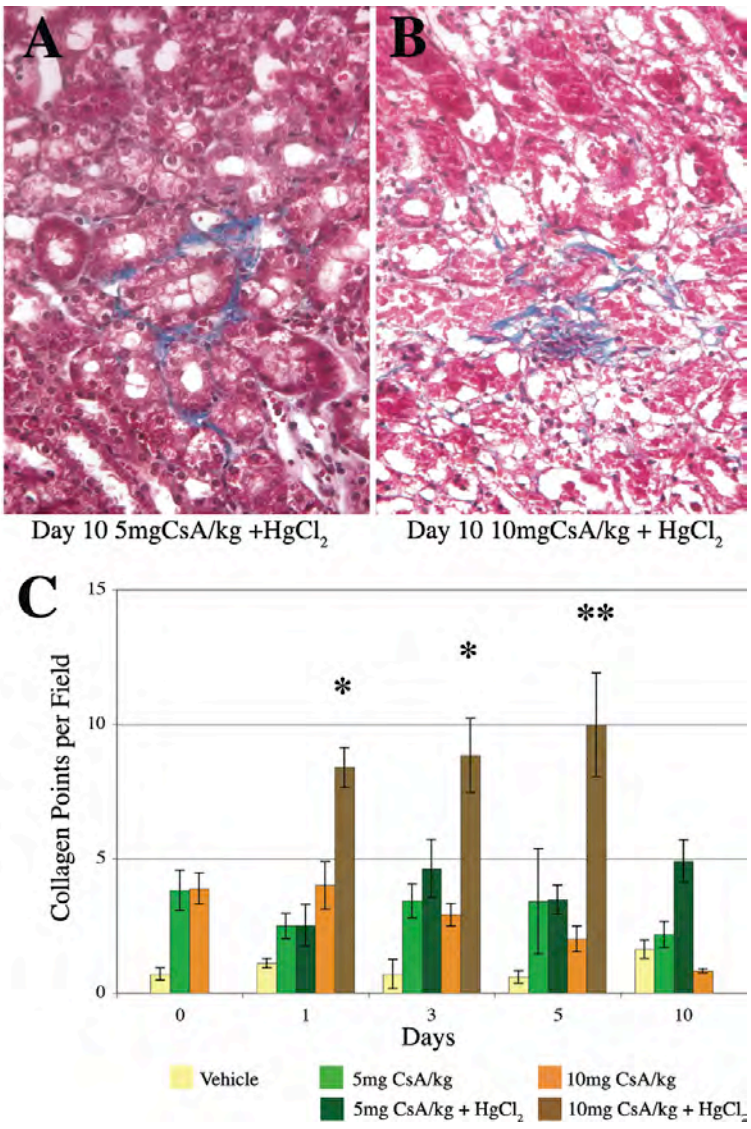

Figure 3.7. ***Following treatment with $HgCl_2$, mice with attenuated NFATc expression have increased interstitial collagen deposits and disrupted proximal tubule segments.*** Trichrome staining 10 days after $HgCl_2$ injury in 5mgCsA/kg treated mice (**A.**) and 10mgCsA/kg treated mice (**B.**). **C.** Quantitative point counting of interstitial collagen deposits show that 10mgCsA/kg treated mice have significantly increased interstitial collagen ($p=0.0013$ WT vs. 10mgCsA/kg treated mice, two-way ANOVA; *$p<0.05$, **$p<0.01$ by two-way ANOVA with Bonferroni posttest verses day 0.

Pharmacologic attenuation of all NFATc proteins with CsA results in increased serum creatinine concentrations

The nephrotoxicity of $HgCl_2$ and CsA was assessed by measuring serum creatinine levels in blood samples collected before daily treatment with CsA, before treatment with $HgCl_2$ (Day 0), and at 1, 3, 5, and 10 days as described above (Fig. 3.8A). Daily treatment with either low or high dose of CsA for one week did not increase serum creatinine concentrations over starting concentrations (data not shown). Serum creatinine concentrations were significantly increased in mice treated with 10mgCsA/kg following $HgCl_2$ induced AKI (Fig. 3.8A, $p<0.0001$ comparing WT vs. 10mgCsA/kg treated mice by two-way ANOVA). The severity of injury in the 10mgCsA/kg treated mice was associated with high mortality and mice did not survive longer than 5 days after $HgCl_2$ treatment. The high serum creatinine concentrations recorded for mice treated with both 10mgCsA/kg and $HgCl_2$ suggest that the high mortality rate within this group was associated with chronic renal failure. Notably, mice treated with vehicle, 5mgCsA/kg, or 10mgCsA/kg and were not exposed to $HgCl_2$ showed no significant change in serum creatinine concentrations throughout the time course.

NFATc1 attenuation results in increased PTC apoptosis

The mechanism of CsA nephrotoxicity has been shown to trigger the apoptotic pathway in mitochondria resulting in CsA-induced tubular cell toxicity, *in vivo* and *in vitro* (Justo et al., 2003). We hypothesized that NFATc1 protected epithelia from apoptosis associated with AKI as NFATc1 has been shown to be upregulated in T cells in order to prevent CsA induced apoptosis (Chuvpilo et al., 2002b; Eckstein et al., 2005; Roy et al., 2006). We therefore quantified TUNEL stained PTCS in the cortex. Mice

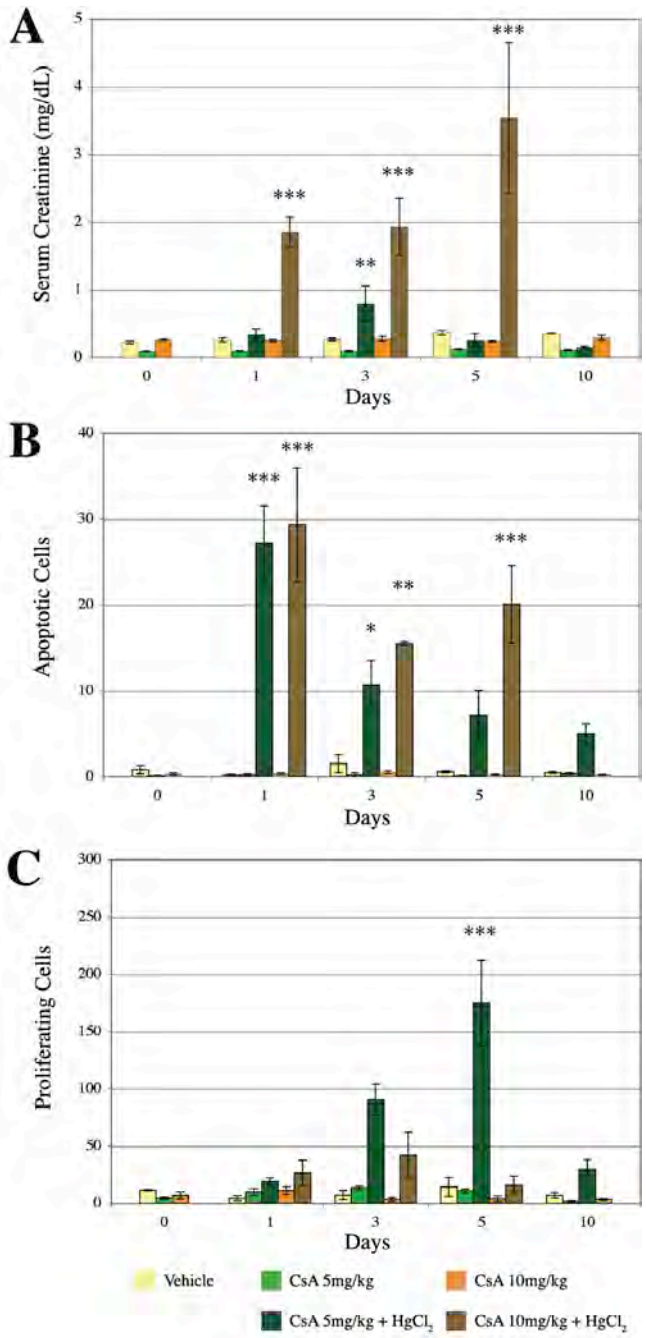

Figure 3.8. ***Attenuation of NFATc with CsA increased serum creatinine concentrations, increased apoptosis and decreased PTC proliferation following $HgCl_2$ injury.*** **A.** Serum creatinine concentrations are significantly increased in mice treated with CsA and $HgCl_2$ ($p<0.0001$ WT vs. 10mgCsA/kg treated mice, two-way ANOVA). **B.** Apoptosis is significant increased in PTCs in mice treated with CsA and $HgCl_2$ ($p=0.0063$ WT vs. 5mgCsA/kg and $p<0.0001$ WT vs. 10mgCsA/kg treated mice, two-way ANOVA). **C.** Proliferation is significantly decreased in mice treated with 10mgCsA/kg following $HgCl_2$ induced AKI compared to WT mice ($p=0.0013$ WT vs. 10mgCsA/kg treated mice, two-way ANOVA). **A-C**, *$p<0.05$, **$p<0.01$, ***$p<0.001$ by two-way ANOVA with Bonferroni posttest verses day 0.

treated with vehicle, 5mgCsA/kg, or 10mgCsA/kg without $HgCl_2$ do not have a significant change in apoptosis throughout the time course. (Fig. 3.8B). The number of apoptotic PTCs was significantly increased in mice treated with 5mgCsA/kg and 10mgCsA/kg (Fig. 3.8B, $p=0.0063$ and $p<0.0001$ comparing WT vs. 5mgCsA/kg and WT vs. 10mgCsA/kg, respectively, by two-way ANOVA). These data indicate that PTCs with uninhibited NFATc1 expression or activation are protected from extensive apoptosis.

Proliferation is inhibited in CsA treated mice

CsA has been shown to reduce cell proliferation (Roy et al., 2006). Immunohistochemistry performed with the proliferation marker PCNA showed that there was not a difference in the amount of proliferating PTCs in the 5mgCsA/kg and 10mgCsA/kg treated mice prior to $HgCl_2$ injury (Fig. 3.8C) compared to WT (Fig. 2.7D). Mice treated with 10mgCsA/kg had significantly decreased PTC proliferation following $HgCl_2$ induced AKI compared to WT mice (Fig. 3.8C, $p=0.0013$ comparing WT vs. 10mgCsA/kg treated mice by two-way ANOVA). Proliferating PTCs were identified in the 5mgCsA/kg treated mice 3 days after $HgCl_2$ injury with the peak in proliferation at day 5. However, the group of mice treated with 10mgCsA/kg had fewer proliferating PTCs at day 5 compared to WT. There were not significant changes in PTC proliferation in mice treated daily with vehicle, 5mgCsA/kg, or 10mgCsA/kg for the duration of the time course without $HgCl_2$.

Discussion

The data presented in this chapter show that WT mice treated with moderately low and high doses of CsA, to pharmacologically inhibit calcineurin and all members of the NFATc family, have lowered Nfatc1 expression in the kidney and when exposed to $HgCl_2$ the regenerative capacity of PTCs is impaired ultimately resulting in renal failure and death. One of the most unexpected results of these studies was the dramatic renal injury that occurred following $HgCl_2$ administration in mice receiving 10mgCsA/kg. Andoh *et al*. administered 100mgCsA/kg, a 10-fold higher dose and reported that this high dose did not alter structure or function in mice on a low-sodium diet (Andoh et al., 1997). However, in our analysis, 10mgCsA/kg resulted in increased PTC apoptosis, decreased proliferation, renal failure and death in all mice following $HgCl_2$ induced AKI. Thus, CsA, even at low doses not associated with chronic changes may result in an increased vulnerability to renal insult resulting in AKI that has not been previously appreciated. We would hypothesize that attenuation of NFATc1 using CsA reduces the number of PTCs due to increased and sustained apoptosis thereby reducing the number of PTCs available to proliferate and regenerate the damaged PTC segment following exposure to a second nephrotoxin.

The toxicity and interstitial fibrosis associated with therapeutic clinical CsA usage is dose independent and it is tempting to speculate that these “side effects” are secondary to inhibition of normal NFATc1 activity in the tubule epithelial cells, although this has not been proven. We would reason that it is critical for the proximal tubule cells to be able to regenerate rapidly as delayed regeneration in 5mgCsA/kg and 10mgCsA/kg treated mice was accompanied by increased interstitial collagen deposition and fibrosis.

Although CsA is pleiotropic and our use of CsA does not reduce NFATc1 in the proximal tubule specifically, it is tempting to speculate that some of the nephrotoxicity associated with clinical use of CsA may result from NFATc1 inhibition and provides an exciting mechanism for future analysis.

Our analysis of the effects of combined treatment with CsA and $HgCl_2$ induced AKI was performed first using the high dose of CsA. After inducing such a high mortality rate, recording high serum creatinine concentrations, and observing severe pathologic damage, we repeated the experiment with the low dose of CsA. Because the experiments were performed in this order, we did not have the foresight to prepare samples from mice treated with the high dose of CsA for electron microscopy and do not feel that it would be ethical to repeat treatment with such a high dose. Therefore, we can only speculate that EM performed on such samples would show a more severe mitochondrial injury defined by large vacuoles and disorganized cristae than the injury observed in Figure 3.6. As presented here, combined treatment with low does of CsA and $HgCl_2$ caused severe mitochondrial injury as the mitochondria contained large vacuoles and showed disorganized cristae. Previously published work has shown that CsA cause tubular cell apoptosis resulting from mitochondrial injury and treatment with $HgCl_2$ alters the structural integrity of the mitochondria, as described above (Justo et al., 2003; McDowell et al., 1976).

However, Whole kidney cortex samples from each mouse were frozen at time of death to be used to extract RNA and protein. qRT-PCR to analyze changes in NFATc1 transcription confirmed that treatment with both low and high doses of CsA significantly reduced Nfatc1 transcription compared to WT mice. We observed a decrease in

transcription of NFATc3 and NFATc4 and increase in NFATc2 transcription in mice treated with 5mgCsA/kg, 5 days after injury. Although NFATc proteins are expressed in cortical tubules during development and in the adult, the expression profile of NFATc2 has not been identified in the adult kidney. Therefore, it is tempting to speculate that NFATc2 may play a role in proximal regeneration as NFATc2 has been shown to play a role in the autoamplification of NFATc1 (Zhou et al., 2002). However, further experiments are required to confirm this mechanism.

The western blots performed using protein samples isolated from the cortex were unsuccessful in identifying NFATc1. We determined that it was unnecessary to repeat these costly experiments in order to measure the decrease in NFATc1 protein expression specifically in the PTCs of mice treated with CsA when we recorded decreased Nfatc1 mRNA expression. CsA inhibits calcineurin thus preventing the dephosphorylation and transcriptional activation of NFATc proteins. Therefore, we would expect to observe a decrease in the amount of dephosphorylated NFATc1 protein similar to *Nfatc1*$^{+/-}$ mice in mice treated with 5mgCsA/kg and a further reduction of NFATc1 protein and possibly no dephosphorylated NFATc1 protein in mice treated with 10mgCsA/kg. The data presented here confer that combined treatment of CsA and exposure to $HgCl_2$ causes nephrotoxicity that is more severe than exposure to CsA or $HgCl_2$ alone.

In conclusion, we have described the significant renal damage that results from the coadministration of CsA and $HgCl_2$. NFATc protein expression was attenuated pharmacologically with moderately low doses of CsA, in mice. Taking into account the clinical nephrotoxicity of calcineurin inhibitors and significant renal injury recorded in mice treated with $HgCl_2$ and CsA, we would hypothesize that NFATc1 plays a role in

modifying epithelial regeneration following renal injury and propose a possible two hit hypothesis as a mechanism to explain CsA induced nephrotoxicity.

These findings are significant, as this is the first study to report that coadministration of CsA and $HgCl_2$ induces a severe renal injury *in vivo*. While the nephrotoxicity associated with CsA is pleiotropic and the PTCs are only one cell population injured, our data would suggest that in addition to adverse vascular effects, CsA also renders the proximal tubule especially susceptible to toxic injuries from exposure to additional nephrotoxins resulting in heightened injury and provides additional insights into the pathology of immunosuppressive nephropathy. This two-hit hypothesis may provide a mechanism for CsA induced nephrotoxicity. However, we do not know what the transcriptional targets of NFATc1 are in the proximal tubule segment, as this is the first report of a role for NFATc1 in the proximal tubule. It is tempting to speculate that NFATc1 targets proteins that maintain the epithelial phenotype of the proximal tubule segment and proteins that control the rate of proliferation and regeneration of this segment following a renal injury. Furthermore, administration of CsA following a transplantation to inhibit the immune system and prevent rejection of the grafted tissue or transplanted organ inhibits the dephosphorylation and transcriptional activation of NFATc1 thus preventing the regenerative response of NFATc1 target proteins. Experiments not performed in this thesis are required to address these questions.

CHAPTER IV

ACCENTUATED EXPRESSION OF NFATC1 IDENTIFIES A PROGENITOR PROXIMAL TUBULE EPITHELIAL CELL POPULATION

Introduction

Recovery from AKI caused by a nephrotoxic insult requires renal tubule cell regeneration. Several investigators have attempted to identify a cell population capable of repairing tubular damage and have focused on identifying a progenitor cell population that is a circulating population originating from bone marrow, an adjacent cell population that undergo EMT or transdifferentiation, or a resident PTC. Taking into account the nephrotoxicity of calcineurin inhibitors and having documented expression of NFATc1 in the kidney, we propose that NFATc1 plays a role in modifying epithelial regeneration following renal injury.

We wanted to identify NFATc1 expression in the proximal tubule segment over the course of injury and repair. To accomplish this, we turned to use NFATc1 transgenic lines that express LacZ [NFATc1-P2-LacZ (Zhou et al., 2005)] under the control of an NFATc1 enhancer domain important for autoamplification of NFATc1. We demonstrated accentuated NFATc1 expression in a subpopulation of proximal tubule cells following $HgCl_2$ injury. This subpopulation did not undergo apoptosis following $HgCl_2$ injury and cells expressing the reporter colocalized with a proliferation marker. We questioned if this subpopulation of cells had regenerative potential and performed lineage analysis using a novel transgenic mouse line that expresses Cre recombinase (NFATc1-P2-Cre) under the control of the NFATc1 enhancer domain. We documented that the NFATc1

labeled PTCs are resistant to apoptosis and subsequently proliferate to repair the damaged proximal tubule segment. These data provide evidence that suggest a self-renewing resident progenitor population of PTCs and further supports a critical role for NFATc1 in regeneration of injured.

Methods

Transgenic mice

NFATc1-P2-LacZ mice have been previously described [BB-HSP-LacZ (Zhou et al., 2005)]. NFATc1-P2-Cre transgenic mice contain the minimal NFATc1-P1 promoter (Zhou et al., 2002), a Cre recombinase cassette, and the NFATc1 enhancer domain (see below, Fig. 4.1). NFATc1-P2-LacZ, NFATc1-P2-Cre, and R26R mice are maintained on the B6D2F1 background and were genotyped using primers listed in Table 2.1.

Experimental Protocol.

All experiments were performed on 6-8 week old female mice using a single subcutaneous dose of 8.14 mg/kg $HgCl_2$ in normal saline to induce significant AKI. NFATc1-P2-LacZ n = 3 for each time point. For lineage tracing, a single bolus of BrdU (GE Healthcare) was administered to *NFATc1-P2-Cre;R26R* mice followed by a 2 hour (Day 0, Day 1, Day 3 and Day 5) or 5 day (Day 10) chase, n = 3 for each time point.

Histology.

Dissected kidneys were bisected and fixed in PBS containing 4% paraformaldehyde overnight at 4˚C, dehydrated in an ethanol and xylene gradient and embedded in paraffin. 5 μm sections were cut on a microtome.

β-Galactosidase detection

Kidneys were bisected, fixed in PBS containing 0.2% glutaraldehyde, 5 mM EGTA, 100 mM $MgCl_2$ for 4 hours at room temperature with a solution change after 2 hours, and cryoprotected in PBS containing 15%- and 30% sucrose before embedding in OCT (Ma et al., 2002). 10 μm sections were cut, dried at room temperature for 30 minutes, washed in a PBS detergent containing 2 mM $MgCl_2$, 0.01% Na-deoxycholate, and 0.02% NP40, stained in X-Gal solution, pH 7.50, and post-fixed in 4% paraformaldehyde, counterstained with eosin or nuclear fast red, and mounted in Permount (Fisher).

Antibody staining

Immunofluorescence with the anti-β-Gal antibody (Dr. Lim, University of Michigan) and anti-cleaved caspase 3 (Cell Signaling) were detected on adjacent 10 μm cryosections with TRITC and FITC labeled goat anti-rabbit antibodies (Jackson), respectively, nuclei stained using Hoechst Dye 33342 (Molecular Probes), and mounted in Vectashield Mounting Media (Vector). Anti-E-Cadherin (BD Biosciences) and anti-β-Gal antibody immunofluorescence was performed on paraffin sections Immunohistochemistry with X-Gal and biotinylated lotus tetragonolobus lectin (LTL,

Vector) were detected on 10μm cryosections. BrdU labeled PTC nuclei were identified using the anti-BrdU antibody (Abcam) and biotinylated-LTL on X-Gal stained slides to score the NFATc1-P2-Cre expression pattern.

Statistics

All data are presented as mean ± SEM. All scoring was performed blinded. Differences between groups were assessed with two-way ANOVA and posttest using Bonferroni correction to compare Day 1, 3, 5, and 10 to Day 0 for each genotype and to reduce Type I error. A result was considered to be significant when $P<0.05$.

Results

Transgenic NFATc1-P2-LacZ reporter expression documents that NFATc1 is upregulated in a subpopulation of PTCs

Our lab developed a transgenic strain of mice, NFATc1-P2-LacZ (Fig. 4.1A), containing an enhancer element located within the first intron of NFATc1 that expresses nuclear localized β-Gal in a subset of endocardium of the developing mouse heart recapitulating endogenous NFATc1 expression during development (Zhou et al., 2005). This P2 enhancer element plays an important role in controlling auto-amplification of NFATc1 (Zhou et al., 2002; Zhou et al., 2005). We used NFATc1-P2-LacZ mice to delineate NFATc1 activation in the adult kidney and observed expression in smooth muscle cells of large renal arteries, but no expression in glomerular, interstitial, or tubular cell populations (Fig. 4.1B). We repeated the $HgCl_2$ dosage and time course as described above using this NFATc1-P2-LacZ transgenic line. LacZ expression is activated 1 day

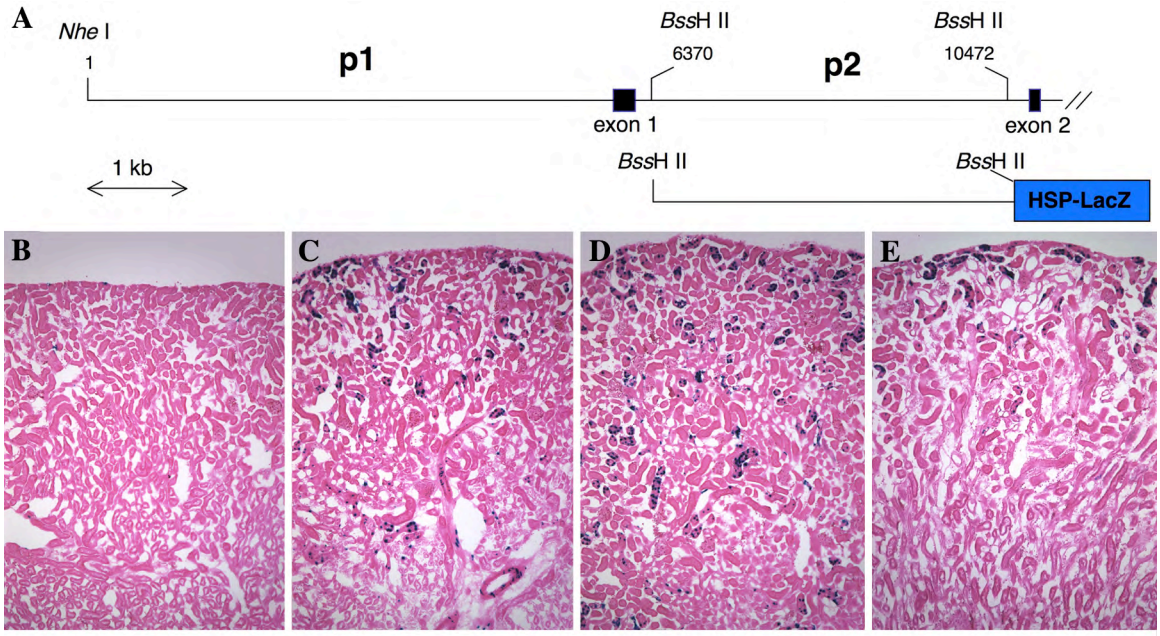

Figure 4.1. ***The NFATc1-P2-LacZ reporter is activated and expressed in the outer cortex after $HgCl_2$ induced AKI.*** The $HgCl_2$ time course was repeated in NFATc1-P2-LacZ mice. **A.** Schematic of the NFATc1-P2-LacZ transgenic construct. **B.** Before treatment with $HgCl_2$, the NFATc1-P2-LacZ reporter is not active in any tubule epithelial, glomerular, or interstitial cell populations. Following $HgCl_2$ injury, the NFATc1-P2-LacZ reporter is expressed in cortical tubules at day 1 as seen by the nuclear localized X-Gal stain (**C.**). The NFATc1-P2-LacZ expression expands on day 3 (**D.**) and expression is decreased by day 5 (**E.**). B-E X-Gal staining with nuclear fast red counterstain. Magnification, 100X.

after $HgCl_2$ injury as seen with X-Gal staining (Fig. 4.1C). The number of cells expressing LacZ increases at Day 3 (Fig. 4.1D) and subsequently decreases at Day 5 (Fig. 4.1E). By day 10, the number of LacZ positive PTCs is greatly reduced (data not shown), a trend analogous to the Real-time PCR expression analysis of NFATc1 described above (Fig. 2.3).

Expression of the NFATc1-P2-LacZ reporter after $HgCl_2$ was not observed in any glomerular or interstitial cell type. The expression was apparent in tubular epithelial cells in the outer cortex and minimal expression in the inner cortex. We performed dual label immunohistochemistry with tubular segmental markers to further delineate the specific cellular identity of NFATc1 expressing cells. Immunofluorescence performed with anti-β-Gal and the proximal tubule specific marker *Lotus tetragonolobus* lectin (LTL, Fig. 4.2A) show that activation of LacZ is in the proximal tubule segment. Furthermore, activation of LacZ was specific to a subset of PTCs as all proximal tubules were not labeled with β-Gal. NFATc1-P2-LacZ was not expressed in any distal tubule or collecting duct as seen by immunofluorescence with anti-E-cadherin (Fig. 4.2B). E-cadherin has been previously shown to be expressed differentially on the basal and lateral membranes of distal tubules, collecting ducts, and in the medulla with very weak expression in the proximal tubule (Prozialeck et al., 2004).

We were intrigued that the expression of the NFATc1-P2-LacZ reporter was detected in only a subset of PTCs. To further characterize this subpopulation, immunofluorescence was performed on adjacent sections with β-Gal and Cleaved Caspase 3 antibodies and showed that NFATc1-P2-LacZ expression in PTCs did not colocalize with apoptotic PTCs (Fig. 4.2C). This is consistent with TUNEL quantification

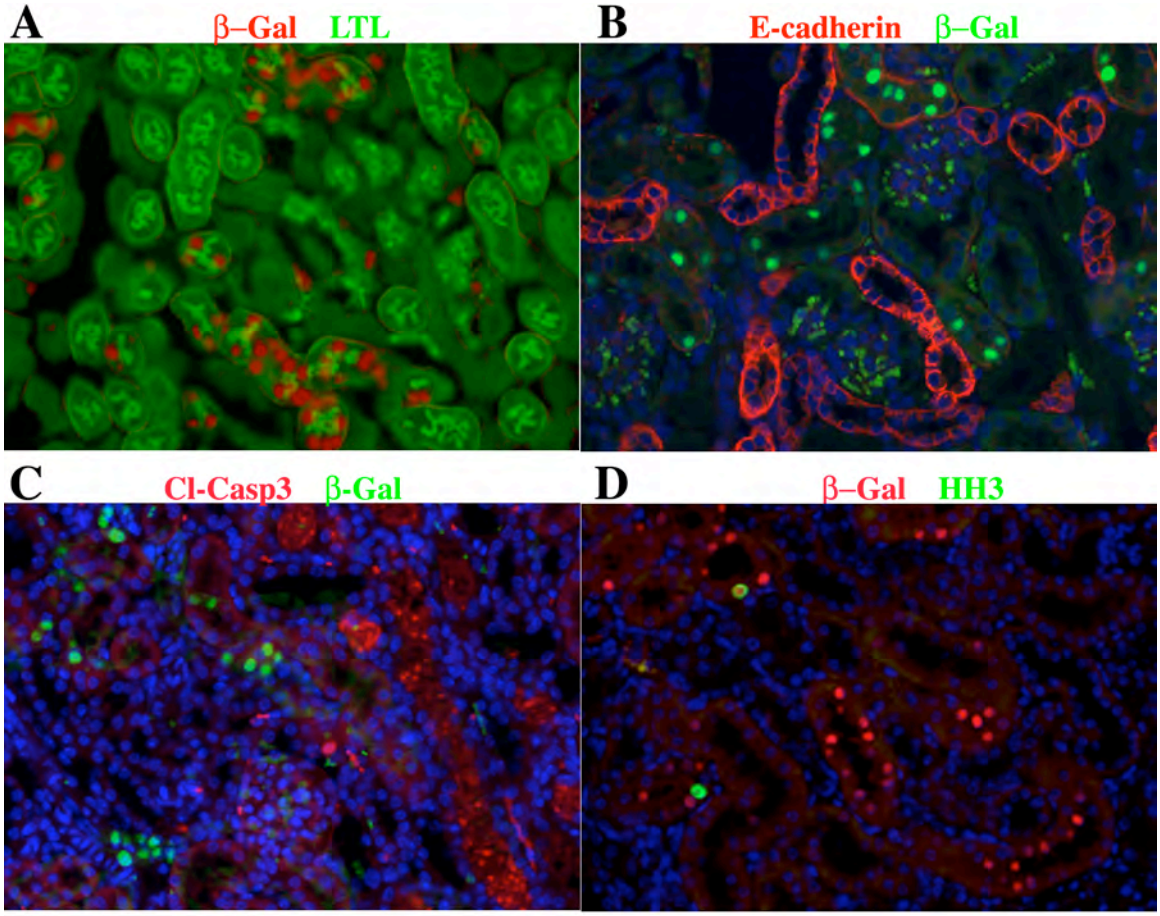

Figure 4.2. ***NFATc1-P2-LacZ is expressed in a subset of proximal tubules that escape apoptosis after $HgCl_2$ induced AKI.*** **A.** Immunohistochemistry performed using anti-B-Gal antibody and proximal tubule specific marker, lotus tetragonolobus lectin reveals that the NFATc1-P2-LaZ reporter is expressed specifically in the proximal tubule segment of the nephron in a subset population of PTCs. Representative image from Day 3. **B.** E-cadherin is expressed in distal tubules and collecting duct and does not colocalize with the majority of NFATc1-P2-LacZ expression after $HgCl_2$. C. Immunofluorescence performed with β-Gal (red) and cleaved caspase 3 antibodies show 3 days after injury, the NFATc1-P2-LacZ PTCs are not apoptotic. **H.** Immunofluorescence performed with β-Gal and cleaved caspase 3 antibodies before $HgCl_2$ injury. F. Hematoxylin stained nuclei. G + H. DAPI stained nuclei (blue). Magnification. 200X.

performed previously (Fig. 2.7). In addition, immunofluorescence with anti-phosphorylated histone-H3 (pHH3), a marker of the S-phase, showed that although only a few cells were in S-phase and labeled with pHH3, the expression colocalized with anti-β-Gal positive PTCs suggesting that these cells proliferate to regenerate the damaged proximal tubule segment (Fig. 4.2D). These data suggest that the P2 locus, which reports NFATc1 autoamplification, is activated in and identifies a subpopulation of PTCs that are resistant to apoptosis following AKI and this subpopulation subsequently undergoes proliferation.

Because the NFATc1-P2-LacZ transgenic construct contains the minimal HSP promoter, we were concerned that the LacZ reporter was being activated by HSP activity following $HgCl_2$ injury and not exclusively by the NFATc1-P2 enhancer element. To confirm that the NFATc1-P2 enhancer element was responsible for the activation of the LacZ reporter, LLC-PK1 cells, a porcine proximal tubule epithelial cell line, were transfected with NFATc1-P2-LacZ (containing the minimal HSP promoter) and an HSP-LacZ plasmid. Cells transfected with NFATc1-P2-LacZ had a significant 3-fold increase in X-Gal staining cells following treatment with $HgCl_2$ compared to LLC-PK1 cells transfected HSP-LacZ (Fig. 4.3, $p=0.001$, Mann-Whitney U test).

The NFATc1-P2-Cre reporter identifies a progenitor subpopulation of PTCs

We questioned whether the apoptotic resistant population of PTCs marked by the NFATc1-P2 enhancer domain contributed to regeneration of the PTCs. To investigate this possibility, NFATc1-P2-Cre mice (Fig. 4.4A), a transgenic strain that utilizes the NFATc1-P2 enhancer element to drive Cre recombinase expression, were crossed to

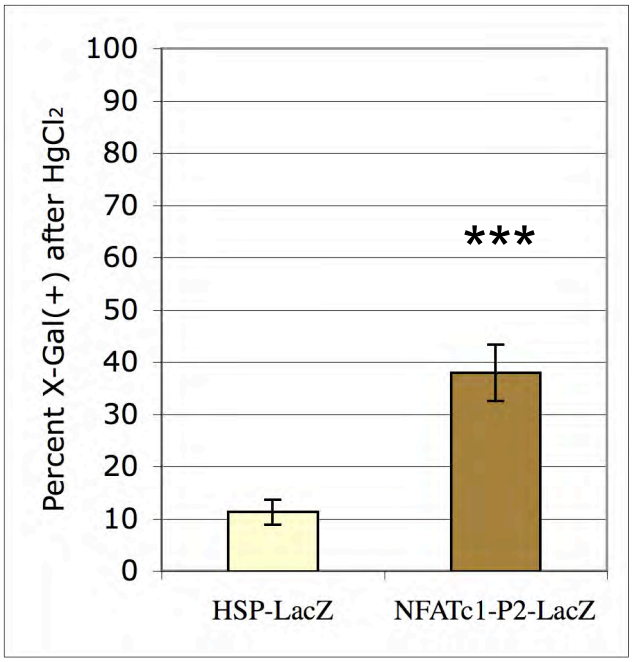

Figure 4.3. ***NFATc1-P2-LacZ is activated in LLC-PK1 cells following treatment with $HgCl_2$, in vitro.*** LLC-PK1 cells, a porcine proximal tubule cell line, transfected with NFATc1-P2-LacZ have a significant increase in X-Gal labeled cells compared to cells transfected with control plasmid, HSP-LacZ. (*** p=0.001, Mann-Whitney U)

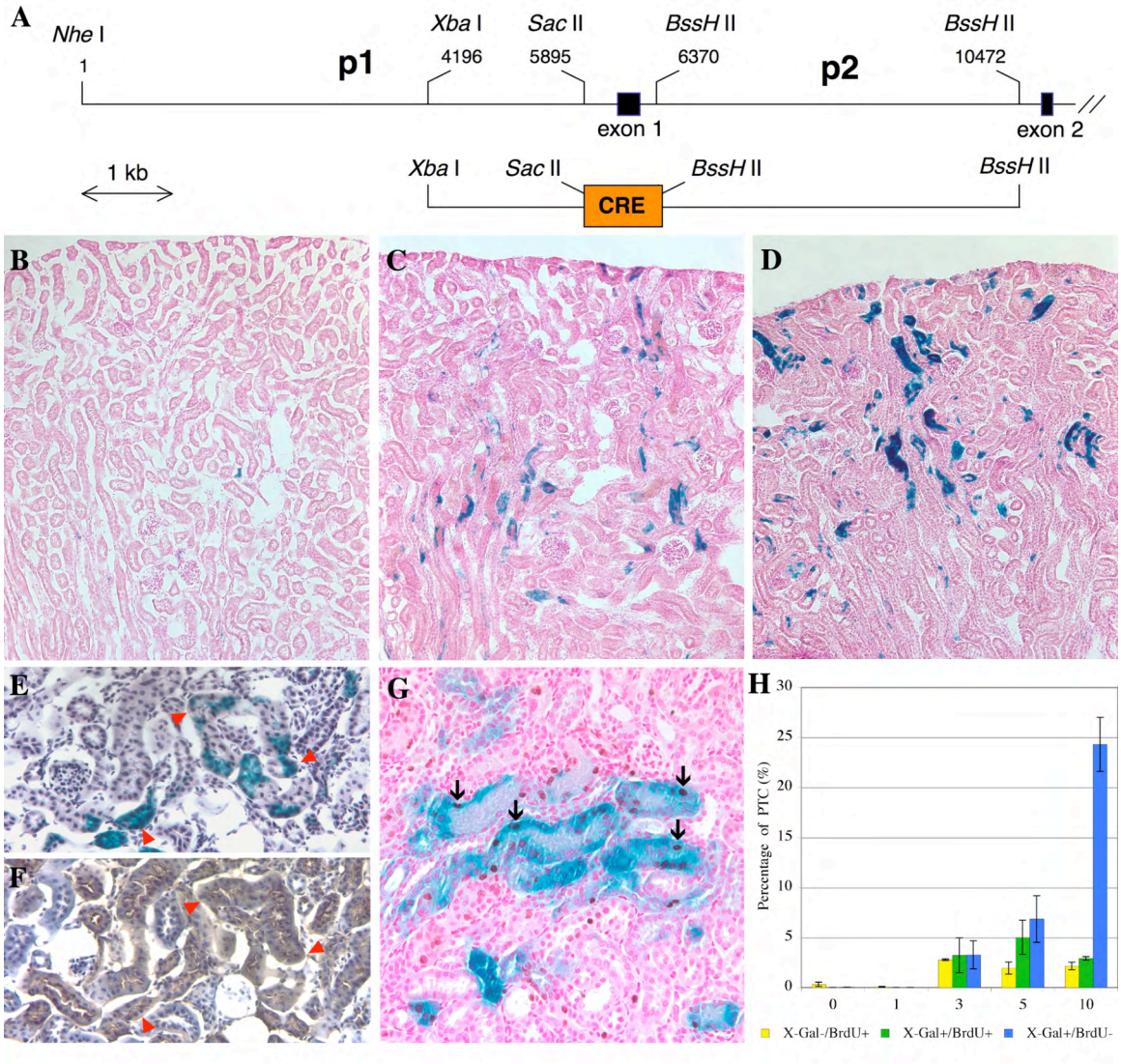

Figure 4.4. ***Lineage analysis using the NFATc1-P2-Cre reporter marks a progenitor subpopulation of PTCs that regenerate PTCs.*** **A.** Schematic of the NFATc1-P2-Cre transgenic construct. **B**. Before $HgCl_2$ treatment, NFATc1-P2-Cre is not expressed in any tubule epithelial, glomerular, or interstitial cell population, confirming that the reporter construct was not activated previously during development. **C.** Following $HgCl_2$ injury, the NFATc1-P2-Cre reporter is activated and expressed in PTCs cells at day 5 and the number of X-Gal positive cells increases by day 10 (**D.**). **E-F**. Staining of serial sections with Xgal (E.) and LTL (F.). Red arrows reference proximal tubule segments on adjacent sections. **G.** Costaining 5 days after $HgCl_2$ injury shows colocalization of the NFATc1-P2-Cre (blue, X-Gal staining of R26R reporter) and BrdU-labeled (brown, arrows) PTC identifying a subset population of PTCs that proliferate after injury. **H.** Quantification of PTCs cells that are positive for X-Gal, BrdU, or both X-Gal and BrdU reveal that at Day 3 there were an equal number of X-Gal+/BrdU+ and X-Gal-/BrdU+ population each composing approximately 5% of the PTC counted cells. At day 10, 27% of the PTCs are NFATc1-P2-Cre derivatives. B-E, Nuclear fast red counterstain. Magnification, B-D. 100X; E. 400X.

R26R reporter mice (Soriano, 1999). This lineage analysis approach allowed us to genetically identify most, if not all, PTCs in which NFATc1-P2 was activated as well as their progeny. We repeated the $HgCl_2$ time course as described above with NFATc1-P2-Cre mice. Prior to treatment with $HgCl_2$, LacZ was not expressed in any tubular, glomerular, or interstitial cells confirming that as previously documented by the NFATc1-P2-LacZ transgenic line, the P2 promoter element was not activated during renal development (Fig. 4.4B). As with the NFATc1-P2-LacZ mice, treatment with $HgCl_2$ activated the Cre reporter and cytoplasmic β-Gal was observed at day 5 (Fig. 4.4C). Interestingly, in contrast to previous experiments with the NFATc1-P2-LacZ where the number of LacZ positive cells decreased 5 days after $HgCl_2$ treatment indicating decreased NFATc1 expression, the number of X-Gal stained PTCs in NFATc1-P2-Cre mice increased by day 10 (Fig. 4.4D). Immunolabeling of serial sections with X-Gal and LTL confirms that NFATc1-P2-Cre expression was specific to the PTC population (Fig. 4.4E-F). Because or experiments with NFATc1-P2-LacZ mice documented an attenuation of NFATc1 expression by day 5, we conclude that the increased number of positive PTCs in the cortex of NFATc1-P2-Cre mice after 10 days represents the clonal expansion of the PTCs in which NFATc1 was originally expressed.

To quantify the regenerative potential of NFATc1-P2-Cre expressing PTCs, we stained sections with X-Gal and performed dual-labeling immunohistochemistry with the anti-BrdU antibody and quantified X-Gal$^-$BrdU$^-$, X-Gal$^-$BrdU$^+$, X-Gal$^+$ BrdU$^+$, X-Gal$^+$ BrdU$^-$PTCs (Fig. 4.4G-H). Before treatment with $HgCl_2$, 0.32% of the PTCs were X-Gal$^-$ BrdU$^+$ and 0.03% of PTCs were X-Gal$^+$ BrdU$^-$. 3 days after $HgCl_2$ injury there was not a significant difference in the number of X-Gal$^-$BrdU$^+$ and X-Gal$^+$ BrdU$^+$ cells. However, 5

days after $HgCl_2$ injury, the number of X-Gal$^+$ BrdU$^+$ PTCs was 2.5-fold greater than X-Gal$^-$BrdU$^+$ PTCs. 10 days after $HgCl_2$ treatment, greater than 25% of PTCs were derived from NFATc1-P2-Cre PTCs. The number of PTCs that label X-Gal$^-$BrdU$^+$ does not change significantly throughout the time course consistent with results for PCNA staining shown in Figure 2.7. These data indicate that the PTCs that are labeled by the NFATc1-P2 enhancer serve as a progenitor population that proliferates to help repair the damaged proximal tubule segment of the nephron. Furthermore, the close approximation of NFATc1-P2-Cre positive cells and their X-Gal$^+$BrdU$^+$ progeny suggests that the damaged PTC segment is regenerated by clonal expansion of an apoptosis-resistant subpopulation of cells that reside in the proximal tubule.

Discussion

Using NFATc1-P2-LacZ mice, we identified a subpopulation of resident PTCs that express the reporter following $HgCl_2$ injury and these cells are resistant to apoptosis. Using a novel transgenic reporter mouse line, NFATc1-P2-Cre, we identified a resident subpopulation of PTCs that serve as a progenitor cell population to regenerate the damaged proximal tubule segment. This study provides the first *in vivo* experimental evidence using transgenic mouse lines to define a resident proximal tubule cell population repopulates the damaged proximal tubule segment following an AKI.

The NFATc1-P2-LacZ transgenic line was created in order to characterize the expression of the autoamplification of NFATc1 as marked by reporter activation (Zhou et al., 2005). This line was further characterized to recapitulate the endogenous expression of NFATc1 in the developing endocardium. Although we have not been successfully able

to report enhanced NFATc1 expression in the proximal tubule segment using antibodies, we believe these genetic studies provide a more sensitive method of NFATc1 expression and that the expression of NFATc1-P2-LacZ recapitulates endogenous NFATc1 expression in the PTC after injury. As discussed in Chapter II, we were unable to document a change in NFATc1 protein expression by immunohistochemistry using currently available antibodies. This is at least partially the result of the inefficiency of this antibody (mouse monoclonal 7A6) when used for immunohistochemistry as experienced in our laboratory and others. In addition, we have previously documented a basal level of NFATc1 in normal PTCs prior to injury. The current study attempted to delineate an increase in autoamplification of NFATc1 expression above that detected in normal cells and thus it is not surprising that an increase of NFATc1 (verses the presence or absence of NFATc1) was not possible given the limitations of this antibody in immunohistochemical studies.

This study provides additional insights into the basic mechanisms of PTC regeneration and repair following acute toxic insult. The injured kidney must undergo a program of regeneration and proliferation in order to restore renal function. The precise origin of cells that repair the damaged PTCs is unknown. It has been postulated that these cells arise from either adjacent less injured cells, a proximal stem cell population, or an external stem cell population circulating in the blood stream (Gupta et al., 2006; Morigi et al., 2006b; Sagrinati et al., 2006). The identification of an adjacent less injured population of progenitor cells has been difficult to identify because such a population remains phenotypically indistinguishable from their terminally differentiated counterparts. Our use of the NFATc1-P2-LacZ and NFATc1-P2-Cre mice suggest a

subpopulation of resident PTCs, which we identified using the NFATc1-P2 enhancer, act as progenitor cells that are resistant to apoptosis. This population subsequently undergoes proliferation to reconstitute a significant number of the damaged proximal tubule cells.

Recent work has described a role for NFATc1 in controlling the quiescence and proliferation of stem cells found in the hair follicle (Horsley et al., 2008). NFATc1 expression is activated by BMP signaling and represses CDK4 signaling in order to maintain stem cell quiescence and when the stem cells are activated to grow a hair, NFATc1 is downregulated, removing the repression of CDK4 and allowing proliferation. When Horsley *et al*. inhibited NFATc1/calcineurin signaling by deleting a conditional allele of NFATc1 or treated mice with CsA, the quiescent phase of the stem cell was removed resulting in rapid hair growth (Horsley et al., 2008). In contrast, Runx1, a protein required for blood formation, was conditionally deleted in keratinocytes. These mice produced normal hair follicles during development but the stem cells failed to proliferate and were trapped in the quiescent phase and therefore unable to sustain hair growth past 3 weeks of age. Following repeated periods of skin injury and repair, WT and Runx1 conditional knockouts had skin hair growth at the injured area and adjacent areas; however, Runx1 conditional knockouts eventually reentered the quiescent phase. The Runx1 mutant phenotype emphasizes the differences in hair growth that occurs during development compared to hair growth triggered by injury (Osorio et al., 2008). Taken together, these studies suggest a role for NFATc1 in the maintenance of quiescence and proliferation of stem cells in the hair follicle. Therefore, we hypothesize that NFATc1 may play a role in the regeneration of the proximal tubule segment after injury.

CHAPTER V

ISOLATION AND CHARACTERIZATION OF PROXIMAL TUBULE PROGENITOR CELLS

Introduction

The source of the progenitor cells that proliferate to regenerate the PTCs following an AKI is a clinically important question as described in Chapter I. The source of these cells has been proposed to come from one of three sources: BMCs circulating in the blood stream that undergo migration and transdifferentiation to repopulate the proximal tubule, adjacent uninjured cells that undergo MET and/or transdifferentiation adopting an epithelial phenotype, or less injured PTCs that self-renew. In Chapter IV, I presented data using NFATc1-P2-Cre mice crossed onto the R26R reporter line to show that the NFATc1 enhancer was activated in a subpopulation of proximal tubule cells that do not undergo apoptosis and proliferate to regenerate the damaged kidney following AKI. This is the first reported use of transgenic model system to identify a population of self-renewing proximal tubule progenitor cells (PTPCs) and introduces many questions. How does the gene expression profile for PTPCs differ from the gene expression profile of non-progenitor PTCs? Do the PTPCs have "stemness" - expressing markers associated with multipotent stem cells? Are these PTPC differentiated PTCs or do they share a common expression profile with developmental proximal tubule precursors?

To address these questions we created a single cell suspension of the renal cortex and used FACS to isolate the PTPCs demonstrating NFATc1 enhancer/reporter expression before and after $HgCl_2$ induced AKI. Labeling proximal tubules with a

fluorescent reporter is key to the isolation of the progenitor population by flow cytometry. A transgenic line expressing a fluorescent reporter protein under the control of the NFATc1 enhancer/regulatory element is not available. Therefore, we initially used NFATc1-P2-LacZ mice to address the question: how does the gene expression profile of labeled PTPCs actively expressing the NFATc1 reporter differ from unlabeled PTCs? However, incorporation of a fluorescent dye required to sort the NFATc1-P2-LacZ PTPCs was toxic (see below). We altered our experimental approach to use the NFATc1-P2-Cre mice crossed with mice that had a conditional fluorescent GFP reporter.

We then isolated mRNA from GFP+ PTCs and GFP– PTCs and performed Real-time PCR on candidate genes to characterize the expression of proximal tubule, stem cell, and developmental markers. Our results show that the GFP+ PTCs have a 2-fold increase in NFATc1 expression compared to the GFP– PTCs. Furthermore, the GFP+ PTCs have increased expression of genes identifying them as differentiated proximal tubules (AQ-1, KAP, KSP, Lim1), have increased expression of stem cell markers (c-Myc, Klf-4, Nanog, Oct-4, Sox-2), proliferative (CDK4) and genes characteristic of early tubular development (BMP-2, BMP-4, BMP-7, Pax-2, Wnt-4, Wnt11). This analysis confirms that the GFP+ PTC population - comprised of PTPCs accentuated by NFATc1 and their progeny - have a unique gene expression profile and suggests that this population could be targeted to improve clinical outcomes of acute and chronic renal failure.

Methods

$HgCl_2$ induced AKI

All experiments were performed on 8-10 week old female mice. Primer sequences used to genotype mice are listed in Table 2.1. A single subcutaneous dose of 12 mg/kg $HgCl_2$, a 1.5 fold increase compared to the dose used in previous Chapters, was administered in order to produce a similar injury in mice on a B6D2F1//C57BL/6 mixed genetic background.

Protocol for FACS with NFATc1-P2-LacZ mice and ImaGene Red substrate

Kidneys from 3 mice were dissected removing the renal capsule and papilla. The remaining cortex was minced into $1mm^3$ pieces, and placed in 30 ml of ice-cold Krebs-Henseleit saline (KHS, pH 7.4, containing 115 mM NaCl, 24 mM $NaHCO_3$, 5 mM KCl, 1.5 mM $CaCl_2$, 10 mM $MgSO_4$, 2 mM NaH_2PO_4, 10 mM HEPES, 5 mM glucose, 1 mM alanine) with 1.5% fetal bovine serum (KHS+). After 3 washes with KHS+, the tissue was digested in KHS+ supplemented with 7.5 mg/ml collagenase B (Roche), 1.2 U/ml dispase II (Roche), 0.01% DNAse I (Invitrogen) for 20 minutes in a 37˚C water bath (ideally with shaking at 40rpm). A 23 G needle and syringe were used to further digest the tissue, passing the digested mix through the needle 5-10 times. Red blood cells were lysed using 0.5 ml/kidney of red blood cell lysing buffer (Sigma), incubated for 1 minute, diluted with KHS+, and centrifuged at 1000 rpm for 5 minutes. This step was repeated if necessary. The resulting single cell suspension was strained through a 40um filter (BD

Falcon) and washed 3-times with KHS+. The kidney digestion protocol was adapted from Challen *et al*. and Vinay *et al*. (Challen et al., 2006; Vinay et al., 1981).

ImaGene Red $C_{12}RG$ substrate staining (Invitrogen)

Cells are resuspended 10^6/ml in 10 mM HEPES, 2% FBS. The supplied chloroquine reagent (1:100, 300 uM final concentration) was added and incubated for 30 minutes at 37˚C. ImaGene Red substrate and FITC labeled LTL (2 mg/ml, Vector) are added (1:100, 1:1000, respectively) and incubated at RT for 30 minutes. The mixture was washed twice with KHS+ buffer and resuspended in 10^6/mL KHS+.

Protocol for FACS with NFATc1-P2-Cre mice

Five days after treatment with $HgCl_2$, kidneys from 3 mice were dissected, renal medulla removed, cortex minced into 1 mm^3 pieces, and washed 3 times with 30 ml of ice-cold KHS+. The minced tissue was digested in 10ml of KHS+ containing 0.05% collagenase type I (5 mg/ml, Sigma), 0.1% DNase I (RNase-free, Invitrogen), and 0.01% soybean trypsin inhibitor (Sigma) for 45 minutes in a 37˚C water bath (ideally with shaking at 40 rpm). The suspension was filtered through a 100 um sieve (BD Falcon). The filter was washed with 30 ml of KHS+ and centrifuged at 1000 rpm for 30 seconds (Beckman Allegra 2IR) and repeated. Red blood cells were lysed in red blood cell lyses buffer (Sigma, 0.5 ml/kidney), mixed gently for 1 min, diluted with KHS+, and centrifuged at 1000 rpm for 5 minutes. This step was repeated if necessary and washed with KHS+. The tissue was resuspended in 0.25% trypsin (Gibco) diluted in KHS+, incubated 4 times at 37˚C for 5 minutes and pushed through a 23 G syringe 10-times

between incubations. Undigested tubules were removed by with a 40 um sieve, and the single cell suspension was washed with KHS+ 3 times.

Cells (10^6/ml) were incubated in biotinylated-LTA lectin (Vector, 2 mg/ml) prepared 1:1000 (2 ug/ml) in KHS+ buffer on ice for exactly 30 minutes. The labeled solution was washed twice with KHS+. Cells were then incubated in streptavidin-APC (Allophycocyanin, Molecular Probes 1 mg/ml) prepared 1:1000 (1 ug/ml) in KHS+ buffer on ice for exactly 15 minutes. The labeled solution was washed twice with KHS+. The cells were resuspended 10^7/ml in KHS for analysis and in KHS+ for cell sorting with 1 μL PI/ml. The labeled cells were covered with foil to protect from light.

Fluorescence activated cell sorting (FACS)

Flow Cytometry experiments were performed in the VMC Flow Cytometry Shared Resource. The VMC Flow Cytometry Shared Resource is supported by the Vanderbilt Ingram Cancer Center (P30 CA68485) and the Vanderbilt Digestive Disease Research Center (DK058404).

For each analysis or sort the following controls were prepared:

- Unstained control – A single kidney cell suspension was prepared as described above using a nonfluorescent mouse (genotype Cre^-/GFP^+ or Cre^+/GFP^-) and this control was used to compensate for the natural fluorescence of the cell population.

Single color controls were prepared in order to individually optimize the voltages used with the photo multiplier tube for each fluorochrome.

- Propidium Iodide (PI) control – Cell viability was recorded as the percentage of cells that exclude PI, which crosses the extracellular and nuclear membranes and

intercalates into double stranded DNA of dead/dying cells. 1 ml of the cell suspension prepared from the nonfluorescent mouse was labeled with 1 μl of PI, vortex.

- Allophycocyanin (APC) control – 1 ml of the cell suspension prepared from the nonfluorescent mouse was stained as described above with both biotinylated-LTL and streptavidin-APC.
- Fluorescent reporter control – A 300 μL aliquot of the single kidney suspension prepared from the kidney sample to be sorted was removed before the sample was stained with biotinylated-LTL and streptavidin-APC.

RNA extraction

Following each cell sort the volume was increased to 15 ml KHS+ and centrifuge for 5 minutes at 3000 rpm. RNA was isolated using the standard Trizol protocol (Invitrogen) followed by a second round of RNA purification was performed using the solid-state column based purification to yield a higher quality RNA (RNeasy Mini Kit, Qiagen). RNA quality and concentration was determined using capillary electrophoresis. (RNA 6000 Nano LabChip Kit and Bioanlyzer, Agilent). cDNA was prepared from 0.35 ug of total RNA using oligo-dT_{16} primer following the manufacturer's protocol (Transcriptor Reverse Transcriptase, Roche).

qRT-PCR

qRT-PCR was performed as described in Chapter 2 with primer sequences in Table 5.1. Three independently sorted samples were used for quantification. Significant changes in expression were calculated using the nonparametric Mann-Whitney U test.

Table 5.1 Oligonucleotides for qRT-PCR analysis of GFP+ PTC and GFP– PTC expression profiles.

Marker gene	Primer sequence	Annealing Temperature (C°)	Product Temperature (C°)	Fragment length(bp)
Aquaporin-1	CATTCTCTCGGGCATCACCT GGGCTGAGCCACCTAAGTCTC	58	80	176
BMP-2	TGAGCGCAATCTCCATGTTGTACC ATTCTTGCTGTGCTAACGACACCC	55	81	105
BMP-4	TGGCTGATCACCTCAACTCAACAA CCAGGTACAACATGGAAATGGCAC	55	81	125
BMP-7	TGTGGCAGAAAACAGCAGCA TCAGGTGCAATGATCCAGTCC	54	81	105
Cadherin-11	ATGGGGCACTGTTGTCCTGT CCTCACCACCCCCTTCATCATCATAG	58	83	219
CDK-4	CTCGTACCGAGCTCCTGAAG TTCTGCAGGTAGGAGTGCTG	55	85	351
c-Myc	AAGCAGATCAGCAACAACCGCAAG TCCTCTGACGTTCCAAGACGTTGT	55	85	100
GAPDH	CACTGGCATGGCCTTCCGTG AGGAAATGAGCTTGACAAAG	55	80	253
KAP	CTTCCTCGTTCTTTCTTCTTTG ACTGTGGCTTTCCCCCTGTC	54	81	429
Klf-4	ACCTTTCACACTGTCTTCCCACGA TCACAAGCTGACTTGCTGGGAACT	55	83	86
KSP	CAACGATTCCCACGCCTACC GCAGCGACACACAATCACTTTG	58	82	130
Lim-1	CGTAGGGGACCCCGGACCACGATCA AGGGGCCGTTGGGGATGAGTTCGCC	58	88	389
Nanog	AAGCCAGGTTCCTTCCTTCTTCCA AGGTCAGGAGTTCAAATCCCAGCA	55	83	173
Nephrin	ATCGCCAAGCCTTCACAGGTA GACCTCAGGCCAGCGAAGG	58	85	155
Nfatc1	GGTGGCCTCGAACCCTATC TCAGTCTTTGCTTCCATCTCCC	55	86	204
Oct-4	GGCGTTCTCTTTGGAAAGGTGTTC CTCGAACCACATCCTTCTCT	58	80	312
Pax-2	AGACTCGGCCGGAGACTGAGC GGGCTGGGCGAGTTAGGACTG	62	88	461
Pax-6	GAGAAGAGAAGAGAAACTGAGGAACCAGA ATGGGTTGGCAAAGCACTGTACG	58	80	201
Pax-8	TGTTTGCTTGGGAGATCCGGGAC CCACTGCTGCTGCTCTGTGAGTCGAT	58	85	351
Podocalyxin	CCAGAGGAAGGACCAGCAA CACCTTCTTCTCCTGCATCT	58	80	120
Pod-1	CCAAGCTGGACACTCTCAGG CCATAAAGGGCCACGTCAG	58	82	120
Sox-2	GAGGAAAGGGTTCTTGCTGGGTTT GGTCTTGCCAGTACTTGCTCTCAT	55	72	142
Wnt-4	GTGGCCAACCTGGCGGAAGGG GTGGTGCCCAGCTGGCCATCG	65	88	491
Wnt-11	GTGAAGTGGGGAGACAGGCT CACGTCCTGGAGCTCTTGC	58	83	119

Sequences are listed in the order antisense, sense-primer. Primer sequences for Aquaporin-1, KSP, Nephrin, Podocalyxin, Pod-1, Wnt-11 (Bruce et al., 2007), Cadherin-11, Oct-4, Pax-6 (Vigneau et al., 2007), CDK-4 (Schmidt et al., 2007), and Lim-1, Pax-8 (Kramer et al., 2006) have been previously published. BMP2, BMP4, c-Myc, Klf-4, Nanog, and Sox-2 primers were graciously provided by the laboratory of Trish Labosky.

Experimental mouse models for PTPC isolation

NFATc1-P2-LacZ mice

Our initial experimental approach was to use NFATc1-P2-LacZ mice and sort β-Gal+ PTPCs and compare them to β-Gal– PTCs. This approach allowed us to isolate the PTPC population actively expressing β-Gal by the NFATc1 enhancer throughout the time course of AKI. A complication of this approach was the requirement for incorporation of a fluorescent β-Gal substrate, ImaGene red, necessary for sorting. Because the β-Gal expressed by NFATc1-P2-LacZ mice is localized to the nucleus, the fluorescent substrate was required to cross both the extracellular and nuclear membranes. The ImaGene red substrate incorporated into cells as seen by fluorescent microscopy (data not shown). However, further staining with PI revealed that the staining protocol necessary to incorporate the ImaGene substrate was toxic as fluorescently labeled cells retained the PI label (data not shown).

NFATc1-P2-Cre//R26R-EYFP mice

As labeling of proximal tubules expressing a fluorescent reporter is key to the isolation of the progenitor population by flow cytometry, we adapted our experimental approach to use the NFATc1-P2-Cre mice and a conditional fluorescent reporter system, R26R-EYFP (enhanced yellow fluorescent protein) (Srinivas et al., 2001). In this line, an EYFP cDNA floxed by loxP sites has been targeted to the *ROSA26* locus. FACS has been successfully used in this cell line to isolate numerous cell types including pancreatic α-cells (Quoix et al., 2007).

An alternative labeling method was proposed to use an antibody to label the Cre reporter. However, similar to the problems we experiences trying to label the nuclear localized LacZ, Cre recombinase is nuclear localized thus trying to label cells that are actively expressing Cre would involve transport of an antibody or substrate across the nuclear membrane and was equally toxic.

As described in the previous chapter, the NFATc1-P2-Cre expressing cells should recombine the EYFP locus and express EYFP constitutively in all progeny. The EYFP positive cell population would be a heterogeneous population consisting of EYFP+ PTPCs and EYFP+ progeny. We would expect the labeled PTPC progeny to have a gene expression profile that is distinct from both the labeled PTPC and EYFP– PTC populations. 5 days after $HgCl_2$ injury, FACS analysis revealed that the R26R-EYFP reporter mice had fewer cells that had recombined the EYFP locus (data not shown) compared to the anticipated number based on our previous quantification (Fig. 4.4H). This was due either to the inefficiency of the NFATc1-P2-Cre to recombine the R26R-EYFP allele or from weak EYFP expression in the proximal tubule.

NFATc1-P2-Cre//Z/EG mice

Finally, we altered our strategy to use a robust fluorescent reporter, the transgenic Z/EG mice. The Z/EG transgenic mice constitutively express a floxed lacZ reporter and stop codon under the control of the CMV enhancer/chicken β-actin promoter and, following Cre mediated recombination, the lacZ gene and polyadenylation sequence is excised allowing the second reporter, green fluorescent protein (GFP) to be expressed constitutively (Novak et al., 2000). When *NFATc1-P2-Cre//Z/EG* mice are treated with

$HgCl_2$ to induce AKI, the NFATc1-P2-Cre should be activated in the PTPCs activating expression of GFP, and because GFP expression is constitutive, all progeny will express GFP allowing for further analysis of this lineage. GFP+ and GFP– populations were analyzed using FACS, as described below.

Results

FACS with NFATc1-P2-Cre//Z/EG mice

NFATc1-P2-Cre//Z/EG treated with $HgCl_2$ were analyzed after 5 and 10 days and compared to mice that were not treated with $HgCl_2$. Cryosections were stained with X-Gal to report LacZ activity and GFP activity was analyzed in kidney cortex slices. Before treatment with $HgCl_2$, NFATc1-P2-Cre was not expressed in any tubule epithelial, glomerular, or interstitial cell population as seen by ubiquitous X-Gal staining suggesting that there was no recombination (Fig. 5.1A). Ten days after injury, ubiquitous X-Gal staining was observed in distal tubules and in the glomerulus (Fig. 5.1B, inset) but not in proximal tubules. The increased dose of $HgCl_2$ administered to *NFATc1-P2-Cre//Z/EG* mice increased the number of proximal tubules that demonstrate recombination and excision of the LacZ reporter compared to R26R reporter recombination presented in Chapter IV. At an earlier time point 5 days after injury, GFP expression was observed in the outer cortex (OC) and inner cortex (IC, Fig. 5.1C). GFP expression was observed in proximal tubules and no GFP expression was observed in the glomeruli (Fig. 5.1D). GFP expression was also observed in other cell types. We would predict that the additional, non-PTCs populations expressing GFP are endothelial cells that form interstitial blood

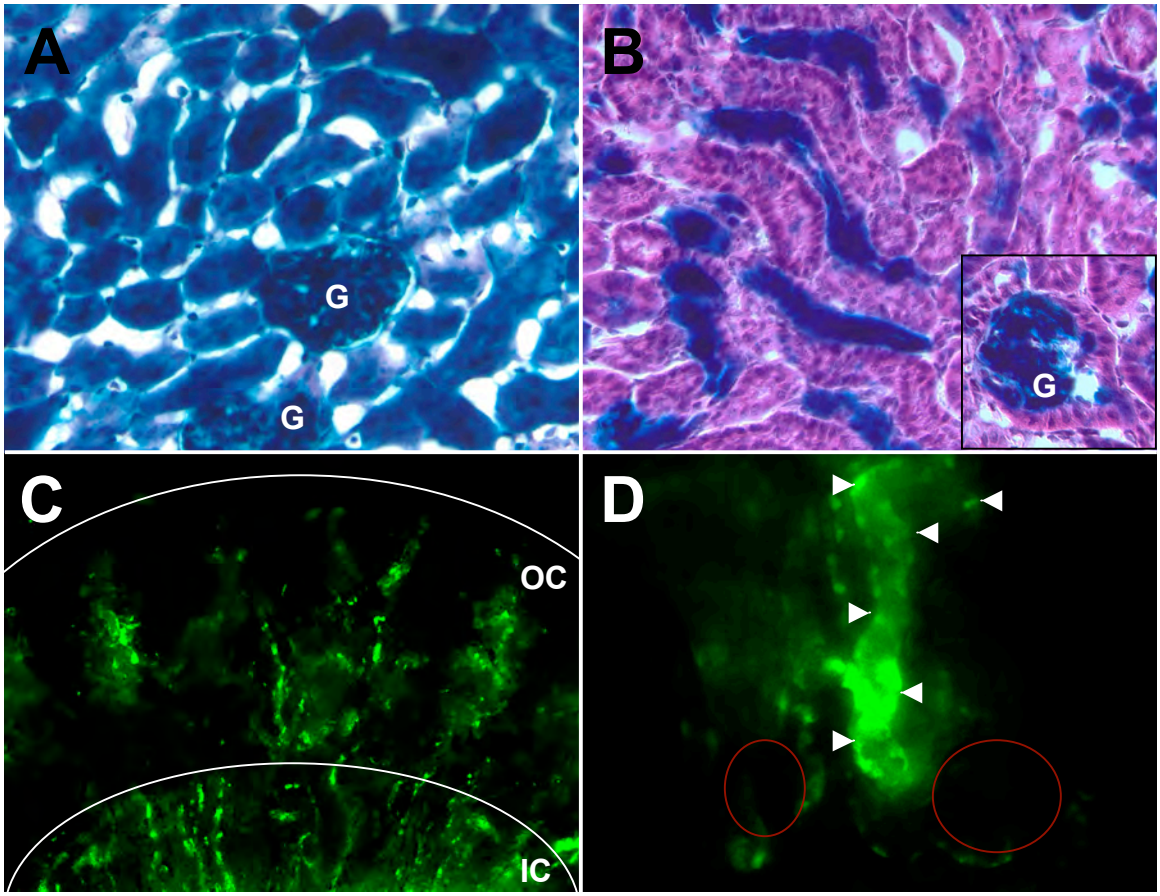

Figure 5.1. ***Expression of LacZ and GFP in NFATc1-P2-Cre//Z/EG before and after $HgCl_2$ injury.*** **A.** Before $HgCl_2$ treatment, NFATc1-P2-Cre is not expressed in any tubule epithelial, glomerular, or interstitial cell population as seen by X-Gal staining. **B.** 10 days after injury, X-Gal staining is observed in distal tubules and in the glomerulus (inset) but not in proximal tubules. **C.** 5 days after injury, GFP expression observed in the outer cortex (OC) and inner cortex (IC). 300mm optical slice. **D.** High power magnification of shows staining in the proximal tubule (arrowheads) and no staining in the glomeruli (red ellipses). 75um optical slice. Magnification: A,B 100X; C, 40X; D, 200X.

vessels and smooth muscle cells, as the NFATc1-P2-LacZ reporter was expressed in this population. Attempts to use anti-GFP antibody for dual immunofluorescence in combination with other cell specific antibodies to confirm the identity of these populations was unsuccessful. However, the single cell population was able to be labeled with PTC specific biotinylated-LTL and streptavidin-APC allowed for PTCs to be distinguished from non-PTCs by FACS analysis.

Populations of cells, GFP+ PTCs and GFP– PTCs were analyzed and sorted by flow cytometry before treatment with $HgCl_2$ and 5 days after $HgCl_2$ induced AKI (Fig. 5.2). We calculated the percentage of GFP+ PTCs and GFP– PTCs in the total cell population - all cellular events recorded that includes both PTCs and non-PTCs - and as the percentage of the defined cell population – restrictions placed on the total cell population to gate for cell viability, cell size, and intensity of the fluorescent labeling (Table 5.2). The viability of the single cell suspension was measured using PI labeling to record the percentage of cells that exclude PI. We documented that 83.1% and 67.9% of the defined cell population was viable at day 0, and day 5, respectively. Treatment with $HgCl_2$ did not significantly reduce viability in either the total cell population or the defined cell population.

Proximal tubule cells were labeled using biotinylated-LTL and streptavidin-APC. We treated *NFATc1-P2-Cre//Z/EG* mice with $HgCl_2$ and sorted GFP+ PTCs and GFP– PTCs 3 days after injury. There was an insignificant increase in the GFP+ PTC population, which comprised 0.45% of the defined population of cells and 0.1% of the total cell population. We were unable to isolate RNA from this population, and therefore used the samples isolated at day 5 for gene profile analysis. Treatment with $HgCl_2$ did not

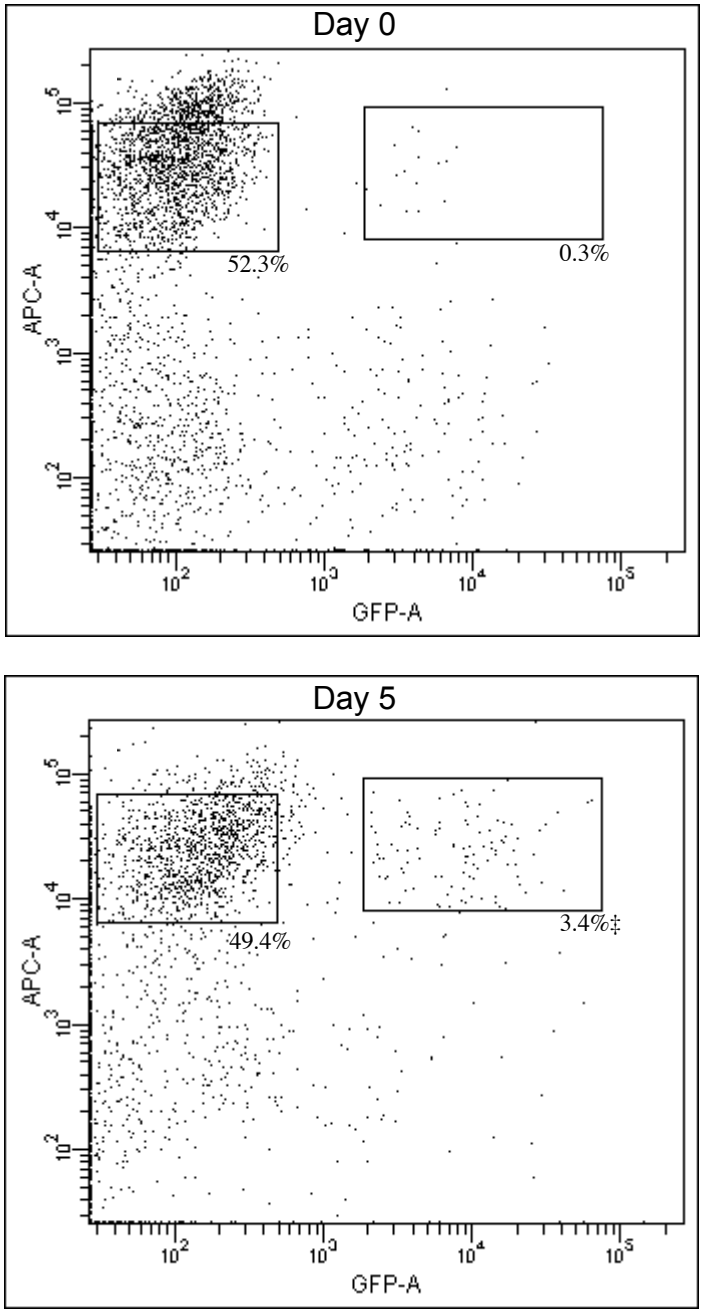

Figure 5.2. ***Quantification of FACS to sort GFP+ PTC and GFP– PTPC.*** GFP+ PTCs are significantly increased 5 days after $HgCl_2$ treatment compared to untreated samples at day 0 (‡, p=0.0001, student's T-test). GFP was constitutively expressed following NFATc1-P2-Cre expression and recombination of the Z/EG transgenic allele. APC fluorescently labeled proximal tubule cells using biotinylated-LTL and streptavidin-APC. The same numbers of events are shown in each dot plots and the percentages are representative of the viable cells sorted in 3 independent samples.

Table 5.2. FACS: percentage of viable, GFP+ PTC, and GFP– PTC populations.

Time Point	Sample	Defined Cells (%)	Total Events (%)
Day 0	Viable cells	83.1 ± 1.7	18.5 ± 7.0
	APC+GFP–	52.3 ± 9.6	16.6 ± 6.6
	APC+GFP+	0.3 ± 0.1	0.13 ± 0.07
Day 5	Viable cells	67.9 ± 2.1	42.5 ± 0.6
	APC+GFP–	49.4 ± 8.8	25.3 ± 7.9
	APC+GFP+	3.4 ± 0.2‡	1.7 ± 0.2†

Percentages are for 3 independently sorted samples; mean ± SEM. Statistics comparing Day 0 and Day 5 cell populations using student's T-test. ‡p = 0.0001, †p=0.003.

significantly change the number of GPF– PTCs (APC+GFP–) in the total cell population or the defined cell population 5 days after injury. Prior to treatment with $HgCl_2$, 0.3% of the sorted population was GFP+, suggesting that this population is a quiescent progenitor population (discussed in Chapter VI). 5 days after treatment with $HgCl_2$, there was a significant increase in the number GFP+ cells as 3.4% of the defined cell population was GFP+ PTCs (APC+GFP+).

Nfatc1 transcription is increased in GFP+ PTCs

After obtaining 3 independently sorted populations of GFP+ PTCs and GFP– PTCs 5 days after $HgCl_2$ injury, gene expression profiles were analyzed using qRT-PCR. Nfatc1 expression was increased 2-fold in the GFP+ PTCs compared to GFP– PTCs (Fig. 5.3). Nfatc1 expression accentuated in the GFP+ PTCs after $HgCl_2$ induced AKI confirmed that the increase in Nfatc1 observed previously over the time course of AKI in renal cortex samples and increased protein in isolated proximal tubule (Fig. 2.3, Fig 2.5) was in the GFP+ PTCs.

GFP+ PTCs are fully differentiated proximal tubules and have decreased transcription of mesenchymal and glomerular markers

We analyzed the transcription of genes expressed in fully differentiated proximal tubules: Aquaporin 1, KAP, KSP, and Lim1 (Fig. 5.3). Aquaporin 1 is expressed in convoluted and straight proximal tubules and the thin descending limb (Sabolic et al., 1992). KAP or kidney androgen-regulated protein is expressed in the S3 segment of the proximal tubule because and in the S1/S2 segment of the proximal tubule in male mice and in androgen-induced females (Meseguer and Catterall, 1990). KSP or Kidney

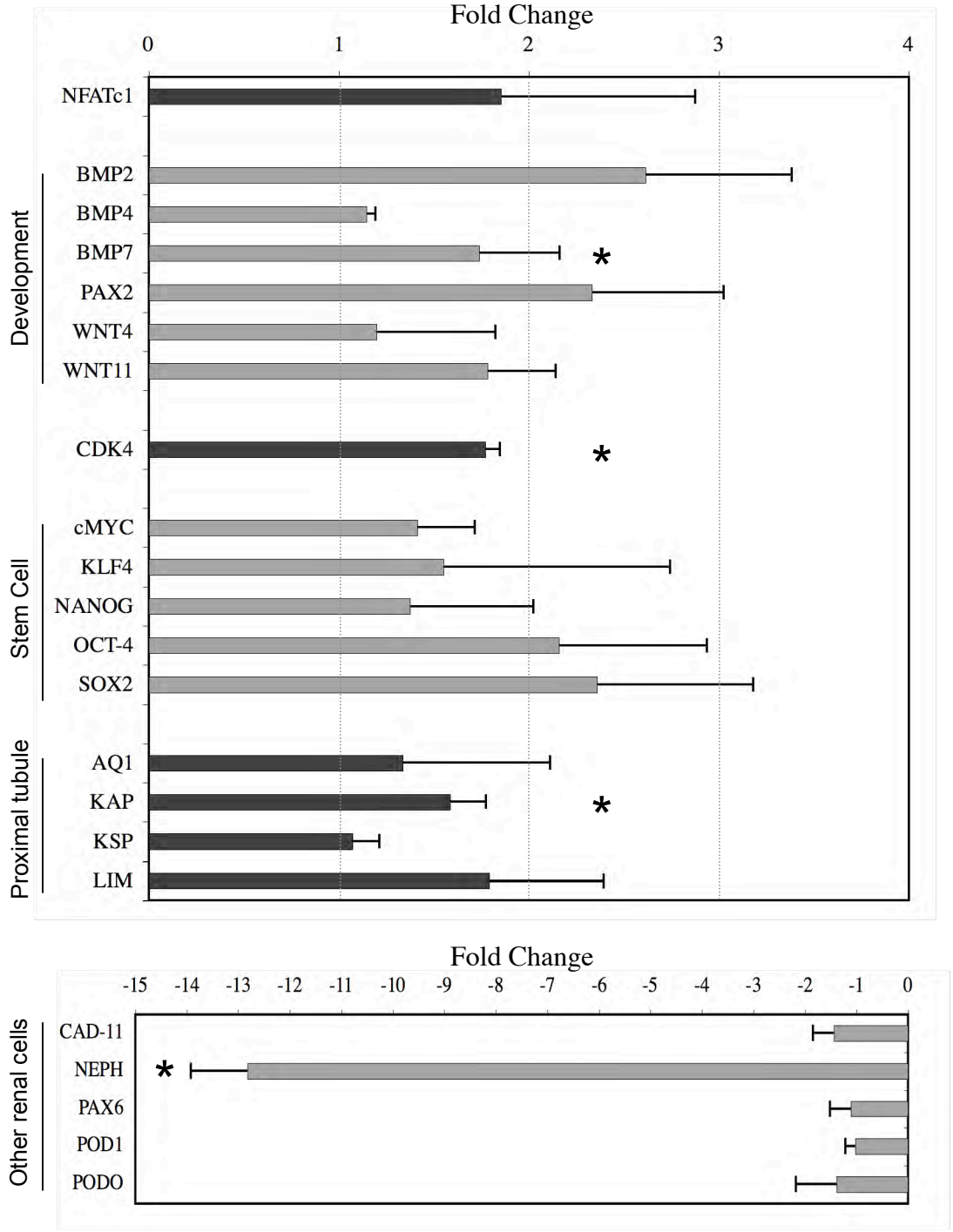

Figure 5.3. ***qRT-PCR analysis of NFATc1 and markers of tubular development, stem cells, differentiated proximal tubules, and other renal cell populations in GFP+ PTCs compared to GFP– PTCs.*** cDNA samples were derived from 3 independently sorted GFP+ PTC and GFP– PTC samples. Fold change in expression of GFP+ PTCs compared to GFP- PTCs is represented as mean ± SEM. (*, $p<0.05$, Mann-Whitney U)

specific protein (also known as cadherin 16) is expressed in proximal and distal tubules (Igarashi, 2003). Lim1 alternatively named Lhx1, plays an important role in patterning the segmental tubular structures of the nephron (Kobayashi et al., 2005). The expression of these proximal tubule markers were either slightly increased (AQ1, KAP, LIM) or unchanged (KSP) in the GFP+ PTCs compared to the GFP– PTCs suggesting that GFP+ PTCs are differentiated proximal tubules and are not undergoing a program of dedifferentiation or EMT.

Transcription of developmental markers is increased in GFP+ PTCs

Expression of genes known to be expressed during kidney development in the condensed metanephric mesenchyme (Pax-2, Wnt-4), developing tubules (BMP7, Lim-1, Wnt4) and ureteric bud tips (BMP7, Pax-2, Wnt11) were increased in GFP+ PTCs compared to GFP– PTCs (Fig. 5.3). Pax-2, the paired-box DNA-binding transcription factor expression was observed in stem cells isolated from the metanephric mesenchyme (Gupta et al., 2006). BMP-7 expression was not observed in adult proximal tubule cells, but has been proposed to possibly have therapeutic benefit following AKI (Kopp, 2002). Adult rats administered ^{125}I-labeled BMP7 showed that the labeled BMP7 bound to proximal convoluted tubules and was used to identify BMPR-II in the proximal tubule (Bosukonda et al., 2000) and significant increase in BMP7 expression in the PTPCs may contribute to the repair process.

Transcription of stem cell markers is increased in PTPCs

Induced pluripotent stem cells (iPSC) have been shown to be derived from murine and human somatic cells by inducing the expression of several ES cell genes including c-Myc, Klf-4, Nanog, Oct-3/4, and Sox-2 (Nakagawa et al., 2008; Okita et al., 2007; Yu et al., 2007b). We analyzed the expression of these stem cell markers c-Myc, Klf-4, Nanog, Oct-4, and Sox-2 using qRT-PCR in order to evaluate the "stemness" of the GFP+ PTCs (Fig. 5.3). Expression of c-Myc, Klf-4, and Nanog was increased 1.5-fold in the GFP+ PTCs compared to GFP– PTCs. c-Myc is a transcription factor that regulates proliferation and constitutive expression of c-Myc in iPSC leads to formation of teratomas. Klf-4 is a member of the Kruppel-like factor family of zinc-finger proteins that share amino acid sequence homology with the Drosophila embryonic pattern regulator Kruppel. Nanog was expressed in pluripotent stem cells in vivo and in vitro and loss of Nanog expression was associated with stem cell differentiation.

Expression of Oct-4 and Sox-2 was increased 2-fold in the GFP+ PTCs compared to GFP– PTCs (Fig. 5.3). Oct-3 and Oct-4 belong to the octamer-binding (Oct) family of transcription factors also known as the POU family of transcription factors expressed in pluripotent undifferentiated embryonic and adult stem cells. Sox-2, a member of the sex-determining region of the Y chromosome (SRY-related) high-mobility group (HMG) box (SOX) family of transcription factors, maintains the self-renewal of undifferentiated stem cells. The increased expression of these genes in the GFP+ PTCs is suggestive that this subset of PTCs represents a progenitor cell population.

In addition, we looked at expression of BMP2, BMP4 and cyclin-dependent kinase 4 (CDK4) as these genes have recently been shown together with NFATc1 to

control quiescence and proliferation of stem cells in the hair follicle (Horsley et al., 2008). In hair follicle bulge cells, BMP signaling increased expression of NFATc1 in turn inhibiting CDK4 activity, maintaining quiescence in these stem cells and attenuation of NFATc1 signaling increased CDK4 expression and activated proliferation in the stem cells (Horsley et al., 2008). CDK4 inhibits proliferation by blocking the G0-G1 transition and progresses proliferation by promoting G1-S [reviewed in (Malumbres and Barbacid, 2005)]. In mice, CDK4 expression was increased in renal tubule epithelial cells during the phase of proliferation following I/R injury (Park et al., 1997). The qRT-PCR analysis performed showed a significant increase in CDK4 expression, a 2.5-fold increase in BMP2 expression, and slight increase in BMP4 expression in the GFP+ PTCs compared to GFP– PTCs.

Because the GFP+ PTCs express markers of pluripotent ES cells, we questioned if they had potential to adopt other fates in order to repair other damaged cell populations of the kidney. Genes expressed in mature podocytes (Nephrin, Pod-1, Podocalyxin) and metanephric mesenchyme (Cadherin11) were downregulated in GFP+ PTCs. Expression of Nephrin was significantly decreased in the GFP+ PTC population. The decrease in expression of glomerular and mesenchymal markers further supports that the GFP+ PTCs are a differentiated progenitor cell population and that the GFP+ PTCs are not initiating transformation to undergo EMT.

Discussion

Here we describe the use of flow cytometry to isolate GFP+ and GFP- PTCs from *NFATc1-P2-Cre//Z/EG* mice after $HgCl_2$ induced AKI. The NFATc1-P2-Cre is a novel

transgenic resource and we believe that we are the first to describe the use of a transgenic model system to identify and perform lineage tracing on a renal progenitor cell population that regenerates the damaged nephron following AKI.

GFP+ PTCs and GFP– PTCs were isolated in order to characterize the gene expression profile that defined the PTPCs accentuated by NFATc1 expression and their progeny following AKI and to identify how that expression profile differed from the GFP– PTCs. qRT-PCR performed on these cell populations showed that NFATc1 expression was increased in the GFP+ PTCs. In addition, the GFP+ PTCs had increased expression of differentiated proximal tubule markers, tubular development markers, and markers of pluripotent stem cells. It is possible that adult renal stem cell population, MRPC previously identified by Gupta *et al*. could be the population of PTPCs identified here (Gupta et al., 2006). MRPC were identified to be a tubular epithelial cell population characterized by expression of Oct-4 and Pax-2 and the gene expression profile of the GFP+ PTCs showed increased transcription of Oct-4 and Pax-2 compared to GFP- PTCs. However, this gene expression profile is complex and further analyses are necessary to determine the differences in the gene expression profile of the GFP+ progeny and GFP+ PTPCs accentuated by NFATc1 and the localization of proximal tubule, stem cell, and developmental markers in each population, as proposed in Chapter VI.

Lineage analysis of the NFATc1-P2-Cre//R26R mice over the $HgCl_2$ time course allowed us to estimate the heterogeneity of the GFP+ PTC population (Fig. 4.4H). As shown in Figure 4.4G, at day 5 there was an increase in number of XGal+BrdU– progeny compared to XGal+BrdU+ PTPCs. Thus, we would estimate that the population of GFP+ PTCs contains more GFP+ progeny than GFP+ PTPCs accentuated by NFATc1.

However, this estimate was approximate due to the short 2-hour BrdU pulse. The GFP+ PTC progeny could have a gene expression profile that is distinct from both the GFP+ PTPCs and GFP- PTCs, which could not be analyzed with this FACS analysis model system.

Our initial experimental design proposed to use NFATc1-P2-LacZ mice to characterize the gene expression profile that defined the subpopulation of PTCs accentuated by NFATc1 expression (PTPCs) compared to PTCs that were unlabeled. However, the fluorescent substrate required to label the NFATc1-P2-LacZ reporter for flow cytometry was toxic. Subsequently, we used the NFATc1-P2-Cre mice crossed with conditional fluorescent reporter. The most significant limitation of this approach is that it results in identification and subsequent sorting of a heterogeneous population of cells. There are at least two distinct populations of cells that should be sorted: 1) the parent population and 2) the progeny. As expression of the NFATc1-P2-Cre labeled PTPCs as well as their progeny with GFP, we would be analyzing the difference in the gene expression profile that defines the GFP+ PTC – a heterogeneous population of PTPCs and their progeny- compared to GFP– PTCs.

A limitation to the use of the NFATc1-P2-Cre mice is that expression of Cre recombines the Z/EG reporter allowing for constitutive expression of GFP in a population of PTPCs, as described in Chapter IV, and the expression of the GFP reporter is inherited by their progeny. Therefore, our gene expression profile analyzed the changes in expression of candidate genes of the GFP– PTCs compared to the GFP+ PTCs – a heterogeneous population that contained the PTPCs accentuated by NFATc1 expression and their GFP+ progeny. This could explain the results of our gene expression profile

analysis where we measured increased expression of stem cell and tubular developmental markers, which are likely to be upregulated in the PTPC parent population and an increase in the expression of mature proximal tubule markers, which are likely to be upregulated in the progeny of PTPCs. The increase expression of CDK4 and Nfatc1 suggest that regulation of cell cycle progression in PTPCs is likely via a different mechanism than in the bulge cells of the hair follicle. In GFP+ PTCs, BMP7 expression and CDK4 expression were significantly increased and act may act synergistically to promote progression through the cell cycle. In Chapter VI, I will outline future experiments and propose a new transgenic mouse line designed to isolate the PTPCs.

The data reported here should be important to the field of renal regenerative medicine, as this is the first report of a transgenic model system that has been used to genetically label a renal progenitor cell population and to monitor the subsequent proliferation and lineage analysis of this population in mice. Most importantly, we identify a resident progenitor population of cells that is fully differentiated expressing relatively unchanged levels of proximal tubule specific genes yet increasing the expression of stem cell markers and markers of tubular development. Using the transgenic tools available we were able to isolate and characterize the gene expression profile of GFP+ PTPCs and GFP+ progeny cells compared to GFP– PTCs. However, characterization of the gene expression profile that defines the subpopulation of PTPCs accentuated by *active* NFATc1 expression following AKI will require derivation of new transgenic reporter lines and is addressed in the final chapter.

CHAPTER VI

DISCUSSION AND FUTURE DIRECTIONS

The primary focus of my research was to determine the function of NFATc1 in murine renal proximal tubules over a time course of renal injury and regeneration. After documenting a phenotype in *Nfatc1*$^{+/-}$ mice, transgenic mice that express reporters under the control of NFATc1 regulatory elements were used to identify a resident population of PTPC. We analyzed the expression profile of candidate genes in this unanticipated population distinguished by accentuated NFATc1 expression. The work presented here lays the groundwork for studies to further characterize the role of NFATc1 in proximal tubule regeneration and should help advance the field of renal regenerative medicine by providing mechanisms to characterize this population of PTPCs. I will conclude with a discussion of the significance of identification of a self-renewing resident PTPC and suggest future experiments to further determine the function of NFATc1 in renal regeneration.

Model for the role of NFATc1 in proximal tubule injury and repair

We propose a model for the regeneration of PTCs (Fig. 6.1). When the proximal tubule is exposed to an injury stimulus, some of the PTCs undergo apoptosis, a population of PTCs survive but do not proliferate, and a third PTPC population, genetically marked using the NFATc1-P2 auto-amplification/enhancer domain, is resistant to apoptosis and proliferates under a program of self renewal to repair the

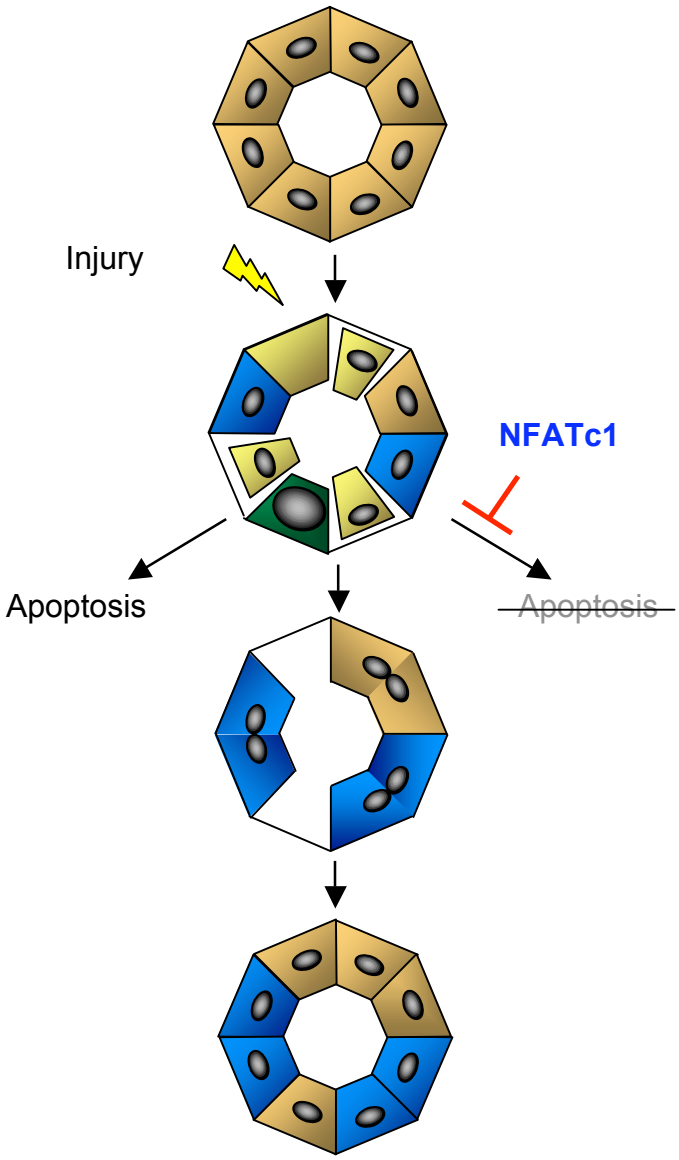

Figure 6.1. ***The proposed model for the role of NFATc1 in regenerating PTCs.*** See text for details.

damaged proximal tubule. While this study does not allow us to determine the contribution of non-Nfatc1 expression cells to PTC regeneration, it does document that a significant portion of the regenerated PTCs are derived from NFATc1 progeny. Further investigation is warranted to delineate the molecular basis for PTC heterogeneity and to enhance the regenerative activity of the resident progenitor population. Regulation of NFATc1 activation could have therapeutic benefits by providing a possible target for regeneration following acute and chronic injury. By specifically altering NFATc1 in PTCs, it may be possible to pharmacologically separate the immunosuppressive and nephrotoxic effects caused by calcineurin inhibitors and other pharmaceuticals and overcome the nephrotoxicity of environmental/occupational toxins.

NFATc1 in AKI and repair

Genetic attenuation of NFATc1

When I began my thesis research to investigate the role of NFATc1 in proximal tubules, there was little known about expression of NFATc1 in the kidney. NFATc proteins were shown to be expressed in cortical tubules of adult mice and during tubular development and NFATc1 was shown to be expressed in mesangial cells grown in culture (Puri et al., 2004; Sugimoto et al., 2001). We adopted a simple and reproducible model of AKI achieved by administering a single bolus of $HgCl_2$ in WT mice and mice with genetic deletion of one allele of Nfatc1, *Nfatc1*$^{+/-}$. This modest attenuation of NFATc1 expression resulted in increased apoptosis in PTCs, sustained tubular injury, delayed regeneration, and increased fibrosis in response to PTC injury. I further

demonstrated using qRT-PCR analysis and immunoblotting that NFATc1 mRNA and protein are upregulated during the period of regeneration following $HgCl_2$ induced AKI in WT mice. NFATc1 mRNA and protein are decreased in the *Nfatc1*$^{+/-}$ mice during the period of regeneration suggesting that even a modest attenuation of NFATc1 perturbs the normal course of regeneration.

Pharmaceutical attenuation of NFATc1 activity

Nfatc1$^{+/-}$ mice had a 20% reduction in transcription of Nfatc1 mRNA in the renal cortex and a 10% reduction of NFATc1 protein in the proximal tubule compared to WT *before* treatment with $HgCl_2$. In response to $HgCl_2$, we observed significant histopathological accentuation of renal injury. But, the serum creatinine and proliferation rates of the *Nfatc1*$^{+/-}$ mice were not significantly different compared to WT mice. This suggests that residual expression of NFATc1 in *Nfatc1*$^{+/-}$ mice is sufficient to maintain renal function. Because NFATc1 homozygous null mice die *in utero* from cardiovascular defects and are therefore not available for adult studies, we wanted to further reduced the amount of NFATc1 activity in the proximal tubule. WT mice were treated daily with CsA prior to and following $HgCl_2$ induced AKI. Treatment with both CsA and $HgCl_2$ resulted in elevated serum creatinine concentrations, interstitial fibrosis characterized by increased extracellular matrix deposition, and progression to renal failure and death not seen with either CsA or $HgCl_2$ treatment alone.

Mice treated with 5mgCsA/kg had a 20% reduction in Nfatc1 transcription in the renal cortex, similar to *Nfatc1*$^{+/-}$ mice and mice treated with 10mgCsA/kg had a 40% reduction in transcription of Nfatc1 in the renal cortex before $HgCl_2$ injury compared to

WT mice. Following $HgCl_2$ treatment, Nfatc1 transcription was suppressed in both 5mgCsA/kg and 10mgCsA/kg treated mice and was not significantly increased in 10mgCsA/kg treated mice. However, because of the toxicity and high mortality in mice treated with both $HgCl_2$ and 10mgCsA/kg and the pleiotropic effects of CsA, we were not able to attribute renal failure specifically to the severely damaged proximal tubule segment. Therefore, in order to address the requirement of NFATc1 expression in the proximal tubule segment during acute kidney injury, it will be necessary to develop a strategy for tissue specific and temporally regulated NFATc1 deletion.

PTC specific gene ablation

Throughout my graduate career, we have been working with Dr. Bin Zhou to create a conditional floxed NFATc1 allele to remove the RHD and germ line transmission of a floxed NFATc1 allele has been established. During the preparation of this dissertation, Horsley *et al* published work with a conditional allele of NFATc1 (*Nfatc1fl*) that was generated by flanking exon 3 with lox P sites, which excises the NHR domain following Cre mediated recombination (Horsley et al., 2008). An important issue that I was not able to address during my thesis work was how regeneration of the proximal tubule segment is affected when NFATc1 is not expressed in this population. To address this important question, mice containing the *Nfatc1fl* allele should be breed with R26R reporter mice and their progeny should be breed with mice containing a proximal tubule specific Cre, sglt2-Cre (Rubera et al., 2004). Sglt2 is a low-affinity sodium-dependent glucose cotransporter that is involved in glucose reabsorption in the S1, S2, and S3 segments of the proximal tubule (Tabatabai et al., 2001; Wright, 2001;

You et al., 1995). The sglt2-Cre strain of mice were created by fusing the 5' upstream promoter region, the first exon, the first intron, and part of the second exon of sglt2 to the Cre coding sequence (Rubera et al., 2004). By crossing the sglt2-cre mice with R26R reporter mice, X-Gal staining confirmed proximal tubular specificity and importantly no Cre activity was detected in the lung, intestine, colon, liver, heart, brain, spleen, and muscle (Rubera et al., 2004). *Nfatc1fl/fl//sglt2-Cre* mice could be used to study the role of NFATc1 in all PTCs over the course of AKI and regeneration. We would expect to see intense injury in the proximal tubule segment marked by vast apoptosis, elevated serum creatinine levels and possible mortality.

Because the *Nfatc1*$^{-/-}$ mice die at E13.5, we were unable to study NFATc1 in later stages of renal development *in vivo*. *In vitro* organ culture experiments performed with E11.5 kidney rudiments isolated from WT, *Nfatc1*$^{+/-}$, and *Nfatc1*$^{-/-}$ did not reveal obvious defects in branching of the ureteric bud (data not shown). Furthermore, *in vitro* metanephric culture conditions do not fully recapitulate *in vivo* renal development as the interstitium and glomeruli are not vascularized. To further investigate if NFATc1 causes renal defects, I engrafted WT and *Nfatc1*$^{-/-}$ E13.5 kidneys under the renal capsule of SCID mice. When engrafted under the renal capsule of adult SCID mice, the structural integrity of the transplanted embryonic kidney rudiment is preserved, normal structure of the glomeruli is maintained, wastes are excreted into the host tissue, and the engrafted tissue becomes vascularized by blood vessels of the host kidney (Hammerman, 2004). We did not identify abnormal renal development in *Nfatc1*$^{-/-}$ kidneys transplanted into normal hosts (data not shown). Thus, we would anticipate that deletion of NFATc1 in the PTC would not result in significant renal developmental abnormalities.

We would expect *Nfatc1fl/fl* to be excised *in utero* as sglt2 is expressed in differentiated PTCs. Deletion of NFATc1 from PTCs may subsequently decrease nephrogenesis and result in post-natal renal failure or mortality, as discussed above. Alternatively, if sglt2-Cre is not efficient in deleting *Nfatc1fl/fl*, the *Nfatc1fl* allele could be deleted by crossing *Nfatc1fl/fl* mice with alternative Cre reporters such as Pax2-Cre to delete NFATc1 from the developing metanephric mesenchyme and Wolffian duct (Dressler et al., 1990; Ohyama and Groves, 2004) or KSP-Cre to delete NFATc1 in renal tubules, collecting duct and ureter (Shao et al., 2002). We would not expect conditional deletion of NFATc1 in this expanded population to attenuate nephrogenesis but may heighten renal injury following $HgCl_2$ induced AKI.

AKI and PTPC specific NFATc1 deletion

A different experimental approach would be to study the role of NFATc1 deletion in the PTPC population by conditionally deleting the *Nfatc1fl/fl* allele specifically in the PTPCs using the NFATc1-P2-Cre mice. *NFATc1fl/fl//NFATc1-P2-Cre* mice would develop normally as NFATc1-P2-Cre is not activated in this population until after $HgCl_2$ injury. Following AKI, we would expect to see ablation of the PTPC population and severe injury as we propose that the work presented here identifies a self-renewing progenitor cell population that is resident in the proximal tubule segment and regenerates the PTC segment following AKI. The qRT-PCR data presented in Chapter 5 suggests that NFATc1 controls cell-cycle progression. Therefore, *NFATc1fl/fl//NFATc1-P2-Cre* mice would have little if any proliferation following $HgCl_2$ induced AKI as only a small percentage of unlabeled PTCs proliferate (Fig. 4.4). However, NFATc1-P2-Cre is

expressed in endocardial cells and attenuation of NFATc1 is likely to result in embryonic lethality due to cardiac valve defects as previously described (de la Pompa et al., 1998; Ranger et al., 1998a). *Nfatc1fl/fl//NFATc1-P2-Cre* mice could be crossed with *Tie2-NFATc1* mice, a transgenic line which rescues the endocardial defects of *Nfatc1*$^{-/-}$ mice (Chang et al., 2004b). Alternatively, it could be necessary to create an inducible transgenic NFATc1-P2-Cre-ER line. Cre-ER is a fusion protein linking Cre recombinase to the ligand-binding domain of the human estrogen receptor allowing for constitutive expression of in active Cre-ER that becomes activated upon treatment with the estrogen homolog 4-hydroxytamoxifen (Metzger et al., 1995). Thus, activation of Cre in the developing endocardial cells would be prevented, as treatment with 4-hydroxytamoxifen would be postponed until after induction of AKI.

Protection from renal injury

An additional experimental approach would be to express constitutively active NFATc1 in proximal tubules in an attempt to expand the population of cells that demonstrate accentuated NFATc1 expression. A constitutively active mutant version of NFATc1 (caNFATc1) was created by introducing serine to alanine mutations in the conserved SRR, SPXX, and SP2/3 motifs (Neal and Clipstone, 2001). However, interestingly ectopic expression of caNFATc1 in T cells resulted in increased gene expression resembling the pattern of expression observed in activated T cells without requiring induction events necessary for activation (Porter and Clipstone, 2002). Ectopic expression of caNFATc1 has been shown to have oncogenic effects. In 3T3-L1 cells, a preadipocyte cell line, inhibited 3T3-L1 cells from differentiating into mature adipocytes

(Neal and Clipstone, 2003). 3T3-L1 cells acquired growth factor autonomy subsequently protecting cells from apoptosis and promoting proliferation following growth factor deprivation and transformed 3T3-L1 cells formed tumors when engrafted suggesting that NFATc1 could function as an oncogene (Neal and Clipstone, 2003). Such "oncogenic" effects might be advantageous to PTPCs in the face of $HgCl_2$ induced AKI.

In order to express caNFATc1 in all PTCs, a new transgenic allele would need to be created. A clone containing a loxP-flanked stop codon followed by the caNFATc1 coding sequence could be synthesized and inserted into the ubiquitous *ROSA26* locus (R26R-caNFATc1). Expression of caNFATc1 would be induced in all PTCs using sglt2-Cre and Cre activity monitored using the R26R reporter. The use of the ubiquitous *ROSA26* locus would allow for a theoretical 1-fold increase in caNFATc1 activity in PTCs of *R26R/R26R-caNFATc1//sglt2-Cre* mice and a theoretical 2-fold increase in caNFATc1 activity in PTCs of *R26R-caNFATc1/R26R-caNFATc1//sglt2-Cre* mice. Proliferation markers such as PCNA, phosphorylated-histone H3 and BrdU pulse-chase labeling in conjunction with proximal tubule markers such as LTL and megalin would be used to analyze changes in the rate of proliferation of PTCs before and after AKI. We would expect to see a dramatic increase in proximal tubule proliferation during the period of postnatal development and following AKI. As caNFATc1 expression has been proposed to function as an oncogene (Neal and Clipstone, 2003), ectopic expression of caNFATc1 could result in excessive PTC proliferation in response to AKI or the formation of renal adenoma/carcinoma due to hyperproliferation of the proximal tubule segment during postnatal development.

CsA nephrotoxicity

Knowing that genetic attenuation of one allele of Nfatc1 resulted in increased apoptosis and sustained AKI but not in significant changes in PTC proliferation or serum creatinine concentration, we sought to pharmacologically inhibit NFATc1 transcription in mice using the calcineurin inhibitor, CsA. Calcineurin isoforms, Aα and Aβ, were identified in the proximal tubule (Tumlin et al., 1995) and NFATc proteins have been identified in cortical tubules (Puri et al., 2004). The localization of NFATc1-calcineurin signaling proteins in the proximal tubule suggests that suppression of NFATc1 activity might contribute to the nephrotoxicity and interstitial fibrosis associated with chronic nephrotoxicity associated with CsA administration. However, the nephrotoxicity of CsA is pleiotropic having dramatic responses in endothelial, epithelial, fibroblast, and immune cells (Esposito et al., 2000b).

The important observation made in these studies is that neither low dose nor high dose of CsA was associated with detectable nephrotoxicity in the absence of AKI. However, combined treatment with CsA and $HgCl_2$ in WT mice reduces NFATc1 expression, elevates serum creatinine concentrations, decreases proliferation, increases interstitial fibrosis, and increases apoptosis in PTCs compared to WT mice treated with either CsA or $HgCl_2$. Initial treatment with low and high doses of CsA showed characteristic morphological features of tubular epithelial injury marked by vacuolization, but continued treatment with CsA alone does not compound the initial damage to the PTCs over the brief period of our study (data not shown). Thus while, some of the nephrotoxicity related to administration of calcineurin inhibitors are thought to arise from secondary renal and systemic vasoconstriction, increased release of endothelin-1,

decreased nitric oxide production and increased TGF-β expression [rev. in (Olyaei et al., 2001)], our data would suggest that CsA also renders the proximal tubule particularly vulnerable to toxic injuries that would otherwise be well tolerated and thus provides additional insights into the pathology of immunosuppressive nephropathy.

The toxicity and involvement of NFATc1 in proximal tubule regeneration and the injury from $HgCl_2$ and CsA share a common phenotype with nephrotoxicity caused by the ifosfamide-metabolite chloroacetaldehyde (CAA). Ifosfamide is a commonly prescribed chemotherapeutic drug used both in pediatric and adult oncology with cytotoxic side effects including hemorrhagic cystitis and nephrotoxicity. While most patients report only acute nephrotoxicity, chronic nephrotoxicity can lead to the development of renal Fanconi syndrome, which is characterized by aminoaciduria, glucosuria, proteinuria, and urinary loss of phosphate and other electrolytes even after discontinued use (Skinner, 2003). CAA induces cell death primarily in proximal tubule cells through necrosis rather than through apoptosis (Schwerdt et al., 2006) and disrupts intracellular concentrations of calcium (Benesic et al., 2005). Interestingly, members of the NFAT-calcineurin signaling pathway including NFATc1 were reduced in human renal proximal tubule epithelial cells (hRPTEC) following exposure to CAA (Benesic et al., 2006). The nephrotoxicity associated with CsA and CAA confirms the importance of calcium homeostasis in the proximal tubule and supports a role for NFATc1 mediated transcriptional regulation in the proximal tubule. Thus, perturbation of NFATc1 activity may be a common component in the mechanism of AKI induced by multiple agents.

Progenitor proximal tubule population

Following an AKI, the precise origin of cells that proliferate in order to regenerate the proximal tubule segment is unknown. As discussed in Chapter I, it has been postulated that these cells arise from an external stem cell population circulating in the blood stream, adjacent less injured cells, or a resident renal stem cell population (Gupta et al., 2006; Morigi et al., 2006a; Sagrinati et al., 2006) (Fig. 1.2). The identification of renal progenitor cells has been difficult because such a population remains phenotypically indistinguishable from their terminally differentiated counterparts. Using NFATc1-P2-LacZ mice, we were able to identify a subpopulation of apoptosis resistant PTCs characterized by autoamplification of NFATc1 as marked by reporter activation and expression following $HgCl_2$ injury. In addition, a novel transgenic reporter mouse line, NFATc12-P2-Cre, confirmed that the resident subpopulation of PTCs serve as a progenitor cell population to regenerate the damaged proximal tubule segment after $HgCl_2$ induced AKI. As described in Chapter IV, less than 1% of the PTCs could be identified as precursor cells before AKI. This number increased to 5% by day 3 following $HgCl_2$ injury and progeny of this discrete population ultimately accounted for 27% of the PTCs following repair at day 10 (Fig. 4.4).

Role for NFATc1 in regulating quiescence and proliferation

As this is the first report identifying a role for NFATc1 in the proximal tubule, the transcriptional targets of NFATc1 in PTPCs following $HgCl_2$ mediated AKI are unknown. Roles for NFATc1 in regulating quiescence and proliferation and maintenance of cellular integrity have been described in the formation/resorbtion of bone and in

controlling pancreatic β-cell mass. NFATc1 is activated and promotes proliferation of osteoblasts that are derived from multipotent mesenchymal progenitor cells to form new bone and, NFATc1 is required for the lineage specification of osteoclasts, derived from hematopoietic cells, to resorb bone. Calcineurin/NFATc1 signaling enhances chemokine expression and secretion to recruit osteoclast precursors thus stimulating proliferation and inhibition of the calcineurin/NFATc1 signaling pathway disrupts bone homeostasis causing osteopetrosis (Winslow et al., 2006). Mice with calcineurin B1 conditionally deleted from β-cells in the pancreas develop age-dependent diabetes and have decreased β-cell proliferation and mass. Constitutive nuclear expression of NFATc1 in calcineurin B1 null β-cells rescues the phenotype by increasing β-cell proliferation and mass. In addition, NFATc1 increases the expression of cell cycle regulators and β-cell genes and treatment with CsA to inhibit calcineurin/NFATc1 signaling caused diabetes (Heit et al., 2006).

A similar mechanism may be occurring in the PTPCs: low levels of NFATc1 expression in the PTPC population maintains cellular quiescence in the uninjured kidney and triggers rapid proliferation and regeneration of the proximal tubule segment following injury. The lineage analysis and isolation of PTPCs suggests that expression of NFATc1 is not induced in this population until after an injury stimulus. However, flow cytometry experiments suggest that prior to treatment with $HgCl_2$, 0.3% of the defined cell population was GFP+ (Fig 5.2). Previously, when we quantified the percentage of proximal tubules that a very small percentage of cells, 0.03%, expressed NFATc1-P2-Cre and stained with X-Gal, prior to treatment with $HgCl_2$. The discrepancy between these measurements could be due to the increased sensitivity of identifying the fluorescent GFP

reporter compared to enzymatic reaction and substrate staining with X-Gal to identify expression of β-Gal. This finding is significant as it suggests that prior to AKI, the NFATc1 may be active in a small population of proximal tubule cells that quiescent, a finding that is similar to the function of NFATc1 in maintaining the quiescence of stem cells of the hair follicle (Horsley et al., 2008). However, the low incidence of labeled cells prior to AKI would require several animals to be pooled before sorting. To further analyze this, GFP+ PTPCs from uninjured kidneys could be sorted and analyzed for DNA content to analyze progression through the cell cycle. GFP+ cells could be cultured *in vitro*, and treated with CsA, $HgCl_2$, growth factors, or antagonists or transfected with gene of interest to analyze factors that balance quiescence and proliferation.

NFATc1 expression has been recently identified in bulge cells, the stem cell population resident in the hair follicle, where NFATc1 retains bulge cells in a quiescent state (Horsley et al., 2008). Thus, the function of NFATc1 to regulate cellular quiescence and proliferation appears to involve different mechanisms and downstream transcriptional targets during normal developmental processes and during stages of injury. A complimentary study showed that mice with Runx1 conditionally deleted from keratinocytes further supports that different mechanisms control hair growth during development and hair growth triggered by injury (Osorio et al., 2008). Taken together, these studies suggest a role for NFATc1 in the maintenance of quiescence and proliferation of stem cells in the hair follicle.

Downstream targets of NFATc1 activation

We initiated a "candidate" gene strategy to quantify changes in expression of genes known to play a role in development, stem cell identity, proximal tubule maturation, and other renal cell populations. We used FACS analysis and qRT-PCR to compare the expression profiles of GFP+ PTCs, a heterogeneous population containing PTPCs with accentuated NFATc1 expression and their progeny, and GFP– PTCs 5 days after injury. Our results document that GFP+ PTCs are fully differentiated proximal tubules and have decreased expression of mesenchymal and glomerular markers. In addition, developmental markers and stem cell markers were increased in GFP+ PTCs compared to GFP- PTCs. In mice, CDK4 expression was increased in renal tubule epithelial cells during the phase of proliferation following I/R injury (Park et al., 1997). The increase expression of CDK4 and Nfatc1 suggest that regulation of cell cycle progression in PTPCs is regulated by a different mechanism than that observed in the bulge cells of the hair follicle (Horsley et al., 2008). We would propose a mechanism in which an increase in NFATc1 significantly increases BMP7 and CDK4 expression to synergistically release PTPCs from their quiescent slow-cycling state thus promoting progression through the cell cycle to regenerate the damaged proximal tubule segment. Furthermore, we would propose that the increased expression of stem cell markers, such as c-Myc, control the rate of proliferation of the PTPCs. The relationship between c-Myc and NFATc1 signaling has been previously studied in B-lymphocytes. C-Myc amplified intracellular Ca^{2+} concentration and promoted NFATc1-dependent proliferation, low levels of Ca^{2+} and/or c-Myc signaling alone resulted in an apoptotic response, and constitutive c-Myc signaling or c-Myc activation with sustained Ca^{2+}/NFATc1 activation

promoted differentiation (Habib et al., 2007). The increase in c-Myc expression may promote proliferation and coordinate a balance between apoptosis and proliferation in this population. Identifying the mechanism of cell cycle regulation involving BMP7, CKD4, c-Myc and NFATc1 warrants further investigation.

As described above, our methods for isolation of GFP+ PTCs resulted in a heterogeneous population of cells composed of 1) the NFATc1-P2-Cre expressing progenitor cells and 2) constitutively labeled GFP+ progeny. Optimally, we want to isolate and exclusively characterize the progenitor population in the process of AKI. Therefore, I have developed a new transgenic line, NFATc1-Venus, using the NFATc1-P2 enhancer element, the minimal HSP promoter, and a yellow fluorescent protein that localizes to the nucleus, Venus (Nagai et al., 2002). The enhanced fluorescence of this reporter construct should allow direct FACS isolation of the PTPC population.

Initial experiments will be required to confirm the expression pattern of the NFATc1-Venus reporter both in developing endocardial cells, as previously characterized for NFATc1-P2-LacZ (Zhou et al., 2005), and in the proximal tubule following $HgCl_2$ injury. These mice will then be used to FACS the Venus+ PTPCs before and after injury. The gene expression profile of the Venus+ PTPCs can be compared to the unlabeled PTC population by using both a candidate gene strategy as well as microarray analysis to survey for evidence of broad activation/repression of specific signaling cascades (cell cycle regulation, apoptosis, calcineurin-NFAT signaling) and to screen for novel, unanticipated factors that may participate in the process (stem cell, developmental, and novel markers). As described for the Z/EG mice, Venus+ PTPCs should have an increase in expression of stem cell and developmental markers, cell cycle regulatory genes

indicative of increased cell proliferation, and anti-apoptotic genes. Identification of NFATc1 transcriptional targets would facilitate a more mechanistic understanding of the function of NFATc1 in mediating renal injury.

Are NFATc1 PTPCs restricted progenitor cells or multipotent stem cells?

It would be informative to determine if the NFATc1+ PTPCs are capable of regenerating additional components of the damaged nephron in addition to regeneration of proximal tubules, as described in this work. Are NFATc1+ PTPCs only progenitor cells or do they possess multipotent stem cell properties? The potential for NFATc1 accentuation to identify other renal progenitor cells provides a potentially fruitful avenue of investigation for potential therapeutic application in regenerative medicine. NFATc1+ PTPCs may adopt a renal differentiation program participating in the development of all renal cell populations, retain an epithelial phenotype contributing to the formation of tubular epithelial cells, or maintain specificity of a proximal tubule cell type. To answer this question, isolation of the NFATc1+ PTPCs from NFATc1-Venus mice could be used to further test the regenerative potential of these cells by analyzing if NFATc1-accentuated cells have the potential to regenerate other renal cell populations, thus testing an alternative hypothesis that adjacent less injured cells have regenerative capabilities. NFATc1+ PTPCs could be sorted and injected into SCID mice after $HgCl_2$, I/R, or glycerol-rhabdomyolysis injury to test if they regenerate proximal and/or distal tubules, glomeruli, or endothelial cells and increase renal function, as performed previously (Gupta et al., 2006; Lazzeri et al., 2007; Sagrinati et al., 2006).

NFATc1+ PTPCs could also be grafted under the renal capsule to see if they will form tubular segments, migrate and incorporate into host nephrons, or adopt other renal cell fates as performed with MRPC (Gupta et al., 2006). In addition, NFATc1+ cells could be microinjected into WT mouse kidney rudiments and grown *in vitro* for 7 to 10 days. Similar experiments were performed with R26R ES cells and injected ES cells were found in tubular epithelial cell populations and in glomerular tufts (Steenhard et al., 2005). Targets of NFATc1 activation as described above could be validated in these cells. Our data suggests that the PTPCs are fully differentiated and proliferate under a program of self-renewal to regenerate only the proximal tubule segment making this possibility less likely, but certainly worthy of investigation

Concluding remarks

The data presented here show that NFATc1 plays a role in proximal tubule regeneration following AKI and genetic and/or pharmacologic attenuation of NFATc1 results in increased proximal tubule apoptosis, increased renal injury, decreased proliferation, and even death. The most significant discovery presented in this thesis is the identification of NFATc1 expression in a subset of proximal tubules following $HgCl_2$ induced AKI, which is characteristic of a unique PTC progenitor cell population. In addition, we provide the first transgenic model system to identify a renal progenitor cell population in the proximal tubule. To our knowledge, the delayed regeneration after AKI is the first example of a phenotype identified in the *Nfatc1*$^{+/-}$ mouse and proposes a role for NFATc1 in the regeneration of injured proximal tubule cells by a resident population of progenitor proximal tubules accentuated by NFATc1 expression.

BIBLIOGRAPHY

Andoh, T., Lam, T., Lindsley, J., Alpers, C., and Bennett, W. (1997). Enhancement of chronic cyclosporine nephrotoxicity by sodium depletion in an experimental mouse model. Nephrology *3*, 471-478.

Aramburu, J., Yaffe, M. B., Lopez-Rodriguez, C., Cantley, L. C., Hogan, P. G., and Rao, A. (1999). Affinity-driven peptide selection of an NFAT inhibitor more selective than cyclosporin A. Science *285*, 2129-2133.

Basile, D. P. (2007). Novel approaches in the investigation of acute kidney injury. J Am Soc Nephrol *18*, 7-9.

Beals, C. R., Sheridan, C. M., Turck, C. W., Gardner, P., and Crabtree, G. R. (1997). Nuclear export of NF-ATc enhanced by glycogen synthase kinase-3. Science *275*, 1930-1934.

Bechstein, W. O. (2000). Neurotoxicity of calcineurin inhibitors: impact and clinical management. Transpl Int *13*, 313-326.

Benesic, A., Mildenberger, S., and Gekle, M. (2006). cAMP Ca2+ NFAT signalling in RPTEC control vs. CAA (Gene Expression Omnibus).

Benesic, A., Schwerdt, G., Mildenberger, S., Freudinger, R., Gordjani, N., and Gekle, M. (2005). Disturbed Ca2+-signaling by chloroacetaldehyde: A possible cause for chronic ifosfamide nephrotoxicity. Kidney Int *68*, 2029-2041.

Bi, B., Schmitt, R., Israilova, M., Nishio, H., and Cantley, L. G. (2007). Stromal cells protect against acute tubular injury via an endocrine effect. J Am Soc Nephrol *18*, 2486-2496.

Blair, J. T., Thompson, A. W., Whiting, P. H., Davidson, R. J. L., and Simpson, J. G. (1982). Toxicity of the immune suppressant cyclosporine A in the rat. J Pathol *138*, 163-178.

Bosukonda, D., Shih, M. S., Sampath, K. T., and Vukicevic, S. (2000). Characterization of receptors for osteogenic protein-1/bone morphogenetic protein-7 (OP-1/BMP-7) in rat kidneys. Kidney Int *58*, 1902-1911.

Bruce, S. J., Rea, R. W., Steptoe, A. L., Busslinger, M., Bertram, J. F., and Perkins, A. C. (2007). In vitro differentiation of murine embryonic stem cells toward a renal lineage. Differentiation *75*, 337-349.

Burdmann, E. A., Young, B., Andoh, T. F., Evans, A., Alpers, C. E., Lindsley, J., Johnson, R. J., Couser, W., and Bennett, W. M. (1994). Mechanisms of cyclosporine-induced interstitial fibrosis. Transplant Proc *26*, 2588-2589.

Burg, M. (2002). Response of renal inner medullary epithelial cells to osmotic stress. Comparative Biochemistry and Physiology - Part A: Molecular & Integrative Physiology *133*, 661-666.

Challen, G. A., Bertoncello, I., Deane, J. A., Ricardo, S. D., and Little, M. H. (2006). Kidney side population reveals multilineage potential and renal functional capacity but also cellular heterogeneity. J Am Soc Nephrol *17*, 1896-1912.

Chang, C. P., McDill, B. W., Neilson, J. R., Joist, H. E., Epstein, J. A., Crabtree, G. R., and Chen, F. (2004a). Calcineurin is required in urinary tract mesenchyme for the development of the pyeloureteral peristaltic machinery. J Clin Invest *113*, 1051-1058.

Chang, C. P., Neilson, J. R., Bayle, J. H., Gestwicki, J. E., Kuo, A., Stankunas, K., Graef, I. A., and Crabtree, G. R. (2004b). A field of myocardial-endocardial NFAT signaling underlies heart valve morphogenesis. Cell *118*, 649-663.

Chuvpilo, S., Jankevics, E., Tyrsin, D., Akimzhanov, A., Moroz, D., Jha, M. K., Schulze-Luehrmann, J., Santner-Nanan, B., Feoktistova, E., Konig, T., *et al.* (2002a). Autoregulation of NFATc1/A expression facilitates effector T cells to escape from rapid apoptosis. Immunity *16*, 881-895.

Chuvpilo, S., Jankevics, E., Tyrsin, D., Akimzhanov, A., Moroz, D., Jha, M. K., Schulze-Luehrmann, J., Santner-Nanan, B., Feoktistova, E., Konig, T., *et al.* (2002b). Autoregulation of NFATc1/A expression facilitates effector T cells to escape from rapid apoptosis. Immunity *16*, 881-895.

Chuvpilo, S., Zimmer, M., Kerstan, A., Glockner, J., Avots, A., Escher, C., Fischer, C., Inashkina, I., Jankevics, E., Berberich-Siebelt, F., *et al.* (1999). Alternative polyadenylation events contribute to the induction of NF-ATc in effector T cells. Immunity *10*, 261-269.

Coghlan, V. M., Perrino, B. A., Howard, M., Langeberg, L. K., Hicks, J. B., Gallatin, W. M., and Scott, J. D. (1995). Association of protein kinase A and protein phosphatase 2B with a common anchoring protein. Science *267*, 108-111.

Crabtree, G. R. (1999). Generic Signals and Specific Outcomes: Signaling through Ca2+, Calcineurin, and NF-AT. Cell *96*, 611-614.

Crabtree, G. R., and Olson, E. N. (2002). NFAT Signaling: Choreographing the Social Lives of Cells. Cell *109*, S67-S79.

de la Pompa, J. L., Takimoto, H., Yoshida, H., Elia, A. J., Samper, E., Potter, J., Wakeham, A., Marengere, L., Langille, B. L., and Crabtree, G. R. (1998). Role of NF-ATc transcription factor in morphogenesis of cardiac valves and septum. Nature *392*, 182-186.

Dressler, G. R., Deutsch, U., Chowdhury, K., Nornes, H. O., and Gruss, P. (1990). Pax2, a new murine paired-box-containing gene and its expression in the developing excretory system. Development *109*, 787-795.

Duffield, J. S., and Bonventre, J. V. (2005). Kidney tubular epithelium is restored without replacement with bone marrow-derived cells during repair after ischemic injury. Kidney Int *68*, 1956-1961.

Dunn, S. R., Qi, Z., Bottinger, E. P., Breyer, M. D., and Sharma, K. (2004). Utility of endogenous creatinine clearance as a measure of renal function in mice. Kidney Int *65*, 1959-1967.

Eckstein, L. A., Van Quill, K. R., Bui, S. K., Uusitalo, M. S., and O'Brien, J. M. (2005). Cyclosporin a inhibits calcineurin/nuclear factor of activated T-cells signaling and induces apoptosis in retinoblastoma cells. Invest Ophthalmol Vis Sci *46*, 782-790.

Esposito, C., Fornoni, A., Cornacchia, F., Bellotti, N., Fasoli, G., Foschi, A., Mazzucchelli, I., Mazzullo, T., Semeraro, L., and Dal Canton, A. (2000a). Cyclosporine induces different responses in human epithelial, endothelial and fibroblast cell cultures. Kidney Int *58*, 123-130.

Esposito, C., Fornoni, A., Cornacchia, F., Bellotti, N., Fasoli, G., Foschi, A., Mazzucchelli, I., Mazzullo, T., Semeraro, L., and Dal Canton, A. (2000b). Cyclosporine induces different responses in human epithelial, endothelial, and fibroblast cell cultures. Kidney Int *58*, 123-130.

Foley, D. P., and Chari, R. S. (2007). Ischemia-reperfusion injury in transplantation: novel mechanisms and protective strategies. Transplantation Reviews *21*, 43-53.

Gauthier, P., and Helderman, J. H. (2000). Cyclosporine avoidance. J Am Soc Nephrol *11*, 1933-1936.

Go, W. Y., Liu, X., Roti, M. A., Liu, F., and Ho, S. N. (2004). NFAT5/TonEBP mutant mice define osmotic stress as a critical feature of the lymphoid microenvironment. Proc Natl Acad Sci U S A *101*, 10673-10678.

Gooch, J. L. (2006). An emerging role for calcineurin Aalpha in the development and function of the kidney. Am J Physiol Renal Physiol *290*, F769-776.

Gooch, J. L., Barnes, J. L., Garcia, S., and Abboud, H. E. (2003). Calcineurin is activated in diabetes and is required for glomerular hypertrophy and ECM accumulation. Am J Physiol Renal Physiol *284*, F144-154.

Gupta, S., Verfaillie, C., Chmielewski, D., Kren, S., Eidman, K., Connaire, J., Heremans, Y., Lund, T., Blackstad, M., Jiang, Y., *et al.* (2006). Isolation and characterization of kidney-derived stem cells. J Am Soc Nephrol *17*, 3028-3040.

Habib, T., Park, H., Tsang, M., de Alboran, I. M., Nicks, A., Wilson, L., Knoepfler, P. S., Andrews, S., Rawlings, D. J., Eisenman, R. N., and Iritani, B. M. (2007). Myc stimulates B lymphocyte differentiation and amplifies calcium signaling. J Cell Biol *179*, 717-731.

Hammerman, M. R. (2004). Growing new kidneys in situ. Clin Exp Nephrol *8*, 169-177.

Heit, J. J., Apelqvist, A. A., Gu, X., Winslow, M. M., Neilson, J. R., Crabtree, G. R., and Kim, S. K. (2006). Calcineurin/NFAT signalling regulates pancreatic beta-cell growth and function. Nature *443*, 345-349.

Held, P. K., Al-Dhalimy, M., Willenbring, H., Akkari, Y., Jiang, S., Torimaru, Y., Olson, S., Fleming, W. H., Finegold, M., and Grompe, M. (2006). In vivo genetic selection of renal proximal tubules. Mol Ther *13*, 49-58.

Hesser, B., Liang, X., Camenisch, G., Yang, S. H., Lewin, D., Scheller, R., Ferrara, N., and Gerber, H. (2004). Down syndrome critical region protein 1 (DSCR1), a novel VEGF target gene that regulates expression of inflammatory markerson activated endothelial cells. Blood *104*, 149-158.

Ho, S., Clipstone, N., Timmermann, L., Northrop, J., Graef, I., Fiorentino, D., Nourse, J., and Crabtree, G. R. (1996). The mechanism of action of cyclosporin A and FK506. Clin Immunol Immunopathol *80*, S40-45.

Hocherl, K., Dreher, F., Vitzthum, H., Kohler, J., and Krutz, A. (2002). Cyclosporin A suppresses cyclooxygenase-2 expression in the rat kidney. J Am Soc Nephrol *13*, 2427-2436.

Hogan, P. G., Chen, L., Nardone, J., and Rao, A. (2003). Transcriptional regulation by calcium, calcineurin, and NFAT. Genes Dev *17*, 2205-2232.

Horsley, V., Aliprantis, A. O., Polak, L., Glimcher, L. H., and Fuchs, E. (2008). NFATc1 Balances Quiescence and Proliferation of Skin Stem Cells. Cell *132*, 299-310.

Huang, A. M., and Rubin, G. M. (2000). A misexpression screen identifies genes that can modulate RAS1 pathway signaling in Drosophila melanogaster. Genetics *156*, 1219-1230.

Hultman, P., and Enestrom, S. (1986). Localization of mercury in the kidney during experimental acute tubular necrosis studied by the cytochemical Silver Amplification method. Br J Exp Pathol *67*, 493-503.

Igarashi, P. (2003). Following the expression of a kidney-specific gene from early development to adulthood. Nephron Exp Nephrol *94*, e1-6.

Iwano, M., and Neilson, E. G. (2004). Mechanisms of tubulointerstitial fibrosis. Curr Opin Nephrol Hypertens *13*, 279-284.

Iwano, M., Plieth, D., Danoff, T. M., Xue, C., Okada, H., and Neilson, E. G. (2002). Evidence that fibroblasts derive from epithelium during tissue fibrosis. J Clin Invest *110*, 341-350.

Justo, P., Lorz, C., Sanz, A., Egido, J., and Ortiz, A. (2003). Intracellular mechanisms of cyclosporin A-induced tubular cell apoptosis. J Am Soc Nephrol *14*, 3072-3080.

Kahan, B. D. (1989). Cyclosporine. N Engl J Med *321*, 1725-1738.

Kobayashi, A., Kwan, K., Carroll, T., McMahon, A., Mendelsohn, C., and Behringer, R. (2005). Distinct and sequential tissue-specific activities of the LIM-class homeobox gene Lim1 for tubular morphogenesis during kidney development. Development *132*, 2809-2823.

Kopp, J. B. (2002). BMP-7 and the proximal tubule. Kidney Int *61*, 351-352.

Kramer, J., Steinhoff, J., Klinger, M., Fricke, L., and Rohwedel, J. (2006). Cells differentiated from mouse embryonic stem cells via embryoid bodies express renal marker molecules. Differentiation *74*, 91-104.

Lazzeri, E., Crescioli, C., Ronconi, E., Mazzinghi, B., Sagrinati, C., Netti, G. S., Angelotti, M. L., Parente, E., Ballerini, L., Cosmi, L., *et al.* (2007). Regenerative potential of embryonic renal multipotent progenitors in acute renal failure. J Am Soc Nephrol *18*, 3128-3138.

Li, C., Lim, S. W., Sun, B. K., and Yang, C. W. (2004). Chronic cyclosporine nephrotoxicity: new insights and preventive strategies. Yonsei Med J *45*, 1004-1016.

Li, J., Chen, F., and Epstein, J. A. (2000). Neural crest expression of Cre recombinase directed by the proximal Pax3 promoter in transgenic mice. Genesis *26*, 162-164.

Li, L., Truong, P., Igarashi, P., and Lin, F. (2007a). Renal and bone marrow cells fuse after renal ischemic injury. J Am Soc Nephrol *18*, 3067-3077.

Li, S. Z., McDill, B. W., Kovach, P. A., Ding, L., Go, W. Y., Ho, S. N., and Chen, F. (2007b). Calcineurin-NFATc signaling pathway regulates AQP2 expression in response to calcium signals and osmotic stress. Am J Physiol Cell Physiol *292*, C1606-1616.

Lim, S. W., Li, C., Sun, B. K., Han, K. H., Kim, W. Y., Oh, Y. W., Lee, J. U., Kador, P. F., Knepper, M. A., Sands, J. M., *et al.* (2004). Long-term treatment with cyclosporine decreases aquaporins and urea transporters in the rat kidney. Am J Physiol Renal Physiol *287*, F139-151.

Livak, K. J., and Schmittgen, T. D. (2001). Analysis of relative gene expression data using real-time quantitative PCR and the 2(-Delta Delta C(T)) Method. Methods *25*, 402-408.

Lopez-Rodriguez, C., Antos, C. L., Shelton, J. M., Richardson, J. A., Lin, F., Novobrantseva, T. I., Bronson, R. T., Igarashi, P., Rao, A., and Olson, E. N. (2004). Loss of NFAT5 results in renal atrophy and lack of tonicity-responsive gene expression. Proc Natl Acad Sci U S A *101*, 2392-2397.

Lopez-Rodriguez, C., Aramburu, J., Jin, L., Rakeman, A. S., Michino, M., and Rao, A. (2001). Bridging the NFAT and NF-KB families: NFAT5 dimerization regulates cytokine gene transcription in response to osmotic stress. Immunity *15*, 47-58.

Lopez-Rodriguez, C., Aramburu, J., Rakeman, A. S., and Rao, A. (1999). NFAT5, a constitutively nuclear NFAT protein that does not cooperate with Fos and Jun. Proc Natl Acad Sci U S A *96*, 7214-7219.

Ma, J., Nishimura, H., Fogo, A., Kon, V., Inagami, T., and Ichikawa, I. (1998). Accelerated fibrosis and collagen deposition develop in the renal interstitium of angiotensin type 2 receptor null mutant mice during ureteral obstruction. Kidney Int *53*, 937-944.

Ma, W., Rogers, K., Zbar, B., and Schmidt, L. (2002). Effects of different fixatives on beta-galactosidase activity. J Histochem Cytochem *50*, 1421-1424.

Macian, F. (2005). NFAT proteins: key regulators of T-cell development and function. Nat Rev Immunol *5*, 472-484.

Malumbres, M., and Barbacid, M. (2005). Mammalian cyclin-dependent kinases. Trends in Biochemical Sciences *30*, 630-641.

Mammucari, C., Tommasi di Vignano, A., Sharov, A. A., Neilson, J., Havrda, M. C., Roop, D. R., Botchkarev, V. A., Crabtree, G. R., and Dotto, G. P. (2005). Integration of Notch 1 and calcineurin/NFAT signaling pathways in keratinocyte growth and differentiation control. Dev Cell *8*, 665-676.

McDowell, E. M., Nagle, R. B., Zalme, R. C., McNeil, J. S., Flamenbaum, W., and Trump, B. F. (1976). Studies on the pathophysiology of acute renal failure. I. Correlation of ultrastructure and function in the proximal tubule of the rat following administration of mercuric chloride. Virchows Arch B Cell Pathol *22*, 173-196.

McKinley, M., and O'Loughlin, V. (2006). Human Anatomy: McGraw-Hill Higher Education).

McMorrow, T., Gaffney, M. M., Slattery, C., Campbell, E., and Ryan, M. P. (2005). Cyclosporine A induced epithelial-mesenchymal transition in human renal proximal tubular epithelial cells. Nephrol Dial Transplant *20*, 2215-2225.

Meseguer, A., and Catterall, J. F. (1990). Cell-specific expression of kidney androgen-regulated protein messenger RNA is under multihormonal control. Mol Endocrinol *4*, 1240-1248.

Metzger, D., Clifford, J., Chiba, H., and Chambon, P. (1995). Conditional site-specific recombination in mammalian cells using a ligand-dependent chimeric Cre recombinase. Proc Natl Acad Sci U S A *92*, 6991-6995.

Mignone, J. L., Kukekov, V., Chiang, A. S., Steindler, D., and Enikolopov, G. (2004). Neural stem and progenitor cells in nestin-GFP transgenic mice. J Comp Neurol *469*, 311-324.

Mihatsch, M. J., Thiel, G., and Ryffel, B. (1988). Cyclosporine nephrotoxicity. Adv Nephrol Necker Hosp *17*, 303-320.

Miyaji, T., Hu, X., and Star, R. A. (2002). alpha-Melanocyte-simulating hormone and interleukin-10 do not protect the kidney against mercuric chloride-induced injury. Am J Physiol Renal Physiol *282*, F795-801.

Miyakawa, H., Woo, S. K., Dahl, S. C., Handler, J. S., and Kwon, H. M. (1999). Tonicity-responsive enhancer binding protein, a rel-like protein that stimulates transcription in response to hypertonicty. Proc Natl Acad Sci U S A *96*, 2538-2542.

Morigi, M., Benigini, A., Remuzzi, G., and Imberti, B. (2006a). The regenerative potential of stem cells in acute renal failure. Cell Transplant *15*, S111-117.

Morigi, M., Benigni, A., Remuzzi, G., and Imberti, B. (2006b). The regenerative potential of stem cells in acute renal failure. Cell Transplant *15 Suppl 1*, S111-117.

Morrison, S. J., and Spradling, A. C. (2008). Stem cells and niches: mechanisms that promote stem cell maintenance throughout life. Cell *132*, 598-611.

Myers, B. D., Sibley, R., Newton, L., Tomlanovich, S. J., Boshkos, C., Stinson, E., Luetscher, J. A., Whitney, D. J., Krasny, D., Coplon, N. S., and et al. (1988). The long-term course of cyclosporine-associated chronic nephropathy. Kidney Int *33*, 590-600.

Nagai, T., Ibata, K., Park, E., Kubota, M., Mikoshiba, K., and Miyawaki, Z. (2002). A variant of yellow fluorescent protein with fast and efficient maturation for cell-biological applications. Nat Biotechnol *20*, 87-90.

Nakagawa, M., Koyanagi, M., Tanabe, K., Takahashi, K., Ichisaka, T., Aoi, T., Okita, K., Mochiduki, Y., Takizawa, N., and Yamanaka, S. (2008). Generation of induced pluripotent stem cells without Myc from mouse and human fibroblasts. Nat Biotechnol *26*, 101-106.

Neal, J. W., and Clipstone, N. A. (2001). Glycogen Synthase Kinase-3 Inhibits the DNA Binding Activity of NFATc. J Biol Chem %R 101074/jbcM004888200 *276*, 3666-3673.

Neal, J. W., and Clipstone, N. A. (2003). A constitutively active NFATc1 mutant induces a transformed phenotype in 3T3-L1 fibroblasts. J Biol Chem *278*, 17246-17254.

Novak, A., Guo, C., Yang, W., Nagy, A., and Lobe, C. G. (2000). Z/EG, a double reporter mouse line that expresses enhanced green fluorescent protein upon Cre-mediated excision. Genesis *28*, 147-155.

Ohyama, T., and Groves, A. K. (2004). Generation of Pax2-Cre mice by modification of a Pax2 bacterial artificial chromosome. Genesis *38*, 195-199.

Okita, K., Ichisaka, T., and Yamanaka, S. (2007). Generation of germline-competent induced pluripotent stem cells. Nature *448*, 313-317.

Oliver, J. A., Maarouf, O., Cheema, F. H., Martens, T. P., and Al-Awqati, Q. (2004). The renal papilla is a niche for adult kidney stem cells. J Clin Invest *114*, 795-804.

Olyaei, A. J., de Mattos, A. M., and Bennett, W. M. (2001). Nephrotoxicity of immunosuppressive drugs: new insight and preventive strategies. Curr Opin Crit Care *7*, 384-389.

Osorio, K. M., Lee, S. E., McDermitt, D. J., Waghmare, S. K., Zhang, Y. V., Woo, H. N., and Tumbar, T. (2008). Runx1 modulates developmental, but not injury-driven, hair follicle stem cell activation. Development *135*, 1059-1068.

Pan, M., Winslow, M. M., Chen, L., Kuo, A., Felsher, D., and Crabtree, G. R. (2007). Enhanced NFATc1 Nuclear Occupancy Causes T Cell Activation Independent of CD28 Costimulation. J Immunol *178*, 4315-4321.

Park, S. K., Kang, M. J., Kim, W., and Koh, G. Y. (1997). Renal tubule regeneration after ischemic injury is coupled to the up-regulation and activation of cyclins and cyclin dependent kinases. Kidney Int *52*, 706-714.

Patschan, D., Michurina, T., Shi, H. K., Dolff, S., Brodsky, S. V., Vasilieva, T., Cohen-Gould, L., Winaver, J., Chander, P. N., Enikolopov, G., and Goligorsky, M. S. (2007). Normal distribution and medullary-to-cortical shift of Nestin-expressing cells in acute renal ischemia. Kidney Int *71*, 744-754.

Porter, C. M., and Clipstone, N. A. (2002). Sustained NFAT signaling promotes a Th1-like pattern of gene expression in primary murine CD4+ T cells. J Immunol *168*, 4936-4945.

Prozialeck, W. C., Lamar, P. C., and Appelt, D. M. (2004). Differential expression of E-cadherin, N-cadherin and beta-catenin in proximal and distal segments of the rat nephron. BMC Physiol *4*, 10.

Puri, S., Magenheimer, B. S., Maser, R. L., Ryan, E. M., Zien, C. A., Walker, D. D., Wallace, D. P., Hempson, S. J., and Calvet, J. P. (2004). Polycystin-1 activates the calcineurin/NFAT signaling pathway. J Biol Chem.

Quoix, N., Cheng-Xue, R., Guiot, Y., Herrera, P. L., Henquin, J. C., and Gilon, P. (2007). The GluCre-ROSA26EYFP mouse: a new model for easy identification of living pancreatic alpha-cells. FEBS Lett *581*, 4235-4240.

Ramesh, G., and Reeves, W. B. (2002). TNF-alpha mediates chemokine and cytokine expression and renal injury in cisplatin nephrotoxicity. J Clin Invest *110*, 835-842.

Ranger, A. M., Grusby, M. J., Hodge, M. R., Gravallese, E. M., de la Brousse, F. C., Hoey, T., Mickanin, C., Baldwin, H. S., and Glimcher, L. H. (1998a). The transcription factor NF-ATc is essential for cardiac valve formation. Nature *392*, 186-190.

Ranger, A. M., Hodge, M. R., Gravallese, E. M., Oukka, M., Davidson, L., Alt, F. W., de la Brousse, F. C., Hoey, T., Grusby, M., and Glimcher, L. H. (1998b). Delayed lymphoid repopulation with defects in IL-4-driven responses produced by inactivation of NF-ATc. Immunity *8*, 125-134.

Rao, A., Luo, C., and Hogan, P. G. (1997). Transcription factors of the NFAT family: regulation and function. Annu Rev Immunol *15*, 707-747.

Rezzani, R. (2004). Cyclosporine A and adverse effects on organs: histochemical studies. Prog Histochem Cytochem *39*, 85-128.

Rothermel, B., Vega, R. B., Yang, J., Wu, H., Bassel-Duby, R., and Williams, R. S. (2000). A protein encoded within the Down syndrome critical region is enriched in striated muscles and inhibits calcineurin signaling. J Biol Chem *275*, 8719-8725.

Roy, M. K., Takenaka, M., Kobori, M., Nakahara, K., Isobe, S., and Tsushida, T. (2006). Apoptosis, necrosis and cell proliferation-inhibition by cyclosporine A in U937 cells (a human monocytic cell line). Pharmacol Res *53*, 293-302.

Rubera, I., Poujeol, C., Bertin, G., Hasseine, L., Counillon, L., Poujeol, P., and Tauc, M. (2004). Specific Cre/Lox recombination in the mouse proximal tubule. J Am Soc Nephrol *15*, 2050-2056.

Sabolic, I. (2006). Common mechanisms in nephropathy induced by toxic metals. Nephron Physiol *104*, p107-114.

Sabolic, I., Valenti, G., Verbavatz, J., Van Hoek, A., Verkman, A., Ausiello, D., and Brown, D. (1992). Localization of the CHIP28 water channel in rat kidney. Am J Pathol *263*, C1225-1233.

Sagrinati, C., Netti, G. S., Mazzinghi, B., Lazzeri, E., Liotta, F., Frosali, F., Ronconi, E., Meini, C., Gacci, M., Squecco, R.*, et al.* (2006). Isolation and characterization of multipotent progenitor cells from the Bowman's capsule of adult human kidneys. J Am Soc Nephrol *17*, 2443-2456.

Satoh, M., Nishimura, N., Kanayama, Y., Naganuma, A., Suzuki, T., and Tohyama, C. (1997). Enhanced renal toxicity by inorganic mercury in metallothionein-null mice. J Pharmacol Exp Ther *283*, 1529-1533.

Schmidt, A., Kuhla, B., Bigl, K., Munch, G., and Arendt, T. (2007). Cell cycle related signaling in neuro2a cells proceeds via the receptor for advanced glycation end products. J Neural Transm *114*, 1413-1424.

Schwerdt, G., Gordjani, N., Freudinger, R., Wollny, B., Kirchhoff, A., and Gekle, M. (2006). Chloroacetaldehyde and acrolein-induced death of human proximal tubule cells. Pediatr Nephrol *21*, 60-67.

Shao, X., Somlo, S., and Igarashi, P. (2002). Epithelial-specific Cre/lox recombination in the developing kidney and genitourinary tract. J Am Soc Nephrol *13*, 1837-1846.

Skinner, R. (2003). Chronic ifosfamide nephrotoxicity in children. Med Pediatr Oncol *41*, 190-197.

Soriano, P. (1999). Generalized lacZ expression with the ROSA26 Cre reporter strain. Nat Genet *21*, 70-71.

Srinivas, S., Watanabe, T., Lin, C. S., William, C. M., Tanabe, Y., Jessell, T. M., and Costantini, F. (2001). Cre reporter strains produced by targeted insertion of EYFP and ECFP into the ROSA26 locus. BMC Dev Biol *1*, 4.

Steenhard, B., Isom, K., Cazcarro, P., Dunmore, J., Godwin, A., St. John, P., and Abrahamson, D. (2005). Integration of Embryonic Stem Cells in Metanephric Kidny Organ Culture. J Am Soc Nephrol *16*, 1623-1631.

Stroud, J. C., Lopez-Rodriguez, C., Rao, A., and Chen, L. (2002). Structure of a TonEBP-DNA complex reveals DNA encircled by a transcription factor. Nat Struct Biol *9*, 90-94.

Sugimoto, T., Haneda, M., Sawano, H., Isshiki, K., Maeda, S., Koya, D., Inoki, K., Yasuda, H., Kashiwagi, A., and Kikkawa, R. (2001). Endothelin-1 induces cyclooxygenase-2 expression via nuclear factor of activated T-cell transcription factor in glomerular mesangial cells. J Am Soc Nephrol *12*, 1359-1368.

Sun, L., Youn, H. D., Loh, C., Stolow, M., He, W., and Liu, J. O. (1998). Cabin 1, a negative regulator for calcineurin signaling in T lymphocytes. Immunity *8*, 703-711.

Tabatabai, N. M., Blumenthal, S. S., Lewand, D. L., and Petering, D. H. (2001). Differential regulation of mouse kidney sodium-dependent transporters mRNA by cadmium. Toxicol Appl Pharmacol *177*, 163-173.

Tanaka-Kagawa, T., Suzuki, M., Naganuma, A., Yamanaka, N., and Imura, N. (1998). Strain Difference in Sensitivity of Mice to Renal Toxicity of Inorganic Mercury. J Pharmacol Exp Ther *285*, 335-341.

Tumlin, J. A., Someren, J. T., Swanson, C. E., and Lea, J. P. (1995). Expression of calcineurin activity and alpha-subunit isoforms in specific segments of the rat nephron. Am J Physiol *269*, F558-563.

Vainio, S., and Lin, Y. (2002). Coordinating early kidney development: lessons from gene targeting. Nat Rev Genet *3*, 533-543.

Vigneau, C., Polgar, K., Striker, G., Elliott, J., Hyink, D., Weber, O., Fehling, H. J., Keller, G., Burrow, C., and Wilson, P. (2007). Mouse embryonic stem cell-derived embryoid bodies generate progenitors that integrate long term into renal proximal tubules in vivo. J Am Soc Nephrol *18*, 1709-1720.

Vinay, P., Gougoux, A., and Lemieux, G. (1981). Isolation of a pure suspension of rat proximal tubules. Am J Physiol *241*, F403-411.

Vogetseder, A., Palan, T., Bacic, D., Kaissling, B., and Le Hir, M. (2007). Proximal tubular epithelial cells are generated by division of differentiated cells in the healthy kidney. Am J Physiol Cell Physiol *292*, C807-813.

Wilkins, B. J., De Windt, L. J., Bueno, O. F., Braz, J. C., Glascock, B. J., Kimball, T. F., and Molkentin, J. D. (2002). Targeted disruption of NFATc3, but not NFATc4, reveals an intrinsic defect in calcineurin-mediated cardiac hypertrophic growth. Mol Cell Biol *22*, 7603-7613.

Winslow, M. M., Pan, M., Starbuck, M., Gallo, E. M., Deng, L., Karsenty, G., and Crabtree, G. R. (2006). Calcineurin/NFAT signaling in osteoblasts regulates bone mass. Dev Cell *10*, 771-782.

Wright, E. M. (2001). Renal Na(+)-glucose cotransporters. Am J Physiol Renal Physiol *280*, F10-18.

Xu, J., Bing, Y., Fan, X., Langworthy, M., Zhang, M. Z., and Harris, R. (2007). Characterization of a Putative Intrarenal Serotonergic System. Am J Physiol Renal Physiol.

Yasutake, A., and Hirayama, K. (1986). Strain difference in mercury excretion in methylmercury-treated mice. Arch Toxicol *59*, 99-102.

You, G., Lee, W. S., Barros, E. J., Kanai, Y., Huo, T. L., Khawaja, S., Wells, R. G., Nigam, S. K., and Hediger, M. A. (1995). Molecular characteristics of Na(+)-coupled glucose transporters in adult and embryonic rat kidney. J Biol Chem *270*, 29365-29371.

Young, B. A., Burdmann, E. A., Johnson, R. J., Alpers, C. E., Giachelli, C. M., Eng, E., Andoh, T., Bennett, W. M., and Couser, W. G. (1995a). Cellular proliferation and macrophage influx precede interstitial fibrosis in cyclosporine nephrotoxicity. Kidney Int *48*, 439-448.

Young, B. A., Burdmann, E. A., Johnson, R. J., Andoh, T., Bennett, W. M., Couser, W. G., and Alpers, C. E. (1995b). Cyclosporine A induced arteriolopathy in a rat model of chronic cyclosporine nephropathy. Kidney Int *48*, 431-438.

Yu, H., van Berkel, T. J., and Biessen, E. A. (2007a). Therapeutic potential of VIVIT, a selective peptide inhibitor of nuclear factor of activated T cells, in cardiovascular disorders. Cardiovasc Drug Rev *25*, 175-187.

Yu, J., Vodyanik, M. A., Smuga-Otto, K., Antosiewicz-Bourget, J., Frane, J. L., Tian, S., Nie, J., Jonsdottir, G. A., Ruotti, V., Stewart, R.*, et al.* (2007b). Induced pluripotent stem cell lines derived from human somatic cells. Science *318*, 1917-1920.

Zalups, R. K. (2000). Molecular interactions with mercury in the kidney. Pharmacol Rev *52*, 113-143.

Zalups, R. K., and Barfuss, D. W. (1996). Nephrotoxicity of inorganic mercury co-administrated with L-cysteine. Toxicology *109*, 15-29.

Zhou, B., Cron, R. Q., Wu, B., Genin, A., Wang, Z., Liu, S., Robson, P., and Baldwin, H. S. (2002). Regulation of the murine NFATc1 gene by NFATc2. J Biol Chem *277*, 10704-10711.

Zhou, B., Wu, B., Tompkins, K. L., Boyer, K. L., Grindley, J. C., and Baldwin, H. S. (2005). Characterization of Nfatc1 regulation identifies an enhancer required for gene expression that is specific to pro-valve endocardial cells in the developing heart. Development *132*, 1137-1146.